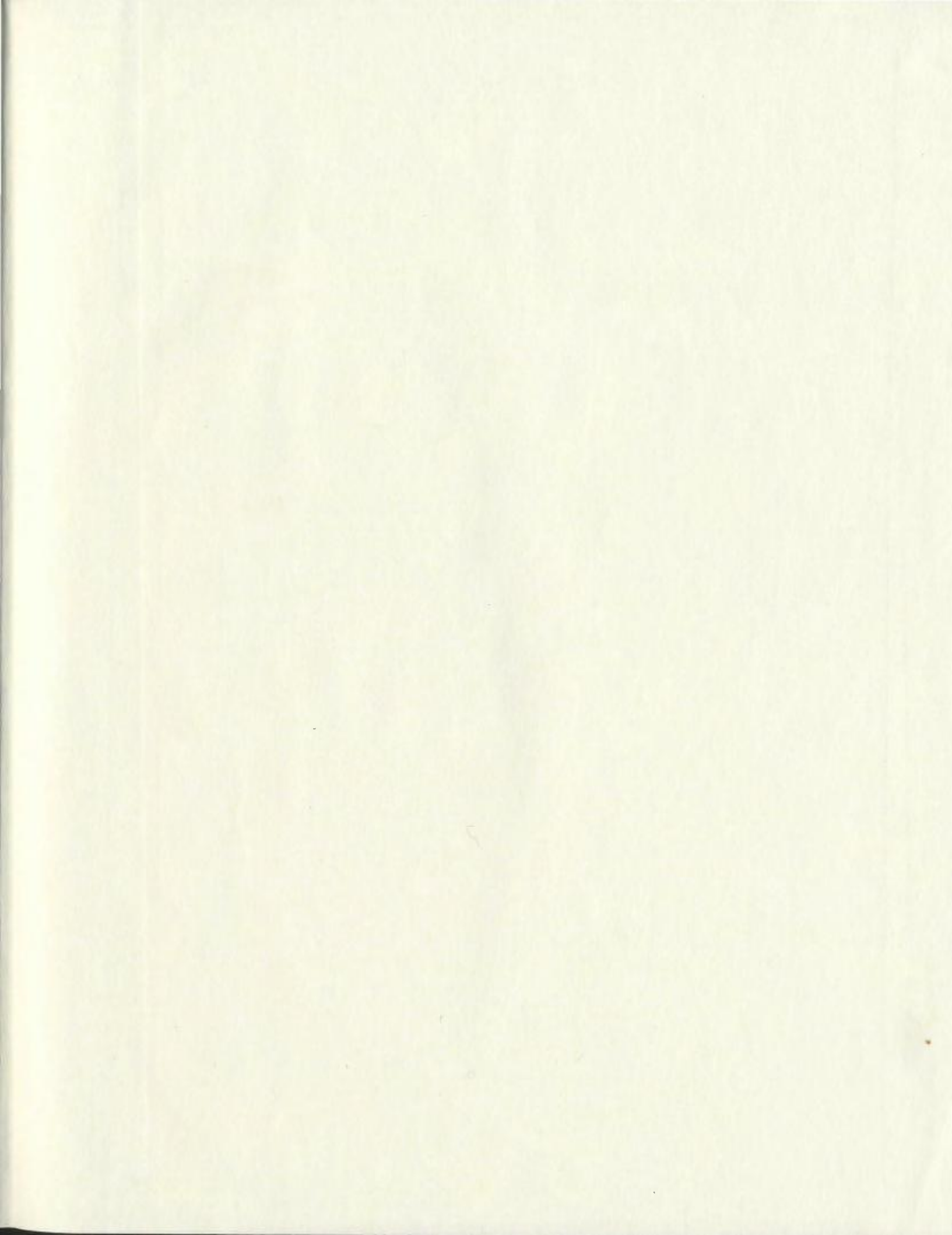


SEISMIC STRATIGRAPHY AND TECTONOSTRUCTURAL
FRAMEWORK OF THE BJARNI AREA,
HOPEDALE BASIN, LABRADOR SEA

MICHELLE RAE MARTIN



SEISMIC STRATIGRAPHY AND TECTONO-
STRUCTURAL FRAMEWORK OF THE BJARNI AREA,
HOPEDALE BASIN, LABRADOR SEA

by

© Michelle Rae Martin, B.Sc. (Honours)

A thesis submitted to the School of Graduate Studies in partial fulfillment of
the requirements for the degree of
Masters of Science

Department of Earth Sciences
Memorial University of Newfoundland
September 2007

St. John's

Newfoundland and Labrador



Abstract

The Labrador shelf and slope Mesozoic sedimentary area is divided by the Okak Arch into two large basins, the Saglek Basin and the Hopedale Basin. The Hopedale Basin is the more southerly basin and extends from the Cartwright Transfer Fault Zone (CTFZ) in the south to the Okak Arch in the North: a distance of approximately 500 kilometres from 55° to 59° latitude North. It is part of a large, oval, tectonic depression having an area of about 175 000 square kilometres. The basin has an uneven basement floor consisting of stretched continental crust, exhumed continental mantle (transitional crust) and oceanic crust. The thickest sediment accumulation is located on the outer shelf and inner slope.

A recent seismic grid collected by Geophysical Service Incorporated (GSI) during 2003, 2004 and 2005 has produced a regional 2D seismic coverage adequately covering this vast area that contains the giant Bjarni/North Bjarni gas field. These non-exclusive seismic lines were graciously donated to Memorial University of Newfoundland to be used for regional tectonic, structural and seismic stratigraphic investigations and mapping.

Using these donated data, several seismic sequences were defined, correlated to well information and mapped throughout the area surrounding the Bjarni/North Bjarni field. The study indicates that the Lower Cretaceous Bjarni Formation is widespread, was deposited in a large rifted area and contains the basin's main reservoir and source rock. Seismic correlations indicate that the Bjarni reservoir extends beyond the shelf and into the outer slope region. This new interpretation increases the probability that there are still many undrilled Bjarni plays on the shelf and on the slope.

On the basis of seismic character observed on lines that extend into deepwater, it is apparent that there was a significant amount of postrift mantle exhumation on the Labrador margin expressed as serpentinized ridges as well as predrift lava flows mapped on continental and transitional crust domains. Thick syndrift and postdrift sediments overlie this oceanic crust.

Kinematic modelling of a representative dip line illustrates that most of the extension took place in a continental setting during the Early Cretaceous. Multiple periods of subsidence followed; the most significant being the prominent thermal subsidence during the Late Tertiary. This subsidence along with margin tilting created the Labrador Shelf as seen today.

As proven by past drilling, the Hopedale Basin contains all elements of a rich petroleum system. With new interpretation of the main reservoir-Bjarni sandstone-combined with previously documented geochemical data, it is evident that there is significant remaining hydrocarbon potential along the Labrador Shelf. Preserved Paleozoic carbonates on top of basement highs as well as draping and onlapping of the Bjarni sandstones on rotated basement blocks are the most significant hydrocarbon plays. Several leads have been indicated during regional mapping.

Currently there is only minor exploration interest in the Hopedale Basin due to its remote location and its vulnerability to natural hazards including high frequency of icebergs, long-lasting pack ice and variable weather. These natural hazards have resulted in no exploration drilling or landsales in the basin for over 25 years even though it has already been proven to hold over 4.2 Tcf of gas. Hopefully, increasing demand for gas,

high commodity prices, new drilling and production technologies and new seismic surveys supplemented by hydrocarbon detection methods (AVO, LMR, etc.) will encourage companies to develop the existing discoveries and explore for new ones.

Acknowledgements

First and foremost I would like to thank my supervisor, Michael Enachescu, who accepted me as his student and has taught and supported me through my thesis. I would also like to thank him for his constant encouragement and his input through the research and writing of this thesis. I would also like to thank my co-supervisor Jim Wright for his help during my time at Memorial University.

I would like to thank Landmark® Graphics for their donation of the software which was used to interpret the data. Also, I would like to thank NSERC for providing computer hardware. Many thanks are extended to Paul and Dave Einarsson with Geophysical Services Incorporated for donating the data used in this thesis. Special thanks are also extended to PanAtlantic Petroleum Systems Consortium (PPSC) for funds and support provided during this degree.

I would like to thank all the technical support who helped in various ways and at different stages of the thesis over the past three years: Tony Kocurko, Craig Rowe, Sharon Deemer, Dan Vasiliu, Clyde Clements, and Peter Bruce. I would also like to thank Trevor Bennett from the C-NLOPB for his help with Landmark® as well as Lisa Clarke at the C-NLOPB library who helped with compilation of well data.

I would like to thank a few extra faculty/staff members in the Department who have helped in many ways. I would like to thank Jeremy Hall for his administrative help during the course of my thesis. I also need to say a special thank-you to Ian Atkinson with PPSC for his help and persistence with all aspects of my research. Also, a big thank-you goes out to Raymond Patzöld and Michelle Miskell for their guidance during my time as a graduate student at Memorial University.

I would like to say thank-you to a large group of fellow graduate students who made my time at Memorial memorable and who have helped in so many ways during my time here. These students include Deanne Duff, my long-time partner in crime, Victoria Hardy, my office mate and friend who always added comic relief to each day and shared in my joys and frustrations. Thank-you to all other graduate students and friends who added insight into my research and kept me smiling through it all: Renee Burton-Ferguson, Stephen Kearsey, Stephen Schwartz, Brad Bonnell, Jordan Stead, Allison Cocker, Nikki Tonkin, Chris Phillips, Angie Dearin, Erin Gillis and so many others. Special thanks to Sean Hayes for his help with the editing of my thesis and Michael Ash for allowing me to use his printer.

Lastly, thank-you to my friends, my parents and my family for continuously asking “are you done yet?” and listening patiently while I listed off my excuses as to why I wasn’t done. I will be forever grateful to my wonderful parents for always believing that I could do it. Finally, thank-you Grant, for everything.

Table of Contents

Title Page	i
Abstract	ii
Acknowledgements	iv
List of Figures	viii
List of Tables	xiv

Chapter 1: Introduction

1.1 Introduction	1
1.2 Background and Previous Work	3
1.3 Purpose	10
1.4 Research Objectives	11
1.5 Data	12

Chapter 2: Labrador Shelf Geography and Geology

2.1 Geography	17
2.2 Regional Geology – Labrador Margin	18
2.3 Basin Development and Stratigraphy	25
2.4 Structural Styles and Elements	39

Chapter 3: Seismic Stratigraphy

3.1 Introduction	41
3.2 Well Control	42
3.2.1 General Well Information	44
3.2.2 Time-Depth Information	44
3.2.3 Well Picks and Seismic Markers	46
3.3 Seismic Data Quality and Horizon Picking	54
3.4 Seismic Sequence Analysis	58
3.4.1 K1 Sequence Boundary: Top Basement Marker	64
3.4.2 Seismic Sequence 1	69
3.4.3 K2 Sequence Boundary	71
3.4.4 Seismic Sequence 2	72
3.4.5 T1 Sequence Boundary	76
3.4.6 Seismic Sequence 3	78
3.4.7 T2 Sequence Boundary	79
3.4.8 Seismic Sequence 4	81
3.4.9 T3 Sequence Boundary	82
3.4.10 Seismic Sequence 5	84
3.4.11 T4 Sequence Boundary	85
3.4.12 Seismic Sequence 6	88
3.4.13 WB Sequence Boundary (Water Bottom)	91
3.4.14 Serpentinized Peridotite Ridges (PR)	92
3.4.15 Lava Flow (LF)	95

<u>Chapter 4: Kinematic modelling of a representative Hopedale Basin dip profile</u>	
4.1 Purpose	100
4.2 Depth Conversion and Kinematic Modelling – Methods	101
4.3 Tectono-stratigraphy	103
4.3.1 Basement Tectonics	104
4.3.2 Evolutionary Stages and Structural Features	107
4.4 Kinematic Model	114
4.5 Discussion	120
4.6 Conclusions	123
<u>Chapter 5: Petroleum System</u>	
5.1 Introduction	125
5.1.1 Producing Depth Maps	126
5.2 Source Rock	128
5.2.1 Markland Formation	128
5.2.2 Bjarni Formation	136
5.3 Reservoir Rock	139
5.3.1 Bjarni Formation	139
5.3.2 Gudrid Member/Cartwright Formation	141
5.3.3 Leif Member	143
5.3.4 Freydis Member	144
5.3.5 Carbonate Reservoirs	144
5.4 Regional Seals	145
5.5 Structural and Stratigraphic Traps	148
5.6 Discussion	154
<u>Chapter 6: Conclusions and Recommendations for Future Work</u>	
6.1 Justification for the Study	159
6.2 Key Conclusions	160
6.3 Recommendations for Future Work	164
<u>References</u>	166
<u>Appendices</u>	
APPENDIX A – Time-depth data for the wells in the study area	179

List of Figures

1.1	Bathymetry and basin locations in the area of the Labrador Shelf. Approximate location of study area shown in orange. The basin is defined by the Okak Arch in the north and the Cartwright Arch in the south. Figure modified from Canada-Newfoundland and Labrador Offshore Petroleum Board (C-NLOPB) and Geological Survey of Canada (GSC). Digitized by Grant Lethbridge.	2
1.2	Bathymetric map showing the locations of wells in the Hopedale Basin as well as their current status, and significant discovery licences (shown in blue).	6
1.3	Lithostratigraphy chart illustrating the major additional sequences and unconformities added to the Labrador Shelf geology by McWhae et al. (1980) in contrast to Umpleby (1979). Ages from Gradstein et al. (2004). Modified from McWhae et al. (1980).	8
1.4	Base map of the Labrador shelf showing the recent GSI seismic coverage along the shelf and the study area shown in blue. These data are of 2003, 2004 and 2005 vintage.	13
1.5	Example of the GSI data set (dip line). The vertical scale is two-way travel time in milliseconds.	15
2.1	Figure from Srivastava and Roest (1999) illustrating the observed and calculated (modelled) anomalies through the Labrador margin. The numbers along the top represent anomaly numbers.	19
2.2	Figure modified after Chalmers and Laursen (1995). This figure demonstrates the observed and calculated fields when considering continental crust after anomaly 27 with oppose to oceanic crust.	21
2.3	Figure from Chian et al. (1995). This figure illustrates the multichannel reflection seismic with velocity values shown as well as colours illustrating the velocity structure.	22
2.4	Crustal thinning of the extinct Labrador rift as suggested by Loudon et al., 1996. (A) Continental crust thickness (yellow) is uniform because the rate of plate separation is equal to the rate of melt supply; (B) Rate of extension exceeds the rate of melt supply thereby thinning the crust. Modified after Loudon et al. (1996).	24
2.5	Generalized lithostratigraphic chart of the Labrador shelf (modified from the GSC and McWhae et al., 1980). Ages after Gradstein et al. (2004).	26

2.6	Pictures of Alexis Basalt. Notice the variation in colour due to possible hydrothermal alteration (A) and weathering (B) as described by Umpleby (1979). Picture A shows Core #4 (boxes 5 & 6 of 7). Picture B shows Core #4 (box 1 of 7). Both pictures are taken from the Roberval K-92 well (~3420 metres depth). Core available from C-NLOPB.	28
2.7	Schematic cross-section through the North Bjarni Field which illustrates typical nearshore structural and tectonic features of the Canadian Labrador margin. Different colours represent different lithological units. Shales are shown in shades of grey, sands are shown in yellow and conglomerates are shown in orange. Red indicates the North Bjarni gas-filled reservoir (modified after GSC and Government of NF and Labrador, Department of Mines and Energy). Note that recent papers and presentations suggests that Bjarni Formation extends into the outer shelf and deep water regions (Enachescu, 2006; Enachescu et al., 2006 and Martin et al., 2006).	29
2.8	Picture (A) shows sandstones from the Bjarni formation from the Roberval K-92 well (Core #2 Box 2 of 5) and picture (~ 3050 metres depth) (B) shows sandstone from the North Bjarni F-06 well (Core #1, Box 1 of 1; ~ 2455 metres depth). Cores available from C-NLOPB.	31
2.9	A typical core section of the Markland shales from the Roberval K-92 well showing Core #1 (Box 1 of 2, ~ 3015 metres depth). Core available from C-NLOPB.	33
2.10	A typical core section of the Cartwright Formation taken from the Snorri J-90 well (Core #1, ~ 2000 metres depth). Core available from the C-NLOPB.	35
3.1	Seismic base map showing current well location and status and the study area (shown in blue rectangle). Coordinates in NAD83.	43
3.2	Time-depth curves for wells in Group A and their respective time-depth functions. Created from data taken from well files in the C-NLOPB archive.	48
3.3	Time-depth curves for wells in Group B and their respective time-depth functions. Created from data taken from well files in the C-NLOPB archive.	49
3.4	Time-depth curves for wells in Group C and their respective time-depth functions. Created from data taken from well files in the C-NLOPB archives.	50
3.5	Schematic diagram illustrating the age, formation names, lithology, horizon number, horizon name, depositional sequence name and the	53

quality and confidence of each of the markers (template for figure modified after Young, 2005; lithostratigraphy modified after McWhae et al., 1980; ages after Gradstein et al., 2004).

3.6	Dip seismic section illustrating good reflection resolution below the shelf break and slope.	55
3.7	Dip seismic section illustrating typical data quality below the shelf break within the study area. Significant loss of resolution and contamination by water bottom multiples of seismic reflectors is visible under the continental slope.	56
3.8	Typical dip seismic section along the shelf and inner channel along the Labrador coast. Arrows are illustrating areas with crossing reflectors. Truncated reflectors at the water bottom are primary reflectors. Areas like this can be difficult to interpret since distinguishing between true reflectors and multiples can be difficult.	57
3.9	Dip seismic section illustrating the quality of data typical of lines in the south-east portion of the study area. This low resolution data makes interpretation very difficult and therefore very little interpretation could be done in this area.	59
3.10	Base map of the study area (blue) illustrating the area where the data is of poor quality and therefore interpretation in this region is limited (red rectangle). Coordinates in NAD83.	60
3.11	Illustration of the four systems tracts define in sequence stratigraphy. HST – highstand systems tract; FSST – falling stage systems tract; LST – lowstand systems tract; TST – transgressive systems tract; SB – sequence boundary; TS – transgressive surface; MFS – maximum flooding surface. Figure modified after Coe et al., (2002).	62
3.12	Schematic diagram illustrating the different types of erosional truncation that are often evident in reflection seismic data. The orange lines represent sequence boundaries while the green line represents a maximum flooding surface (MFS). Figure modified after Coe et al. (2002).	65
3.13	Location map of two significant seismic sections. The red line shows the seismic line passing through the North Bjarni F-06 well (Figures 3.14 and 3.16) and the green line represents the seismic line passing through the Gudrid H-55 well (Figures 3.15 and 3.18).	66
3.14	Dip seismic section illustrating the typical seismic character of the K1 horizon as well as the relationship of the S1 seismic sequence to horizons K1 and K2. S1 seen at the North Bjarni F-06 location shows an obvious	68

flat spot developed below the K2 horizon. Overlying markers and seismic sequences are also shown.

- | | | |
|------|---|----|
| 3.15 | Dip seismic section illustrating the S1 seismic sequence (Bjarni Formation) filling the half grabens on both sides of the Gudrid high. Bjarni Formation (S1 seismic sequence) is missing on the horst block at the Gudrid H-55 well due to erosion or non-deposition. | 70 |
| 3.16 | Dip seismic section illustrating seismic reflectors within S2 (denoted by green) which downlap onto the K2 sequence boundary. Truncation of reflector under K2 boundary (denoted by pink) is also observed. | 73 |
| 3.17 | Dip seismic section showing a family of down-to-basin faults cutting through S2, and seismic sequences S3, S4 and S5 on the shelf. | 75 |
| 3.18 | Dip seismic line through the Gudrid H-55 well showing seismic sequence S3 and its relation to the T1 and T2 sequence boundaries. Notice the apparent downlap of several reflectors within S3 onto T1. | 77 |
| 3.19 | Dip seismic section showing the typical characteristics of the depositional sequence S4. | 80 |
| 3.20 | Regional dip seismic line showing the extent of the T3 seismic boundary coloured in purple. | 83 |
| 3.21 | Dip seismic section illustrating the typical characteristics of depositional sequence S5. | 86 |
| 3.22 | Dip seismic section which shows several faults cutting through seismic sequences S3, S4 and S5. Also note the T3 sequence boundary in purple and the T4 sequence boundary in orange. | 87 |
| 3.23 | Dip seismic section illustrating the S6 sequence as well as at least one unidentified unconformity within S6 (light pink marker). | 90 |
| 3.24 | Bathymetry map of the Hopedale Basin illustrating relevant bathymetric highs and lows. Annotations are: 1 = Nain Bank, 2 = Hopedale Saddle, 3 = Makkovik Bank, 4 = Labrador Marginal Trough, 5 = Harrison Bank, 6 = Cartwright Saddle, 7 = Hamilton Bank. | 93 |
| 3.25 | Dip seismic section showing the interpreted serpentinized peridotite ridge sequence and its relation to the other horizons which have been interpreted in the study area. | 96 |

3.26	Strike seismic section showing the typical seismic characteristics of the interpreted lava flows and its relation to other seismic horizons and sequences within the study area.	98
4.1	Depth structure map of the seismic basement (K1 horizon) in the study area. Black lines represent fault planes and tick marks show direction of normal faulting.	105
4.2	Hopedale Basin tectono-stratigraphic chart. Modified after Figure 2.2 (McWhae et al., 1980, GSC). Geodynamic evolutionary stages after Enachescu (2006) and timescale from Gradstein et al. (2004).	108
4.3	Seismic section illustrating the postdrift Tertiary gravity folds present in the deep water section of the Hopedale Basin.	113
4.4	Depth section near the area of the North Bjarni F-06 well. Red = prerift basement, yellow = synrift stage sequence, green = postrift stage sequence, purple = syndrift stage sequence, blue = postdrift stage sequence, grey = exhumed mantle, black = serpentinized mantle (peridotite ridges), orange = lava flows.	115
4.5	Kinematic model of the Labrador Shelf in the region of the Hopedale Basin. In each figure red = prerift basement, yellow = synrift sedimentary sequence, green = postrift sedimentary sequence, purple = syndrift sedimentary sequence, blue = postdrift sedimentary sequence. (A) This figure represents the basin configuration at the end of rifting (total synrift deposits) at the end of the Early Cretaceous (mid to late Albian time); (B) This figure represents basin configuration at the end of the postrift (mantle exhumation) stage at the end of the Late Cretaceous (late Maastrichtian); (C) The third figure shows the basin configuration after syndrift, that is, at the end of sea floor spreading (late Eocene); (D) The last figure shows the basin configuration at present time after deposition of thick postdrift sedimentary wedges.	118
4.6	Stratigraphic chart illustrating stratigraphic units, evolutionary stages and thermal and tectonic subsidence history of the Hopedale Basin (modified after McWhae et al., 1980 and GSC, 1987 and Enachescu, 2006). Ages after Gradstein et al. (2004).	121
5.1	Depth structure map of the top of the Markland Formation (horizon T1). The map was created in UTM Zone 21, NAD 83.	129
5.2	Depth map of the top Markland Formation (T1 horizon) with an upper maturation limit of 3335.0 metres. Map shows the areas with Markland Formation below top of maturation window. The map has been generated in UTM Zone 21, NAD 83.	134

5.3	Depth map of the top Bjarni Formation (K2 horizon) with an upper maturation limit of 3335.0 metres. This map indicates a large hydrocarbon kitchen for the shales of the Bjarni Formation. The map has been generated in UTM Zone 21, NAD 83.	137
5.4	Depth structure map of the top of the Bjarni Formation (K2 horizon). The map was created in UTM Zone 21, NAD 83.	140
5.5	Depth structure map of the top Cartwright Formation (horizon T2). The map was created in UTM Zone 21, NAD 83.	142
5.6	Depth structure map of the top Kenamu Formation (horizon T3). The map was created in UTM Zone 21, NAD 83.	146
5.7	Depth structure map of the top Mokami Formation (horizon T4). The map was created in UTM Zone 21, NAD 83.	147
5.8	Dip seismic section of the North Bjarni F-06 field illustrating the anticline containing the Bjarni Formation draped over a complex faulted basement high.	149
5.9	Dip seismic section illustrating the Gudrid H-55 well location. Although difficult to image in seismic, there are remnants of Palaeozoic carbonates on top of a basement horst.	150
5.10	Dip seismic section showing rotated basement blocks with Bjarni sandstones draped over rotated basement blocks and which are sometimes fault bounded.	152
5.11	Depth structure map of the top Bjarni Formation (K2 horizon). The map was created in UTM Zone 21, NAD 83. The location of the structure seen in Figures 5.12(A) and 5.12(B) is indicated by a red circle. Other possible structural traps with Bjarni sandstone reservoir potential are indicated by yellow circles.	153
5.12A	Dip seismic section through a potential structural trap. Location of structure is shown in Figure 5.11.	155
5.12B	Strike seismic section through a potential Bjarni structural trap. Location of structure is shown in Figure 5.11.	156
6.1	Stratigraphic chart combining information determined and used in the previous sections of the study (modified after McWhae et al., 1980, GSC, 1987 and Enachescu, 2006).	162

List of Tables

1.1	List of exploration wells in the study area. Well location (NAD 83), TD and Spud Date taken from the C-NLOPB Schedule of Wells (2003).	16
3.1	List of wells in the study area. Well location (NAD 83). Status, TD and elevation information taken from the C-NLOPB Schedule of Wells (2003).	45
3.2	Wells divided into groups based on spatial distribution. See Figure 3.1 for well locations.	47
3.3	List of wells and formation tops in the study area taken from the C-NLOPB Schedule of Wells (2003). These are the picks that were loaded into the LandMark [®] software for seismic sequence interpretation purposes. Depths (metres) are below rotary table (RT).	52
5.1	Measured or projected depths to 0.7% R_o taken from the Labrador Basin Atlas (1989). It is important to note that two wells have unreliable values (Tyrk P-100 and Bjarni O-82). The asterisks (*) indicate the wells which are hydrocarbon bearing.	132

List of Appendices

Appendix A – Time-depth data for the wells within the study area collected from the C-NLOPB.

List of Abbreviations

C-NLOPB: Canada-Newfoundland and Labrador Offshore Petroleum Board
TWT: Two-way Travel Time
DTE®: Depth Team Express
GSI: Geophysical Services Incorporated
TD: Time-Depth
Tcf: Trillion cubic feet
Mmcf: Million cubic feet
AVO: Amplitude versus offset
LMR: Lambda-Mu-Rho analysis

Chapter One: Introduction

1.1 Introduction

The Hopedale Basin is located offshore Labrador between approximately 55 and 59 degrees latitude (Figure 1.1). It is separated from the neighbouring Saglek Basin in the north by the Okak Arch. The basin is characterized by a large glaciated shelf area and by a steeply dipping shelf edge with variable water depths between 100 and 3000 metres (Enachescu, 2005). The Labrador basins formed during the Mesozoic extension and opening of the Northwest Atlantic Ocean and lie just north of the Orphan Basin which is presently an active area of exploration. The Hopedale Basin is also home to 21 industry wells which were all drilled in an earlier exploration phase during the 1970's and the early 1980's.

The rifting of the Labrador Sea was the final stage of a multi-stage rifting sequence affecting the northern hemisphere. The supercontinent of Pangea rifted apart starting from the Scotian margin and rifting continued north to the Labrador Sea, a process that started 200 million years ago in the Late Triassic – Early Jurassic (Enachescu, 1987; Loudon, 2002; Enachescu and Fagan, 2005). Rifting of the Labrador Sea began in the Early Cretaceous (~125 Ma) and ended during the Albian (~85 Ma) producing both the Saglek and Hopedale basins above a complex basement system of rotated horst blocks and half grabens (Balkwill and McMillan, 1990; Enachescu, 2006a). These basins were filled first with continental sediments followed by predominantly marine deposits during the Late Cretaceous and Tertiary. Both thick source rocks and

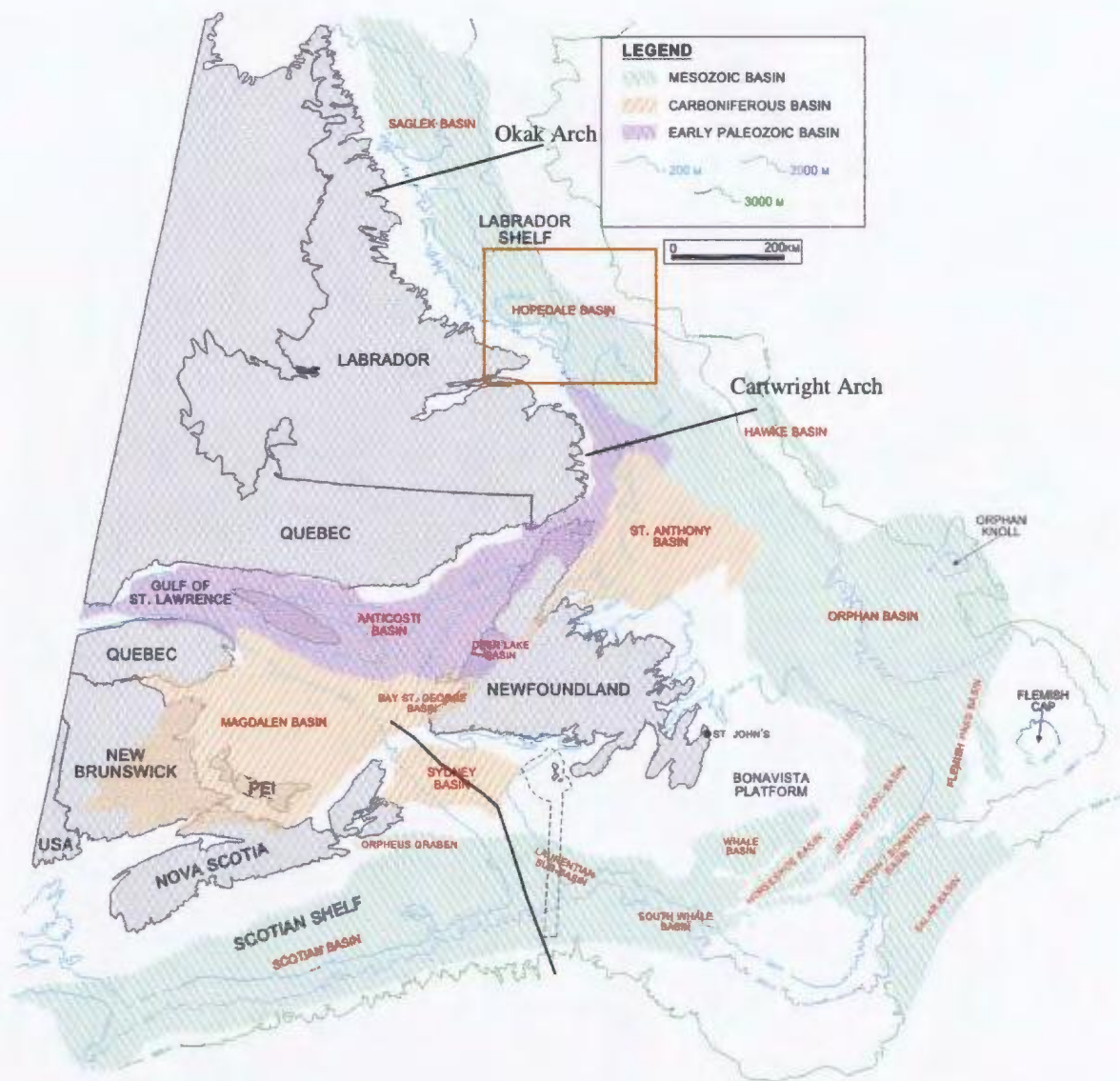


Figure 1.1 – Bathymetry and basin locations in the area of the Labrador Shelf. Approximate location of study area shown in orange. The basin is defined by the Okak Arch in the north and the Cartwright Arch in the south. Figure modified from Canada-Newfoundland and Labrador Offshore Petroleum Board (C-NLOPB) and Geological Survey of Canada (GSC). Digitized by Grant Lethbridge.

quality sandstone were deposited, thus creating an ideal environment for hydrocarbon accumulation.

The Hopedale Basin covers an area of approximately 175 000 square kilometres if its slope and deepwater extension is considered (Enachescu, 2006a). A recent seismic grid collected by Geophysical Service Incorporated (GSI) during 2003, 2004 and 2005 has produced a regional 2D seismic coverage adequately covering this vast area. These seismic speculative lines were graciously donated to Memorial University of Newfoundland. Using these data for university research allows an early public release of valuable regional tectonic, structural and seismic stratigraphic mapping which will result in added insight into the Hopedale Basin's petroleum systems.

Currently there is only minor exploration interest in the Hopedale Basin due to its remote location and its vulnerability to natural hazards including high frequency of icebergs, long lasting pack ice and variable weather (Enachescu, 2006b). These natural hazards have contributed to there being no exploration drilling or landsales in over 25 years. Hopefully increasing demand for gas, high commodity prices and new drilling and production technologies will encourage companies to develop the existing discoveries and explore for new ones.

1.2 Background and Previous Work

Exploration began off the coast of Labrador in the early 1960's with geophysical surveys including refraction and reflection seismology and potential field surveys. In 1966 and 1967 Tenneco completed two aeromagnetic surveys flying over both the eastern

Newfoundland shelf and the Labrador shelf. Several other companies (Geoterrex, EastCan Group and Petro Canada) did their own aeromagnetic surveys in 1974, 1976 and 1980 respectively. Gravity surveys were completed by EastCan (1973) and ESSO Resources (1974) (GSC Atlantic BASIN Website, 2006). Several papers including Laughton (1971), Vogt and Avery (1974), and Srivastava (1978) discussed the results of the aeromagnetic surveys and demonstrated how this ocean basin was formed by continental rifting and sea floor spreading.

Between 1965 and 1969 the Atlantic Geoscience Centre of the Geological Survey of Canada (GSC) led a seismic survey across the Labrador continental margin. All of these surveys indicated that above the plunging Paleozoic and Precambrian basement there is a wedge of sediments thickening away from the shoreline. Several papers were published discussing this sedimentary wedge and the results of exploration drilling in the area including works by Mayhew et al. (1970), Cutt and Laving (1977), Umpleby (1979), Rashid et al. (1980), and McWhae et al. (1980). After studying refraction lines Mayhew et al. (1970) proposed that the sediments were more than 7 kilometres thick with basin infill being confirmed through reflection seismic. These seismic data provided the basis for a paper by Grant (1972) which first described the morphology of the Labrador Shelf.

After the GSC Atlantic Geoscience Centre's early investigation into the geology and geophysics of Labrador and the southern Baffin Island, attention shifted to this area's petroleum potential. This resulted in the awarding of the first petroleum exploration licences in 1966. The first well, Leif E-38, was spudded soon after in 1971. Numerous other wells followed throughout the 1970's including Bjarni H-81 in 1974, Herjolf M-92

in 1976, Hopedale E-33 in 1978 and Tyrk P-100 in 1979. During this time several papers surfaced discussing the general geology of the Labrador Basin including several by Grant (1972, 1975, and 1980) as well as by Srivastava (1978), Keen (1979), Royden and Keen (1980), Srivastava et al. (1981) and McMillan (1982).

Although not the intended target, major gas discoveries were made during the search for oil reservoirs during the 1970's. The first significant discovery well was Bjarni H-81 which was drilled in 1973 by EastCan et al. Drill stem tests were conducted and the well produced 365 287 m³/day (12.9 mmcf/day) (C-NLOPB, 2003A). Several other gas wells followed and there were four significant discoveries in the Hopedale Basin (including Bjarni H-81, Figure 1.2) and one in the Saglek Basin. Unfortunately, due to the poor market for natural gas, lack of infrastructure and the numerous hazards associated with drilling offshore Labrador, each of the wells was abandoned and significant discovery licences were issued in perpetuity to the respective operators. Figure 1.2 illustrates the locations of all the wells relevant to this study as well as the boundaries of these significant discovery licences.

After the 1970s exploration drilling and seismic interpretation, the stratigraphic nomenclature of the Labrador Shelf sequence was developed within the EastCan Group and defined in a key paper by Umpleby (1979). Following Umpleby, McWhae et al. (1980) redefined these sequences into the accepted lithostratigraphic chart published in numerous other documents including the GSC Labrador Atlas (Bell et al., 1989). McWhae et al.'s (1980) revisions evolved from exploration progress on the Labrador

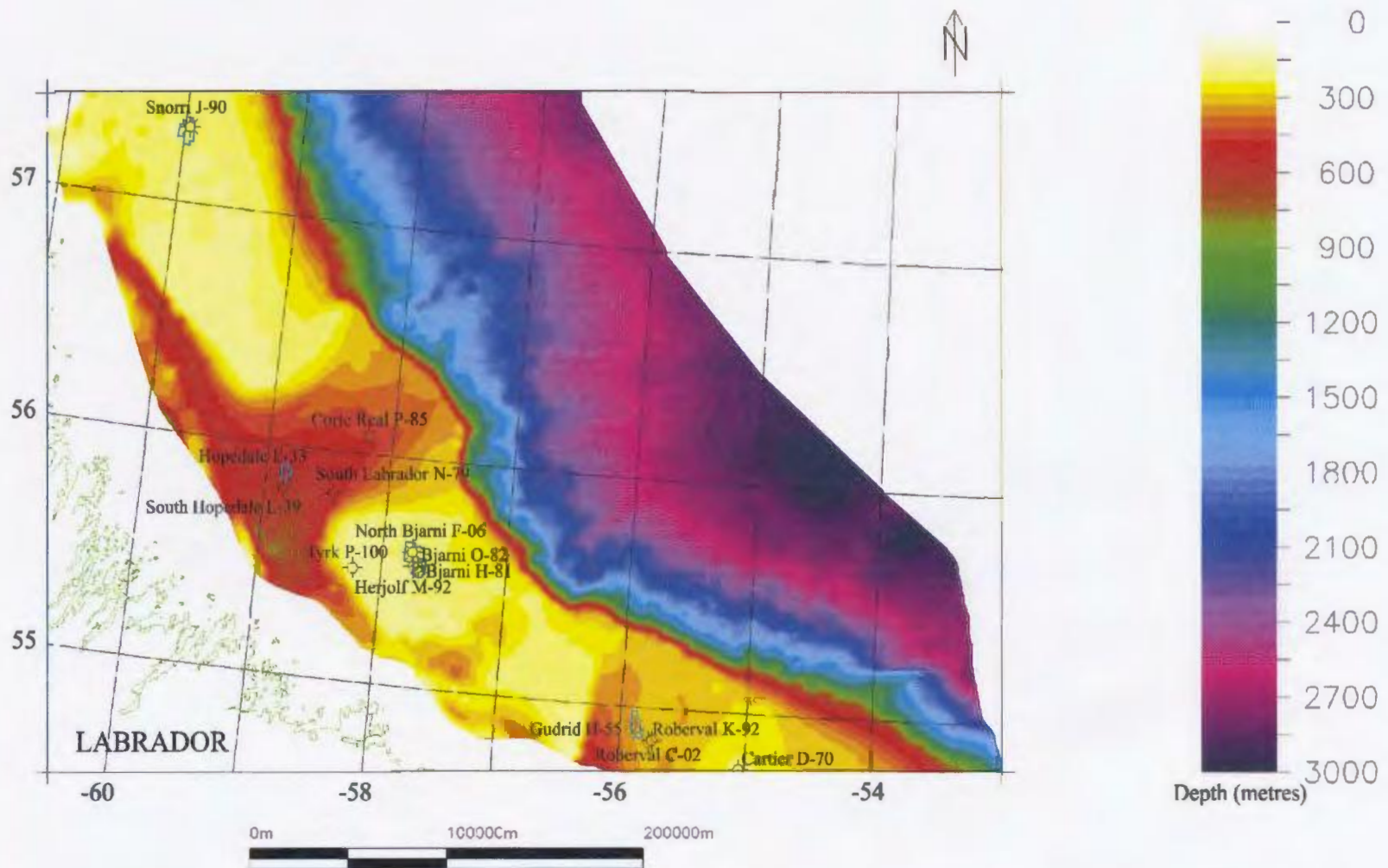


Figure 1.2 – Bathymetric map showing the locations of wells in the Hopedale Basin as well as their current status, and significant discovery licences (shown in blue).

Shelf. The basis of Cretaceous-Cenozoic lithostratigraphic divisions for Umpleby was on well data which included logs, cores and cuttings. With the help of reflection seismic data McWhae et al. (1980) added certain key lithostratigraphic units including the Mokami Formation, the Kenamu Formation and one of the potential source rocks for the area, the Markland Formation. McWhae et al. (1980) also revisited the age of the existing units and produced the lithostratigraphic chart illustrated in Figure 1.3. They also noted and described key unconformities present on the Labrador shelf such as the Labrador, Bylot and Avalon Unconformities (McWhae et al., 1980). For comparison, the lithostratigraphic chart introduced by Umpleby (1979) is included in Figure 1.3.

In 1979 Taylor, Weitmiller, and Judge (1979) first introduced the idea of possible gas hydrate on the Labrador Shelf. Their predictions were based on numerous assumptions and were not confirmed at that time. It was not until 2001 that Majorowicz and Osadetz (2001) using more recent geoscience data estimated between $1.9 \times 10^{13} \text{ m}^3$ and $7.8 \times 10^{13} \text{ m}^3$ of gas hydrates off the coast of Newfoundland and Labrador thereby accounting for up to 43% of Canadian hydrates (Majorowicz and Osadetz, 2001). It was determined that the average thickness of the gas hydrates present is 79 metres and were most often detected in the Saglek and Mokami formations (Majorowicz and Osadetz, 2003). While constituting a possible future resource, the offshore gas hydrate is not presently accessible and it is viewed as a drilling hazard by the petroleum industry rather than an energy source.

During the 1980's, there was very little exploration in the Hopedale Basin and as a result there were few studies published during this time. In 1989 the Geological Survey

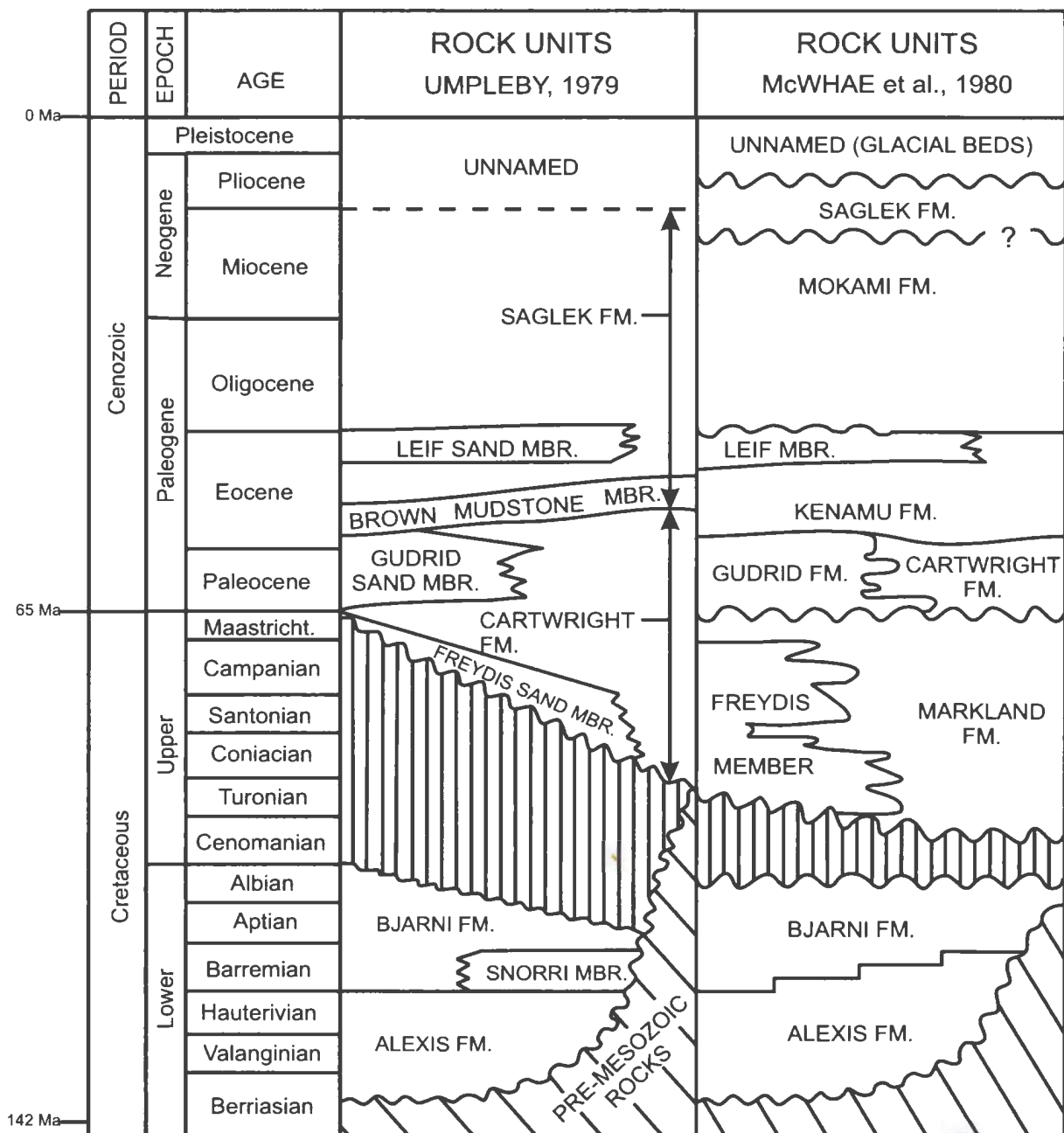


Figure 1.3 – Lithostratigraphy chart illustrating the major additional sequences and unconformities added to the Labrador Shelf geology by McWhae et al. (1980) in contrast to Umpleby (1979). Ages from Gradstein et al. (2004). Modified from McWhae et al. (1980).

of Canada added the Labrador Sea to its East Coast Basin Atlas Series (Bell et al. 1989). This monumental atlas contains a compilation of reports and data from industry and government which includes biostratigraphy, lithostratigraphy, structural and geophysical maps and short articles among others. In 1990 the Geological Survey of Canada published *Geology of the Continental Margin of Eastern Canada* in which a chapter is dedicated to the geology of the Labrador shelf, Baffin Bay and Davis Strait regions (Balkwill and McMillan, 1990).

In recent years, Hall et al. (2002) researched and published on the Lithoprobe Eastern Canadian Onshore-Offshore Transect (ECSOOT). ECSOOT was a major project which integrates onshore data, well data, normal incidence reflection seismic, wide-angle refraction seismic and gravity and magnetic data in an attempt to understand the continental crust's evolution in the northeastern Canadian Shield (Labrador and northeast Quebec).

Shillington et al. (2004) contributed greatly to the understanding of transitional crust along the margin of Newfoundland and Labrador through the SCREECH (Studies of Continental Rifting and Extension on the Eastern Canadian Shelf) program. The multi-channel reflection seismic collected as part of the SCREECH program was collected in the area of the ODP sites 1276 and 1277 located in deepwater south of the Flemish Cap (Arnaboldi et al., 2004). This program identified three zones within the crust (moving seaward): 1. extended continental crust; 2. featureless basement and 3. high relief basement in the form of margin-parallel ridges (Shillington et al., 2004).

These findings may help to understand transitional crust in other areas of eastern Canada such as the Labrador Shelf region.

During the exploration phases of the 1960s and 1970s there were numerous reflection seismic surveys completed. After 1982 however there was a 20 year break in seismic acquisition offshore Labrador which ended in 2002. More recently there have been several surveys completed by GSI from 2003 to 2006 of which data from the 2003, 2004 and some lines from 2005 surveys are used in this thesis. Currently there are no active exploration licences in the Hopedale or Saglek basins but a large landsale is planned for summer of 2008.

1.3 Purpose

Gas discoveries off the coast of Labrador were unexpected discoveries during the hunt for oil reservoirs. Due to the price of natural gas at that time these discoveries were considered a commercial failure although the estimated reserves exceeded those of the White Rose or Sable Island fields (Enachescu, 2005). This, along with the unpredictable metocean conditions, led to a 25-year drought in drilling and seismic exploration. Today, with the continuous rise in natural gas prices and the growing demand for cleaner resources, the reserves on the Labrador shelf are becoming more significant to the international oil and gas industry and to the energy sector of the Province of Newfoundland and Labrador.

Not only has the Labrador shelf been neglected by industry but also by academia in comparison to other potential petroleum areas offshore Newfoundland and Labrador. The purpose of this study is to gain an understanding of the regional geology of the area

and its tectonic history by completing structural mapping, seismic stratigraphic characterization, commenting on the area's future potential and finally building a kinematic model for the Hopedale Basin. By building a kinematic model, a lithospheric stretching model will be presented along with relevant arguments and examples to support the model. This will help understand the depositional environment present on the Labrador Shelf in the area of the Hopedale Basin.

1.4 Research Objectives

The main objectives of this study are to:

- a.) create a generalized velocity model of the Labrador shelf using time-depth data available for the wells within the study area. This velocity function can then be used to convert seismic targets from time to depth in this study as well as in future research;
- b.) complete a seismic structural and stratigraphic study of the area concentrating on the Cretaceous and Cenozoic successions of the Hopedale Basin. This study will include defining seismic sequences including the basement and correlating them throughout the area of interest as well as tying the seismic markers to available well information. The seismic markers will be extended as far as possible on the slope and rise depending on the quality of data;
- c.) develop a concept of how the Hopedale Basin and Labrador margin formed based on newer seismic data and compare this concept with older ideas. This involves regional and detailed mapping of the structural and tectonic features and related seismic-stratigraphic sequences and associating them to various stages of margin evolution;

d.) identify the main rift features such as basin-bounding faults, major extensional faults or transform faults thereby identifying possible transtensional movements;

e.) characterize the seismic stratigraphic units and suggest a kinematic model for the Hopedale Basin;

f.) use depth structure maps of the Bjarni Formation in conjunction with maturation data from available geochemical studies to locate areas of potential hydrocarbon generation; and

g.) identify and illustrate hydrocarbon play types.

1.5 Data

GSI provided Memorial University of Newfoundland with over 22 000 kilometres of 2D seismic data in the Labrador shelf area, approximately 9 700 kilometres of which are included in this thesis. This study area includes fifty-four 96 fold 2D lines of which 39 are dip lines and 15 are strike lines. The spacing of the dip lines and strike lines are 5 and 20 kilometres respectively. Data coverage in the area can be seen in Figure 1.4. These data are of 2003, 2004 and 2005 vintage.

The data were received post-processing in SEG-Y format together with positioning data. During acquisition 6-8 kilometre long streamers were used and data were recorded to 12 000 milliseconds (minimum). The data were migrated using a Kirchhoff pre-stack time migration algorithm. The data were loaded into Landmark® workstations and interpreted using the Landmark 2D SeisWorks® interpretation package.

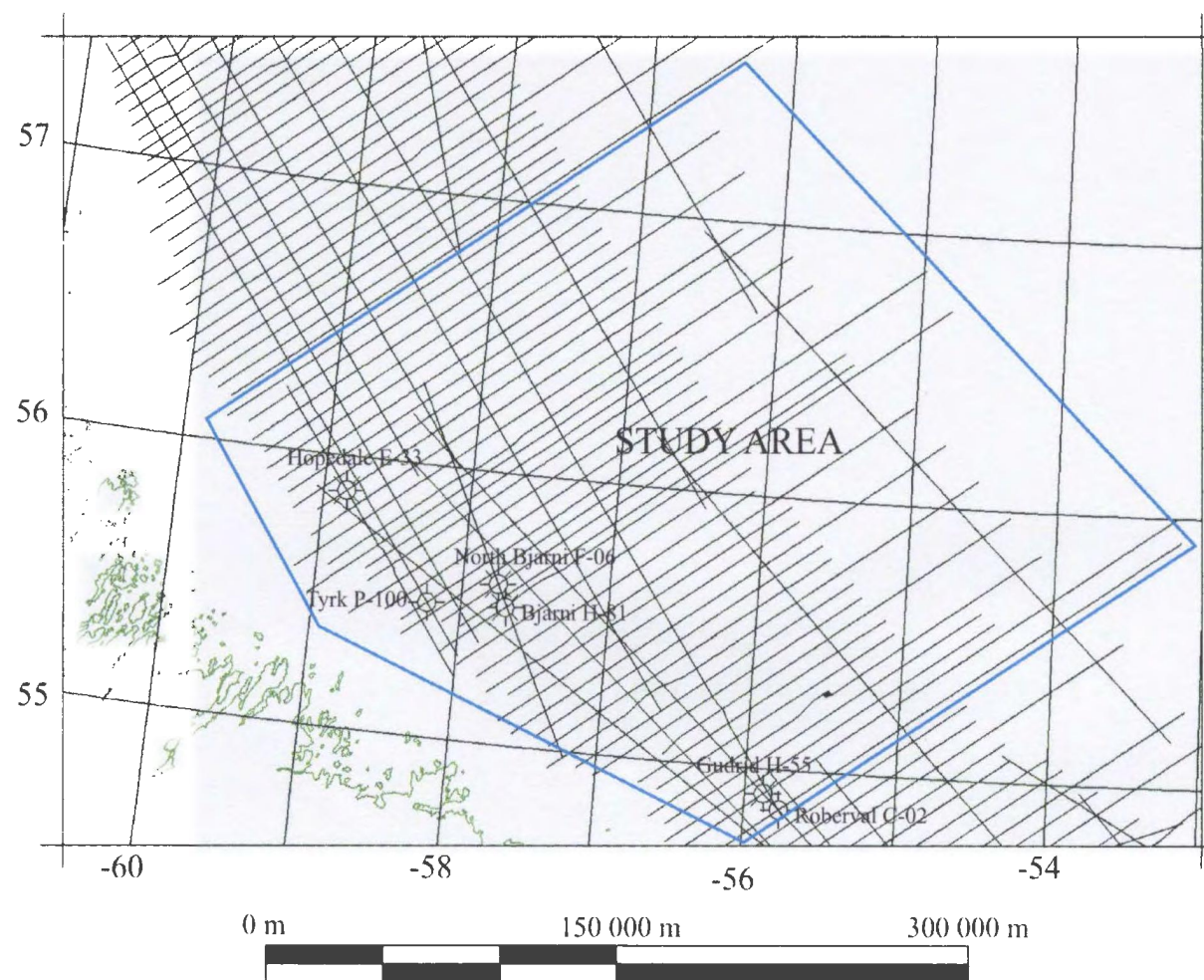


Figure 1.4 – Base map of the Labrador shelf showing the recent GSI seismic coverage along the shelf and the study area shown in blue. These data are of 2003, 2004 and 2005 vintage.

The data quality varies from excellent on the shallow shelf to satisfactory everywhere else on the shelf and deep water, and to poor below the shelf break and upper slope. These differences in data quality are due to the steep slopes present at the shelf edge that generate interfering multiples. An example of the seismic data quality can be seen in Figure 1.5.

Well data for 12 wells (Table 1.1) in the area were collected from the Canada-Newfoundland and Labrador Offshore Petroleum Board (C-NLOPB). In particular, the check-shot surveys including the time-depth tables were collected and loaded into the OpenWorks® database. Also, the C-NLOPB formation picks were loaded to aid in the seismic interpretation.

The interpretation of the 2D seismic data and mapping was done in the time domain. To convert these time horizons to depth the Depth Team Express® and TDQ® software were used. These programs specifically convert horizon reflection times to depth by applying a velocity model generated from existing time-depth data. A further discussion of the time-depth conversion will be presented in Chapter 4. Also, isochron and isopach maps were generated using SeisWorks®. Besides seismic and velocity data, this study used well logs, stratigraphic information and published interpretations of the logs. Cores and cuttings were inspected for certain wells and in certain intervals that were available at the C-NLOPB core laboratory to relate seismic character to rock formations. Although this research does not include the detailed study or logging of the cores, the main formations were observed, their physical properties were related to seismic sequences and cores were photographed to aid in the interpretation of the data.

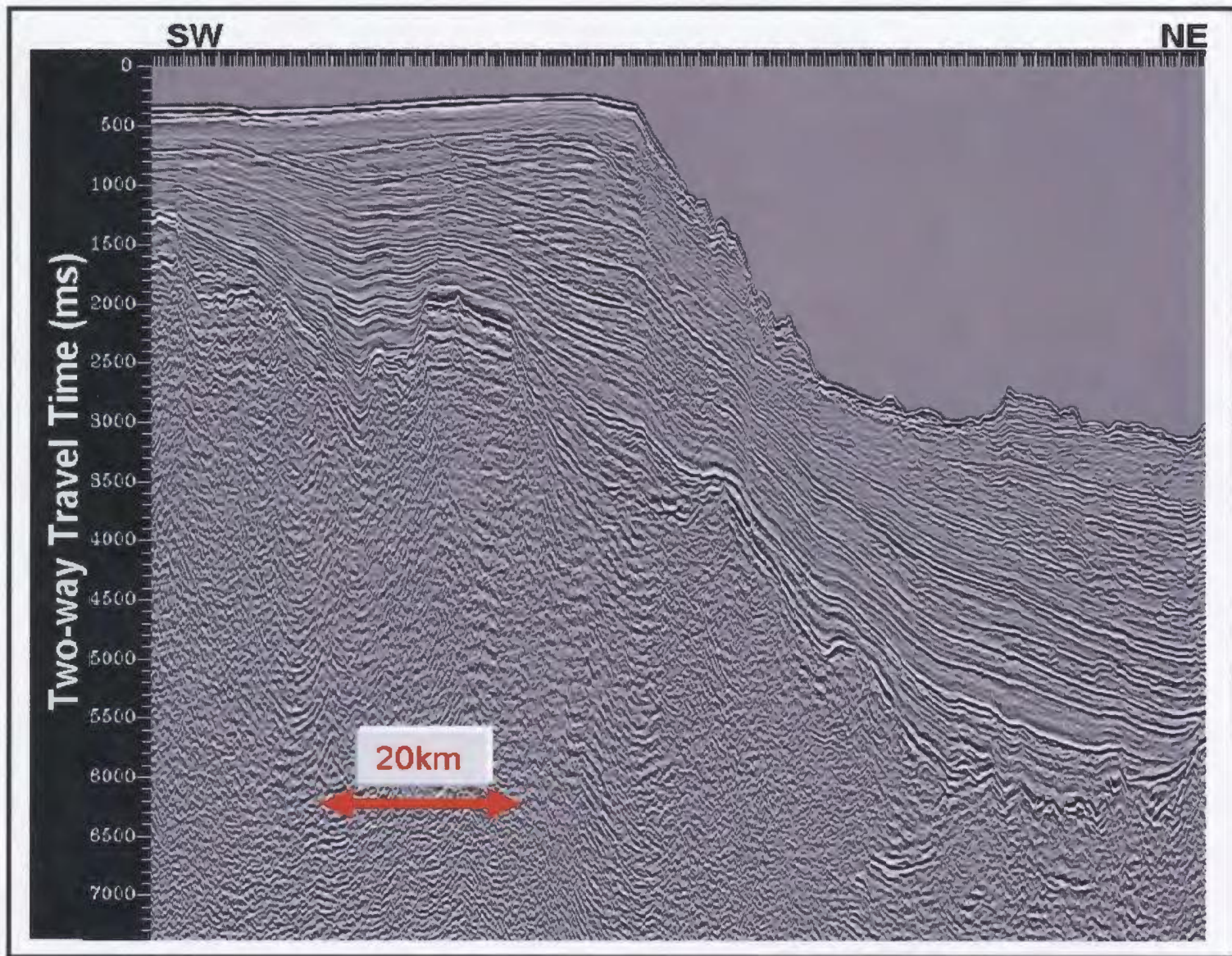


Figure 1.5 – Example of the GSI data set (dip line). The vertical scale is two-way travel time in milliseconds.

Well Name	Latitude	Longitude	Total Depth	Spud Date
Bjarni H-81	55°30'29.58"N	57°42'01.82"W	2514.6 m	1973-08-29
Bjarni O-82	55°31'48.45"N	57°42'30.99"W	2650.0 m	1979-07-30
Corte Real P-85	56°04'49.14"N	58°12'05.46"W	4395.0 m	1981-10-05
Gudrid H-55	54°54'30.19"N	55°52'28.47"W	2838.0 m	1974-07-14
Herjolf M-92	55°31'53.53"N	57°44'48.82"W	4086.2 m	1976-08-31
Hopedale E-33	55°52'24.62"N	58°50'48.78"W	2069.4 m	1978-08-09
North Bjarni F-06	55°35'29.57"N	57°45'45.68"W	2812.0 m	1980-09-28
Roberval C-02	54°51'08.06"N	55°46'00.76"W	2823.0 m	1980-07-07
Roberval K-92	54°51'35.69"N	55°44'32.01"W	3874.0 m	1978-10-02
South Hopedale L-39	55°48'32.85"N	58°50'45.01"W	2364.0 m	1983-07-13
South Labrador N-79	55°48'45.49"N	58°26'29.12"W	3571.0 m	1980-08-03
Tyrk P-100	55°29'49.87"N	58°13'47.05"W	1739.0 m	1979-07-19

Table 1.1 – List of exploration wells in the study area. Well location (NAD 83), TD and Spud Date taken from the C-NLOPB Schedule of Wells (2003).

Chapter Two: Labrador Shelf Geography and Geology

2.1 Geography

The Labrador shelf is divided by the Okak Arch into two large basins, the Saglek Basin and Hopedale Basin (Figure 1.1). The Hopedale Basin is the more southerly basin and extends from the Cartwright Transfer Fault Zone (CTFZ) in the south to the Okak Arch in the North; a distance of approximately 500 kilometres (55° to 59° North) (Enachescu, 2006a; Martin et al., 2006). It is part of a large, oval, tectonic depression having an area of about 175 000 km² with an uneven basement floor consisting of stretched continental crust, exhumed continental mantle (transitional crust) and subsided oceanic crust which serves as part of the connection between the Atlantic and Arctic ocean basins (Balkwill and McMillan, 1990; Enachescu et al., 2005; Enachescu, 2006a; Martin et al., 2006).

The Labrador shelf has prominent attributes consistent with that of Atlantic-type passive margins as described by Bally (1981): the continental shelf is flat compared with the steeply dipping continental slope and the area of the shelf closest to land is made up of a large sedimentary prism on top of extended cratonic crust whereas the outer portion of the shelf prism lies on early Tertiary and Cretaceous peridotites and basalts (Balkwill and McMillan, 1990; Enachescu, 2006a).

Water depths along the Labrador shelf vary substantially from a mere 100 metres on the shelf to nearly 3000 metres on the lower slope. The average declivity of the slope is 3.0°; ranging from 2.5-3.5° (calculated from bathymetry, see Figure 1.2).

The shelf lies to the north of the Newfoundland's Grand Banks and Orphan Basin and has certain geologic affiliation with them but is more critically linked to the geology of the Baffin Bay and Davis Strait to the north and the west Greenland shelf to the east.

2.2 Regional Geology – Labrador Margin

The separation between North America and Europe occurred in the Early Cretaceous localized between Iberia and the Grand Banks followed by the separation of Greenland from Labrador in the Late Cretaceous (Keen, 1982; Enachescu, 1987; Tankard and Welsink, 1989). Unfortunately there is still much confusion regarding the spreading history of the Labrador margin, the extent of exhumed mantle and occurrence of true oceanic crust.

There are three different theories regarding what underlies the continental slope and rise of the Labrador Sea. First, a model exists which explains the presence of small magnetic anomalies along the margins as anomalies brought on by extremely slow seafloor spreading which accounts for the symmetry between the magnetic anomaly trends in reference to mid-ocean ridge axis (Srivastava & Roest, 1999). Srivastava and Roest (1999) also determined that basement topography (from a rough basement to a smooth basement) corresponds with the spreading rate (slow to fast respectively) which may have been a result of a volcanic plume to the west of Greenland. They also believe that oceanic crust extends from Labrador's continental slope to the west Greenland slope. Figure 2.1 shows a figure from Srivastava and Roest (1999) which illustrates the



Figure 2.1 – Figure from Srivastava and Roest (1999) illustrating the observed and calculated (modelled) anomalies through the Labrador margin. The numbers along the top represent anomaly numbers.

modelling of the observed magnetic anomaly with the position of the ridge axis during various times on one of the seismic profiles.

Second theory suggests that basic dyke injections have occurred through stretched continental crust (Chalmers, 1991; Chalmers & Laursen, 1995). These intrusions of igneous material occurred along cracks and faults as seen across passive continental margins which had been subjected to large extensions during rifting creating rotated blocks. Their model was based on their inability to model magnetic anomalies beyond anomaly 27 using purely a seafloor spreading model. Schematic diagrams from Chalmers (1991) and Chalmers and Laursen (1995) illustrating their modelling are seen in Figure 2.2. Also shown in these figures is a display of their models on two seismic lines compared with the models proposed by Roest and Srivastava (1989). From these diagrams it appears that a continental crust model (Chalmers, 1991 and Chalmers & Laursen, 1995) explains the observed magnetic field better than the oceanic crust model proposed by Roest and Srivastava (1989). Chalmers (1991) and Chalmers and Laursen (1995) both illustrate that the models proposed by Roest and Srivastava (1989) seem to be plausible up to and including anomaly 27 but continue to show that models which include a continent-ocean transition zone and larger areas of continental crust appear to fit the observed data better. A variation of this model comes from Chian & Loudon, 1994 and Chian et al., 1995 in that a partly serpentinized mantle (with seismic velocity of 7.4-7.7 km/s) lies beneath the foundered continental crust (Figure 2.3) which has a low velocity of only 4-5 km/s (Osler and Loudon, 1992 and 1995).

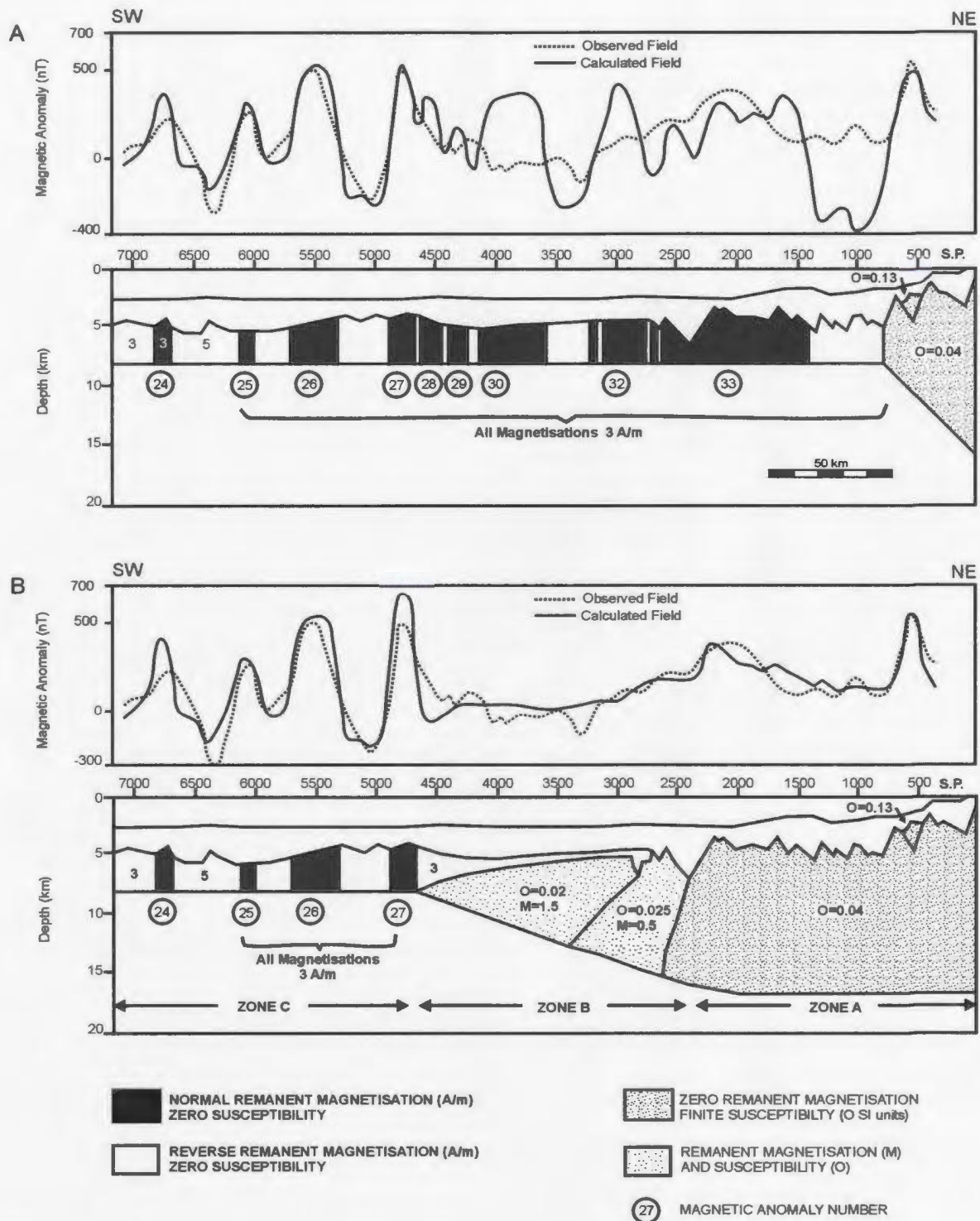


Figure 2.2 – Figure modified after Chalmers and Laursen (1995). This figure demonstrates the observed and calculated magnetic fields when considering continental crust rather than oceanic crust east of anomaly 27.

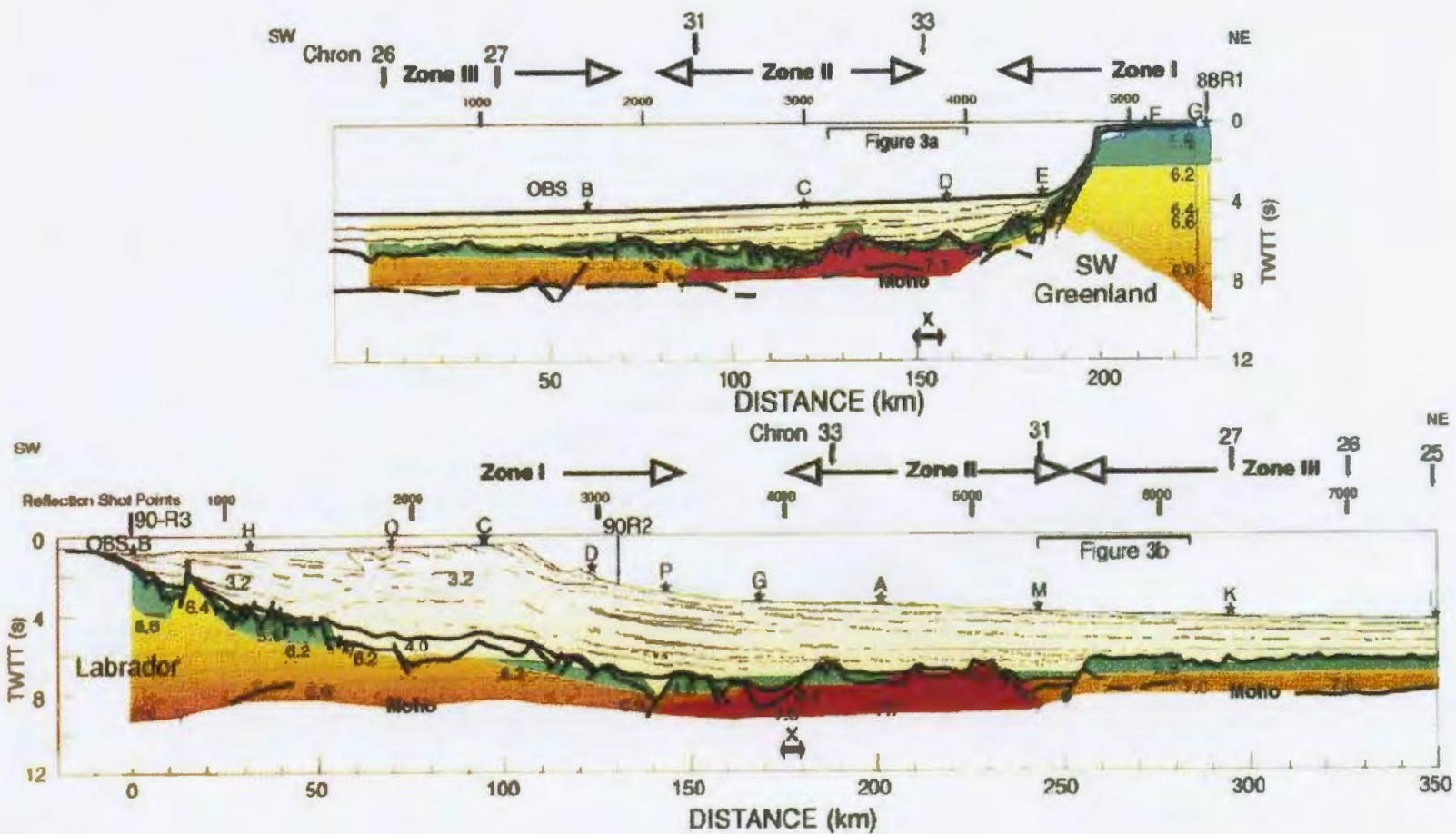


Figure 2.3 – Figure from Chian et al. (1995). This figure illustrates the multichannel reflection seismic with velocity values shown as well as colours illustrating the velocity structure.

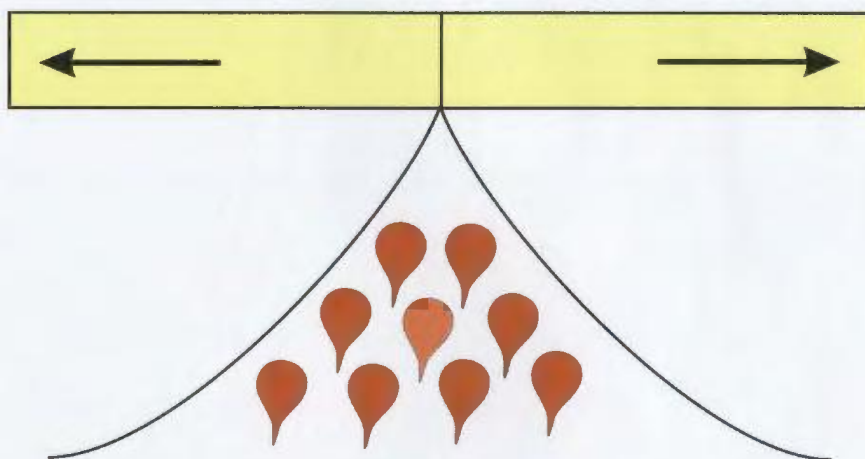
Finally several parties with extensive data and expertise joined together to combine research efforts and suggest an explanation for the Labrador Sea formation (Louden et al., 1996). Louden et al. (1996) used two independent data sets to discuss crustal thinning and spreading rates along the Labrador margin. The first data set was initially analyzed by Osler and Louden (1992, 1995) and consisted of a wide-angle refraction profile situated perpendicular to the strike of the proposed extinct oceanic rift axis. The other set of seismic data was a multi-channel reflection profile which cut through the same rift segment as the refraction profile.

Louden et al. (1996) believe that the crustal thinning of the extinct rift is due to a “complex discontinuous process” which is not represented by the steady-state viscous flow models presented in the past. They postulate that at full spreading rates (>20 km/my rate of melt supply) keeps pace with the spreading therefore causing a uniform thickness between old and new crust. When spreading rates are slower (<20 km/my) the rate of extension exceeds the rate of melt supply given that the melt pulses do not keep pace with spreading. The crust then undergoes tectonic thinning and widening due to the inconsistent pulse rate and plate separation rate. These conclusions are based on one seismic reflection and refraction line thus it is difficult to apply this model to the entire region of the Labrador Shelf. A schematic diagram presented by Louden et al. (1996) can be seen in Figure 2.4.

Although each theory has much evidence supporting it, it is hard to ignore the difficulty of interpreting the low amplitudes of the magnetic anomalies on the

(A) $V > 20 \text{ km/m.y.}$

Rate of Extension = Rate of melt supply



(B) $V < 20 \text{ km/m.y.}$

Rate of Extension > Rate of melt supply

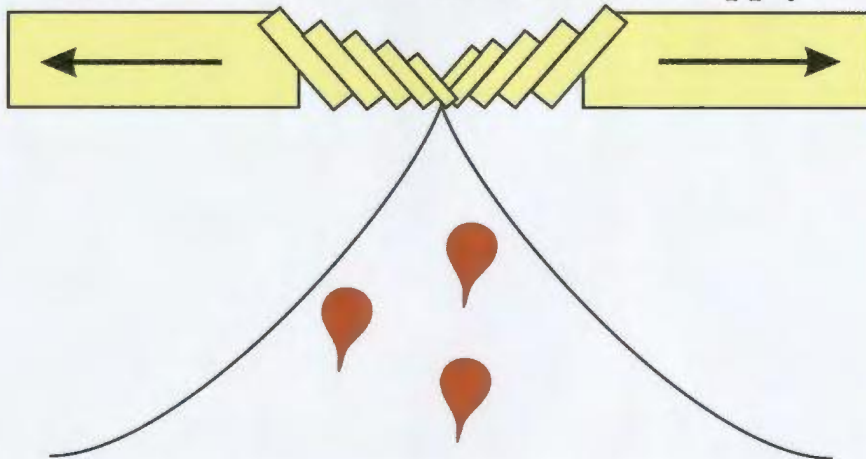


Figure 2.4 – Crustal thinning of the extinct Labrador rift as suggested by Loudon et al., 1996. (A) Continental crust thickness (yellow) is uniform because the rate of plate separation is equal to the rate of melt supply; (B) Rate of extension exceeds the rate of melt supply thereby thinning the crust. Modified after Loudon et al. (1996).

Labrador margin; therefore, with the lack of clear supporting geophysical evidence or drilling, the true nature of the Labrador Sea floor in the deep water area remains unknown.

2.3 Basin Development and Stratigraphy

Plate reconstructions suggest that the separation of North America from Eurasia began sometime before 160 Ma with North America separating from Africa to form the present day Scotian margin. Separation continued to form the Southern Newfoundland margin before 125 Ma (Early Cretaceous – Barremian) as North America parted from Iberia. Prior to 120 Ma North America separated from Ireland thus forming the Northern Newfoundland margin. Finally, the Labrador margin was formed after the separation of North America from Greenland over 70 Ma ago (Late Cretaceous) followed by the separation of Greenland from Europe sometime before 55 Ma (Eocene) (Louden, 2002).

Balkwill and McMillan (1990) and Balkwill (1987) suggest that rifting and break-up of the Greenland/Labrador margins began during the Berriasian and ended during the Albion. Synrift deposition began with the Alexis Formation during late Berriasian (Figure 2.5). Originally named after the Alexis Bay on the southern Labrador coast, Umpleby (1979) established this name in published literature.

The Alexis Formation consists of Early Cretaceous basalts (mid Berriasian) as well as products of their continental erosion and deposition. The Alexis Formation lies below other Cretaceous sediments (McWhae and Michel, 1975, Figure 2.5). These are considered the oldest known Mesozoic rocks on the Labrador shelf. Below the Alexis

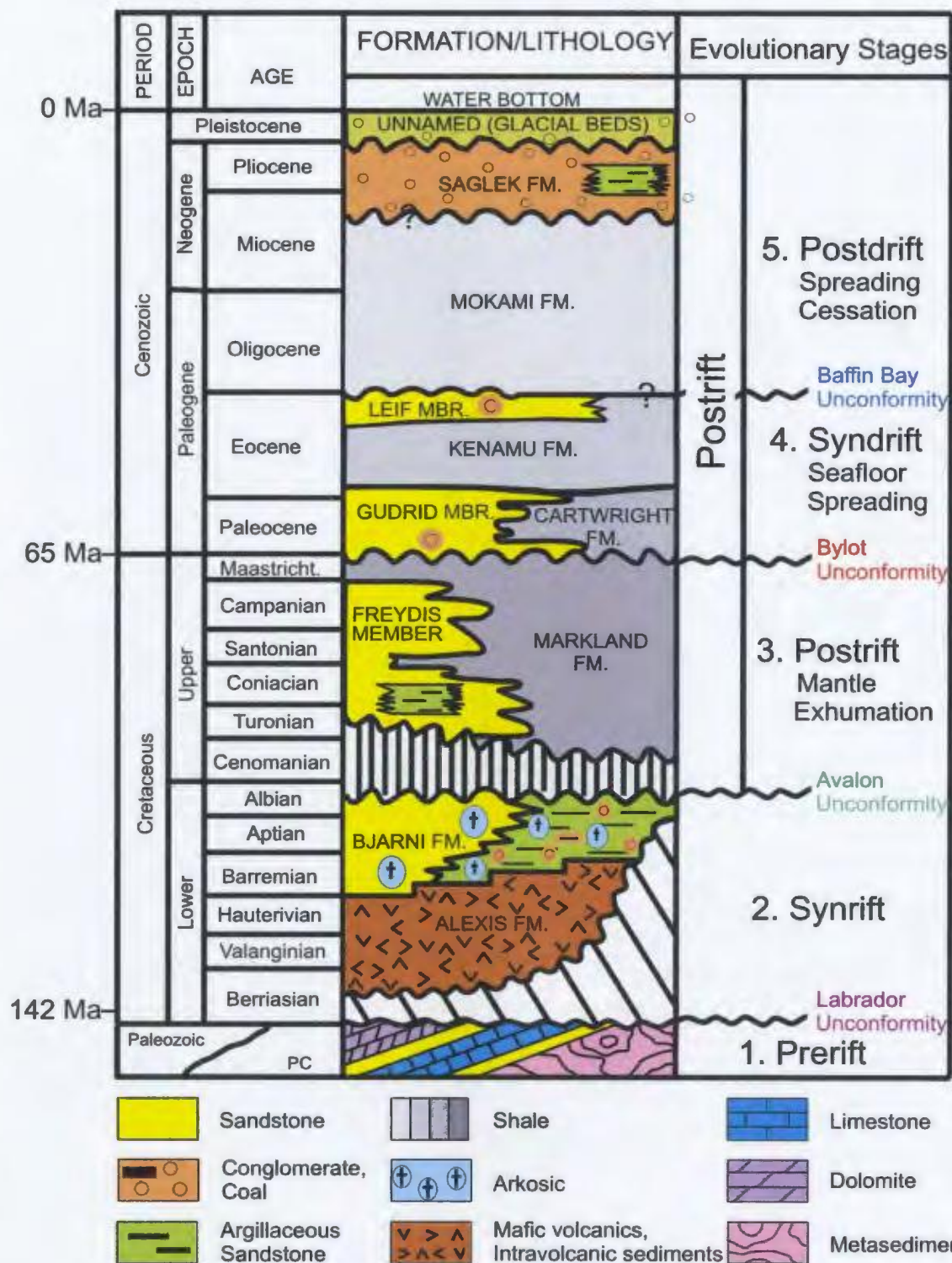


Figure 2.5 – Generalized lithostratigraphic chart of the Labrador shelf (modified from the GSC and McWhae et al., 1980). Ages after Gradstein et al. (2004).

Formation lies the Precambrian basement except in areas where lower Palaeozoic carbonates and clastics were preserved. The Alexis Formation's onshore equivalent may be the Ford's Bight volcanics which are similar in age to the Alexis (King and McMillan, 1975; Wanless et al., 1974). McWhae et al. (1980) describe the lithology of the Alexis Formation as volcanic rocks with lavas and dikes with an approximate thickness of 300 metres. According to Umpleby (1979) there may have been extensive hydrothermal alteration or weathering of these basalts which give the Alexis Formation a variation in appearance as seen in Figure 2.6.

During the Early Cretaceous (Berriasian to Cenomanian) the cratonic crust was laterally stretching which created large horst and graben structures (Balkwill and McMillan, 1990). These grabens were filled with immature lithic arenites rich in feldspar and quartz which were likely derived from local highs (Figure 2.7). According to Balkwill and McMillan (1990) and Umpleby (1979) the clastic sediments were predominantly nonmarine and were partially derived from the erosion of the underlying Alexis Formation. These sediments constitute the hydrocarbon bearing Bjarni Formation which overlies the Alexis Formation and extends beyond the shelf and into the slope. The name Bjarni was formalized by Umpleby (1979) and was used to describe an interval in the Herjolf M-92 well but was informally used in 1975 by McWhae and Michel (1975). According to Barss et al. (1979) these coarse arkosic sands range in age from Barremian to early Cenomanian and Albian (Figure 2.5).

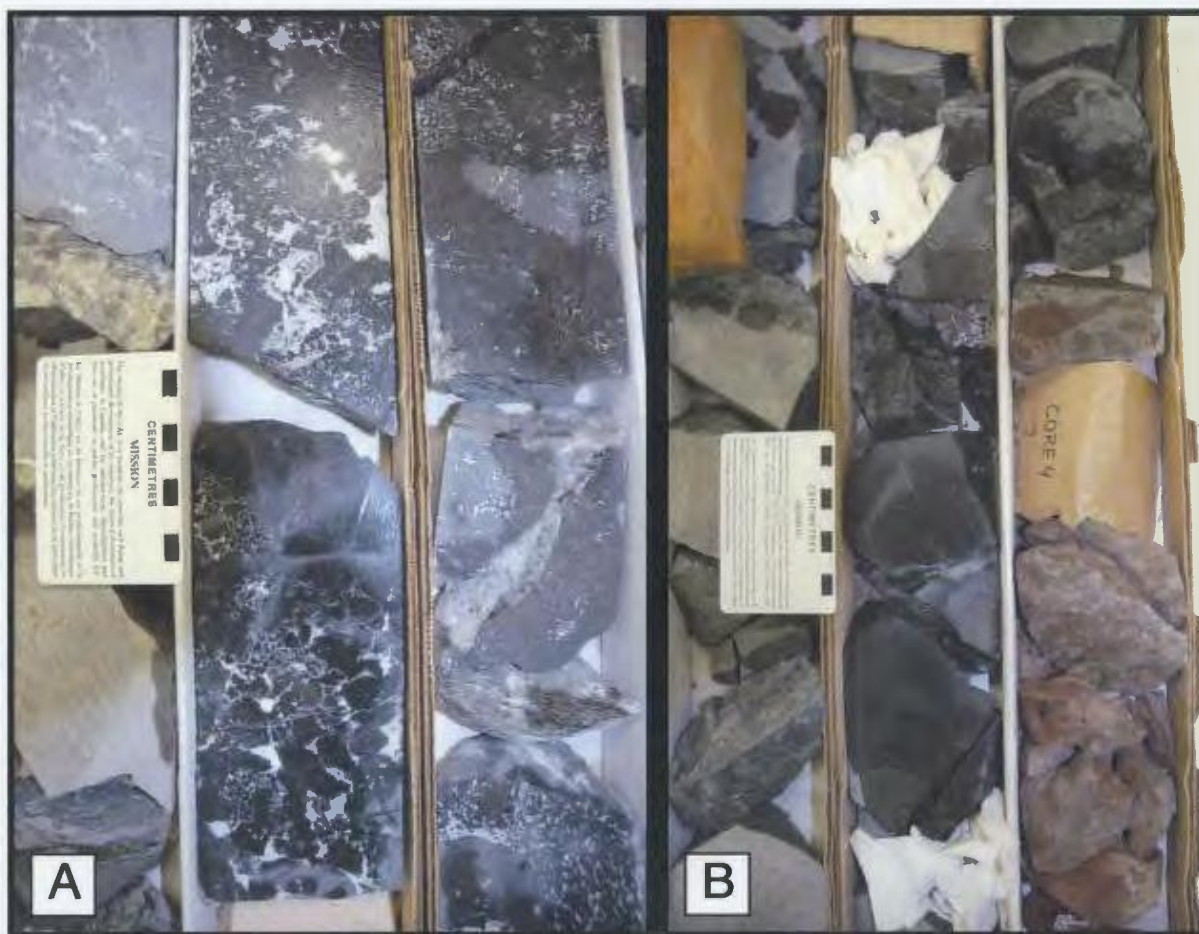


Figure 2.6 – Pictures of Alexis Basalt. Notice the variation in colour due to possible hydrothermal alteration (A) and weathering (B) as described by Umpleby (1979). Picture A shows Core #4 (boxes 5 & 6 of 7). Picture B shows Core #4 (box 1 of 7). Both pictures are taken from the Roberval K-92 well (~3420 metres depth). Core available from C-NLOPB.

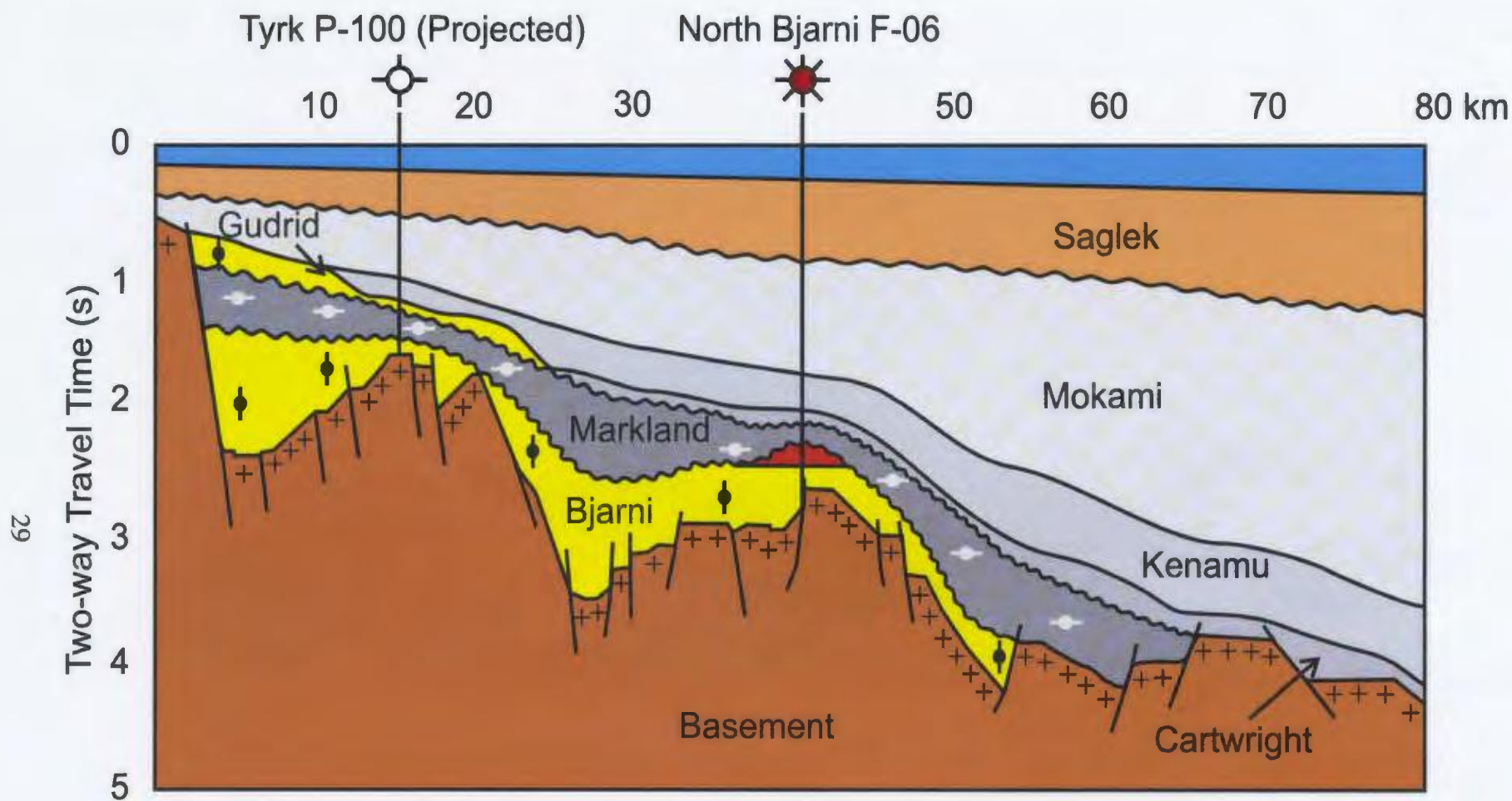


Figure 2.7 – Schematic cross-section through the North Bjarni Field which illustrates typical nearshore structural and tectonic features of the Canadian Labrador margin. Different colours represent different lithostratigraphic units. Shales are shown in shades of grey, sands are shown in yellow and conglomerates are shown in orange. Red indicates the North Bjarni gas-filled reservoir (modified after GSC and Government of NF and Labrador, Department of Mines and Energy). Note that recent papers and presentations suggests that Bjarni Formation extends into the outer shelf and deep water regions (Enachescu, 2006; Enachescu et al., 2006 and Martin et al., 2006).

The lithology of the Bjarni Formation varies significantly; coarse sandstone, fine sandstone, conglomerate, carbonaceous shale and thin coal seams occur. Core photos of the Bjarni Formation from two of the Labrador shelf wells can be seen in Figure 2.8. The Bjarni Formation is separated from the overlying Markland Formation by the Avalon Unconformity, marking the end of intra-continental extension, which produces the strong seismic marker used to distinguish the top of the formation on seismic reflection data. The Bjarni Formation locally lies on the Alexis Formation or directly on Paleozoic and Precambrian rocks. The top basement unconformity or the Labrador Unconformity is defined as the pre-rift unconformity in the Labrador basins (McWhae et al., 1980).

Regionally, the Bjarni Formation is somehow discontinuous and predominately fills in the lows caused by rotated horst blocks in the form of grabens and half-grabens. Some of the ridges are distinct but still preserve a significant thickness of Bjarni Formation (100 – 800 metres), including excellent reservoirs.

By Albian time, the Hopedale Basin had been firmly established as a shallow marine environment. From Cenomanian (98.9 ma) to Coniacian (85.8 Ma) the middle and outer Labrador shelves were practically sediment starved except for small amounts of clastic sediments which accumulated mostly nearshore and formed the Freydis Member of the Markland Formation (Balkwill, 1987; Balkwill and McMillian, 1990). The Markland Formation was named by McWhae et al. (1980) after Markland, the Norse name for Labrador. This formation had not been geologically separated from the Cartwright Formation by Umpleby (1979). This Cartwright marine shelf shale is



Figure 2.8 – Picture (A) shows sandstones from the Bjarni formation from the Roberval K-92 well (Core #2 Box 2 of 5) and picture (~ 3050 metres depth) (B) shows sandstone from the North Bjarni F-06 well (Core #1, Box 1 of 1; ~ 2455 metres depth). Cores are available from C-NLOPB.

widespread throughout the basin and has been dated to be between Cenomanian and Maastrichtian in age (McWhae et al., 1980; Chalmers and Pulvertaft, 2001). This shale is described as a green to dark grey shale. The formation lithology can vary between shale, silty shale, and some siltstone and sandstone with a rare occurrence of brown dolomitic limestone beds (Figure 2.9).

McWhae et al. (1980) believe that the Avalon Unconformity separates the Markland shales from the Bjarni sandstones (Figure 2.5). The Markland Formation is unconformably overlain by the Cartwright Formation in mid to distal parts of the shelf and, on occasion, can be unconformably overlain by the Kenamu Formation (Balkwill and McMillan, 1990).

The Markland Formation was most likely deposited in a shallow marine shelf environment as determined from the presence of dinoflagellates and foraminifera as well as the downlapping of reflections seen in the seismic data (McWhae et al., 1980; Balkwill and McMillan, 1990). After rifting occurred, first mantle exhumation and then sea-floor spreading began in the south at approximately 70-80 Ma (Campanian) and continued northward until approximately 35 Ma (Late Eocene) (Srivastava, 1978, Roest and Srivastava, 1989). During this phase there was shallowing of the shelf and coastal erosion. Seaward progradation of sands and shales commenced and deposition of the Gudrid, Cartwright and Kenamu formations began (Balkwill and McMillan, 1990). Umpleby (1979) originally classified the Gudrid as a member. The following year McWhae et al. (1980) redefined this unit as a formation. In more recent literature, Balkwill (1987) and Balkwill and McMillan (1990), revert back to the Gudrid Member



Figure 2.9 – A typical core section of the Markland shales from the Roberval K-92 well showing Core #1 (Box 1 of 2, ~ 3015 metres depth). Cores are available from C-NLOPB.

but further subdivide it into the upper, middle and lower Gudrid Members. For the purpose of this thesis, these three units will be referred to as the Gudrid Member. The Gudrid Member is composed of quartzose and feldspathic sandstones. They are typically poorly sorted with varying cements. In some areas, remnants of coal clasts are present. This formation is dated between early Paleocene to early Eocene and is confined by the Bylot Unconformity at the base and the conformable contact with the Kenamu Formation at the top. The sands of the Gudrid Member were likely deposited as a turbidite deep sea fan with subsequent feeder channels on the continental slope and rise (McWhae et al., 1980).

The Cartwright Formation was first used in published literature by Umpleby (1979) but later revised by McWhae et al. (1980). Umpleby used the term Cartwright Formation to describe the present day Markland Shale. According to McWhae et al. (1980) the Cartwright Formation consists of brown-grey claystone, silty claystone and siltstone (Figure 2.10). It is believed to be mid-Paleocene to Early Eocene in age (Umpleby, 1979) (Figure 2.5). At its base is the Bylot Unconformity underlain by the shales of the Markland Formation. This unconformity creates a very prominent marker in seismic sections. The depositional environment is possibly that of an outer shelf or slope sequence with turbidite sands according to Balkwill and McMillian (1990) whereas Umpleby (1979) had originally believed that these sandstones were continental.

The Kenamu Formation is named after the Kenamu River in Labrador. It was first introduced by McWhae et al. (1980) and was implemented to divide Umpleby's thick original concept for the Saglek Formation (Figure 1.3). This formation is yet



Figure 2.10 – A typical core section of the Cartwright Formation taken from the Snorri J-90 well (Core #1, ~ 2000 metres depth). Core are available from the C-NLOPB.

another massive shale, brown-grey in colour, with siltstone and fine sandstone interbedded as well as fine marine silty-shales. The age of this unit is often debated but Gradstein and Williams (1981) placed the top of the Kenamu Formation near the Eocene-Oligocene boundary (Figure 2.5). The top of the unit is defined by the Baffin Bay disconformity which separates the formation from the overlying Mokami Formation. The base of the unit is a conformable contact between the Kenamu Formation and the underlying Gudrid and Cartwright Formations. These contacts create distinct seismic markers making the seismic mapping of this formation unproblematic. According to Balkwill (1987) and Balkwill and McMillian (1990), the shales of the Kenamu Formation are likely bed deposits from either a shallow shelf setting or a coastal setting. During Eocene time, the shelf had a slight seaward slope thus the upper surface of the Kenamu Formation dips seaward.

The Leif Member of the Kenamu Formation consists of fine-grained quartzose sandstone which is normally white to light grey-brown in colour and often contains glauconite and siltstone and mudstone (McWhae et al., 1980). It is a clean reservoir with porosities as high as 30%. It is similar in age to the Kenamu Formation (Late Eocene) but may be as young as earliest Oligocene. It was formed at about 38 Ma (Eocene) when the Labrador Sea ceased spreading (Gradstein and Srivastava, 1980) and is possibly a tidal deposit.

During the early Oligocene to the Pleistocene, drifting ceased and deposition of postdrift sediments commenced. At this time, massive thermal subsidence of the stretched continental blocks, the transitional crust and the oceanic basin floor occurred

along with coastal margin uplift. During this period, thick successions of clastic detritus were deposited as a result of uplift of the cratonic margin. This phase of deposition exceeded the thermal subsidence rate which caused progradation basinward creating what is presently the Labrador outer continental shelf and slope. Finer-grained material was deposited beyond the slope creating a thick succession on the basin floor (Balkwill and McMillan, 1990). These successions included the shale-dominated Mokami Formation and a sandstone-dominated Saglek Formation.

The Mokami Formation contains brown, partially consolidated neritic claystones and shales which were named after the Mokami Hill in Labrador. It is overlain unconformably by the Saglek Formation and overlies the Kenamu and Leif Formations. The age of the Mokami is somewhat unclear but publications indicate that it is late Eocene (Early Oligocene) to middle Eocene (Balkwill and McMillan, 1990). A small hiatus at the base of this formation may suggest a minor fall in sea-level at the time of deposition.

The Saglek Formation was redefined by McWhae et al. (1980). Umpleby (1979) had originally established it as a thick succession from mid-Eocene to early Pliocene. It is now used in a more restricted sense and is thought to be mid-late Miocene to Pliocene (McWhae et al., 1980). It is named after the Saglek Bay in Northern Labrador. McWhae et al. (1980) describe it as very porous conglomeratic sandstone which is poorly sorted and can range from fine to coarse-grained. It can appear white to brown to grey and can contain feldspars and cherts. At the top of the succession there is an erosional unconformity separating it from younger glacial beds (currently unnamed). The base of

the unit is another unconformity referred to as the Beaufort Unconformity. This separates the Saglek Formation from the underlying Mokami Formation. The clastic rocks of the Saglek Formation were likely deposited in a continental and lagoonal environment (Balkwill and McMillan, 1990).

To summarize, the sedimentary-tectonic stages of the Labrador Sea is as follows (modified after Chalmers and Pulvertaft, 2001):

- 1.) pre- to early synrift deposition of the Alexis Formation and Lower Bjarni Member during late Berriasian, and Valanginian to Aptian time;
- 2.) synrift deposition of the Upper Bjarni Member onto the hanging walls of the fault blocks which occurred between Aptian and Albian time;
- 3.) postrift deposition of the Markland Formation during a time of thermal subsidence which occurred between Cenomanian to mid-Campanian/Danian time;
- 4.) syndrift deposition of late Paleocene and Eocene-aged Cartwright and Kenamu formations;
- 5.) postdrift sediments of the late Paleogene/Neogene-aged Mokami and Saglek Formations.

An alternate seismic stratigraphic and tectonic chart including 1) prerift basement; 2) synrift; 3) postrift mantle exhumation; 4) syndrift ocean crust creation and 5) postdrift seismic sequences was proposed by Enachescu (2006a) and will be used in this thesis. A further discussion of this seismic stratigraphic and tectonic chart are present in Chapter 4.

2.4 Structural Styles and Elements

On a regional scale, Enachescu (2006b) proposes that the Hopedale Basin is in fact three separate subbasins each in communication with the others. The three subbasins proposed by Enachescu (2006b) are the Hamilton subbasin, Harrison subbasin and the Nain subbasin. Each of the basins contains parallel ridges as well as extended fault blocks and rotated half grabens. These structural elements are separated along strike by transfer faults (with an offset of 10-15 kilometres) and accommodation zones.

Enachescu et al. (2006) also suggest that there are changes in the landward rift system boundary all along the Labrador margin. The rift system boundary changes from a hinge zone to a basin-bounding fault along strike. They also suggest that Mesozoic sediments onlap against this hinge zone/fault bound anywhere from 80 to 100 kilometres from the modern-day shoreline. According to Enachescu et al. (2006), Tertiary beds onlap onto the pre-rift basement around 40 to 75 kilometres from the shoreline on a lineament approximately parallel to the modern coastline.

Although salt structures play a significant role in the overall structural styles of Newfoundland's Grand Banks and the Scotian shelf and slope, to date, salt has not been identified on the Labrador shelf. This means that all structural elements of the Labrador shelf and slope are created during the rifting and ocean-spreading history of the margin. According to Enachescu and Hogg (2005) and Enachescu (2006b), some of these structural features include inversion features, due to strike-slip faulting, and compressional features brought on by gravity sliding.

According to Balkwill and McMillan (1990), the basin master faults strike northwest and can be up to several kilometres long. These master faults are linked to one another through shorter transfer faults which trend orthogonally to the master faults. Although the dip of the master faults can be either seaward or landward there is nearly always a predominant dip direction thus creating the rotated horst blocks and half grabens visible in the seismic data.

Further structural elements will be discussed in later parts of the thesis as they become evident during seismic data interpretation and the regional seismic mapping.

Chapter Three: Seismic Sequence Analysis

3.1 Introduction

Seismic sequence analysis was undertaken in the study area in order to divide the seismic data into regionally mappable seismic sequences and subsequently to associate these with previously described geological formations. Only regional, prominent seismic markers which exist due to large acoustic impedance contrasts were mapped throughout the area. Geologically, these markers are formed due to a sudden variation in sediment lithology or the presence of major unconformities.

In the study area centered on the North Bjarni-Bjarni gas field, seven seismic markers were defined based on specific seismic character and regional continuity. These have been labelled horizons K1, K2, T1, T2, T3, T4 and WB where K and T represent Cretaceous and Tertiary and WB stands for water bottom. These seismic markers thus define 6 major seismic sequences (S): S1, S2, S3, S4, S5, and S6. After picking the seismic markers on representative seismic sections that contain significant exploration wells, these horizons were tied to geological formation tops identified in the well bores using local time-depth conversion curves.

Each of the regional horizons, and thus each of these depositional sequences, was interpreted using the SeisWorks[®] program in Landmark[®] workstation and initially mapped in two-way travel time (ms). After structural time mapping the resulting seismic maps were converted to depth using the TDQ[®] program in Landmark[®] in conjunction with the well information and time-depth information previously obtained from the

C-NLOPB well reports and loaded into the workstation. A further explanation of depth conversion will be described in Chapter 4.

This chapter contains a detailed account of the seven mapped seismic sequence boundaries and six seismic sequences, accompanied with representative workstation illustrations to document the seismic stratigraphy of the area. First, I will introduce all pertinent well data used in the study including general well information, time-depth data and geological top picks.

3.2 Well Control

There is very little well control in most regions offshore Atlantic Canada. The study area contains only 11 wells with another one (Cartier D-70) lying just south of the study area (Figure 3.1). These exploration wells are unevenly distributed in the area. As a consequence, there are huge breaks in well control making correlation of events from line to line difficult in places. This is especially true in the outer shelf, slope and deep water where no wells were yet drilled.

During past exploration drilling in the Hopedale Basin, geophysical well logs were collected; unfortunately they were not available publicly in digital format and all attempts to obtain them from various sources failed. The cost of obtaining digital data or of digitizing paper logs was prohibitive to us and thus made it impossible to import sonic and density logs into the system and generate synthetic seismograms. Likewise there is no digital access to other logs such as gamma ray logs or porosity logs. Certain well

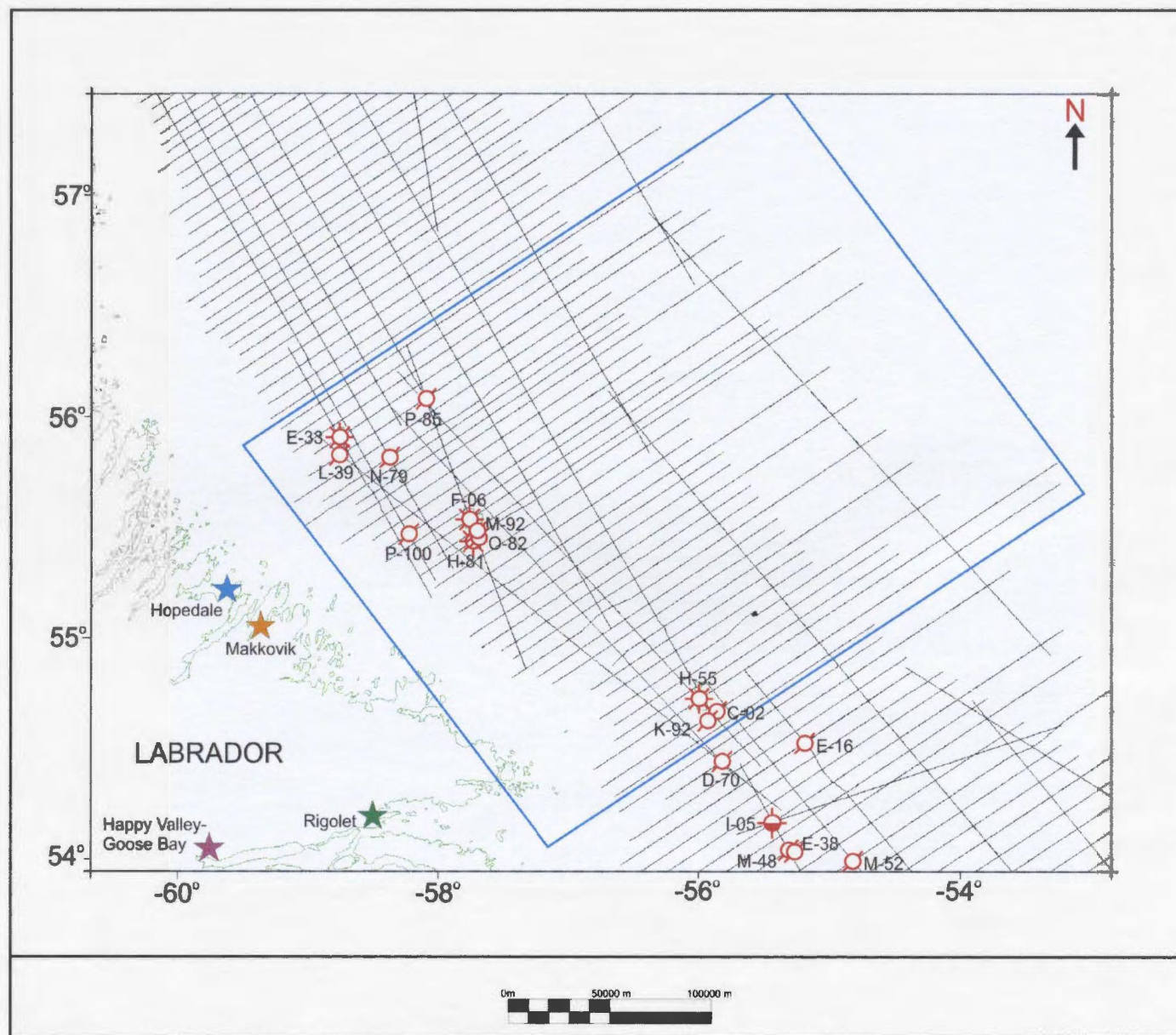


Figure 3.1 –Seismic base map showing current well location and status and the study area (shown in blue rectangle). Coordinates in NAD83.

reports available to us from C-NLOPB had synthetic seismograms and hard copies of well logs. Well logs and log correlation to older seismic data are contained in the Labrador Basin Atlas (Bell et al., 1989). This information was used for visual inspection and correlation to the new GSI seismic lines available for this study (Figure 3.1).

There is also general well information available which includes total depth, elevation datum, time-depth data and formation picks from the C-NLOPB (Schedule of Wells, 2003) and from the GSC Atlantic BASIN website (2006). By accessing these data it was feasible to project the well trajectory and formation picks into the workstation database thereby allowing the seismic data to be adequately correlated to the wells. More information regarding general well information, time-depth pairs and well picks are outlined in the following sections.

3.2.1 General Well Information

In order for the SeisWorks[®] program to properly display the well trajectory the following information was required and had to be loaded into the well header: well location, total depth, and elevation datum. The well information contained in Table 3.1 was taken from the C-NLOPB Schedule of Wells (2003) and was loaded into the project database.

3.2.2 Time-Depth Information

Time-depth values were available for 10 wells located within the study area (Well files, C-NLOPB). From South to North these wells are: Roberval C-02, Roberval K-92,

Well Name	Latitude	Longitude	Status	TD (m)	Elev. (m)
Bjarni H-81	55°30'29.58"N	57°42'01.82"W	Abandoned Gas	2514.6	13.0
Bjarni O-82	55°31'48.45"N	57°42'30.99"W	Abandoned Gas	2650.0	12.3
Corte Real P-85	56°04'49.14"N	58°12'05.46"W	Abandoned	4395.0	13.4
Gudrid H-55	54°54'30.19"N	55°52'28.47"W	Abandoned Gas	2838.0	12.3
Herjolf M-92	55°31'53.53"N	57°44'48.82"W	Abandoned	4086.2	26.8
Hopedale E-33	55°52'24.62"N	58°50'48.78"W	Abandoned Gas	2069.4	12.8
N. Bjarni F-06	55°35'29.57"N	57°45'45.68"W	Abandoned Gas	2812.0	12.0
Roberval C-02	54°51'08.06"N	55°46'00.76"W	Abandoned	2823.0	13.7
Roberval K-92	54°51'35.69"N	55°44'32.01"W	Abandoned	3874.0	13.0
S. Hopedale L-39	55°48'32.85"N	58°50'45.01"W	Abandoned	2364.0	11.6
S. Labrador N-79	55°48'45.49"N	58°26'29.12"W	Abandoned	3571.0	11.3
Tyrk P-100	55°29'49.87"N	58°13'47.05"W	Abandoned	1739.0	11.8

Table 3.1 – List of wells in the study area. Well location (NAD 83). Status, TD and elevation information taken from the C-NLOPB Schedule of Wells (2003).

Gudrid H-55, Bjarni H-81, Bjarni O-82, Herjolf M-92, North Bjarni F-06, Tyrk P-100, South Hopedale L-39, and Hopedale E-33. There was no reliable time-depth information collected for South Labrador N-79. The time-depth data for each of the wells are included in Appendix A.

The wells are located in three distinct areas: one in the north of the study area, one in the south of the study area and one located in between (Figure 3.1). These clusters of wells will be designated Group A (North), Group B, and Group C (South). The wells included in each of these groups are listed in Table 3.2. The time-depth data for each group were plotted using Microsoft Excel and regression functions were fitted to each of these data sets. Figure 3.2 is a time-depth plot for the wells in Group A, Figure 3.3 is for wells in Group B and Figure 3.4 is for wells in Group C. These curves give equations for the time-depth data which can be used to interpolate between the data points and to obtain deeper depth conversions. It also shows the R^2 value of the curve. A perfect correlation would have an R^2 value of 1.0 therefore these curves match the well data with accuracies of approximately 98%. These graphs are visual representations of the data listed in Appendix A. Another program (Depth Team Express) will be used to apply the velocities to the seismic horizons.

3.2.3 Well Picks and Seismic Markers

Several formation pick sets exist for Labrador wells put forward by various groups and individual researchers. For consistency, well picks provided by the C-NLOPB in the Schedule of Wells (2003) were used to correlate seismic events with

Group A	Group B	Group C
Hopedale E-33	North Bjarni F-06	Gudrid H-55
South Hopedale L-39	Tyrk P-100	Roberval K-92
Corte Real P-85	Herjolf M-92	Roberval C-02
	Bjarni O-82	
	Bjarni H-81	
Table 3.2 – Wells divided into groups based on spatial distribution. See Figure 3.1 for well locations.		

Time-Depth Curves for Group A wells

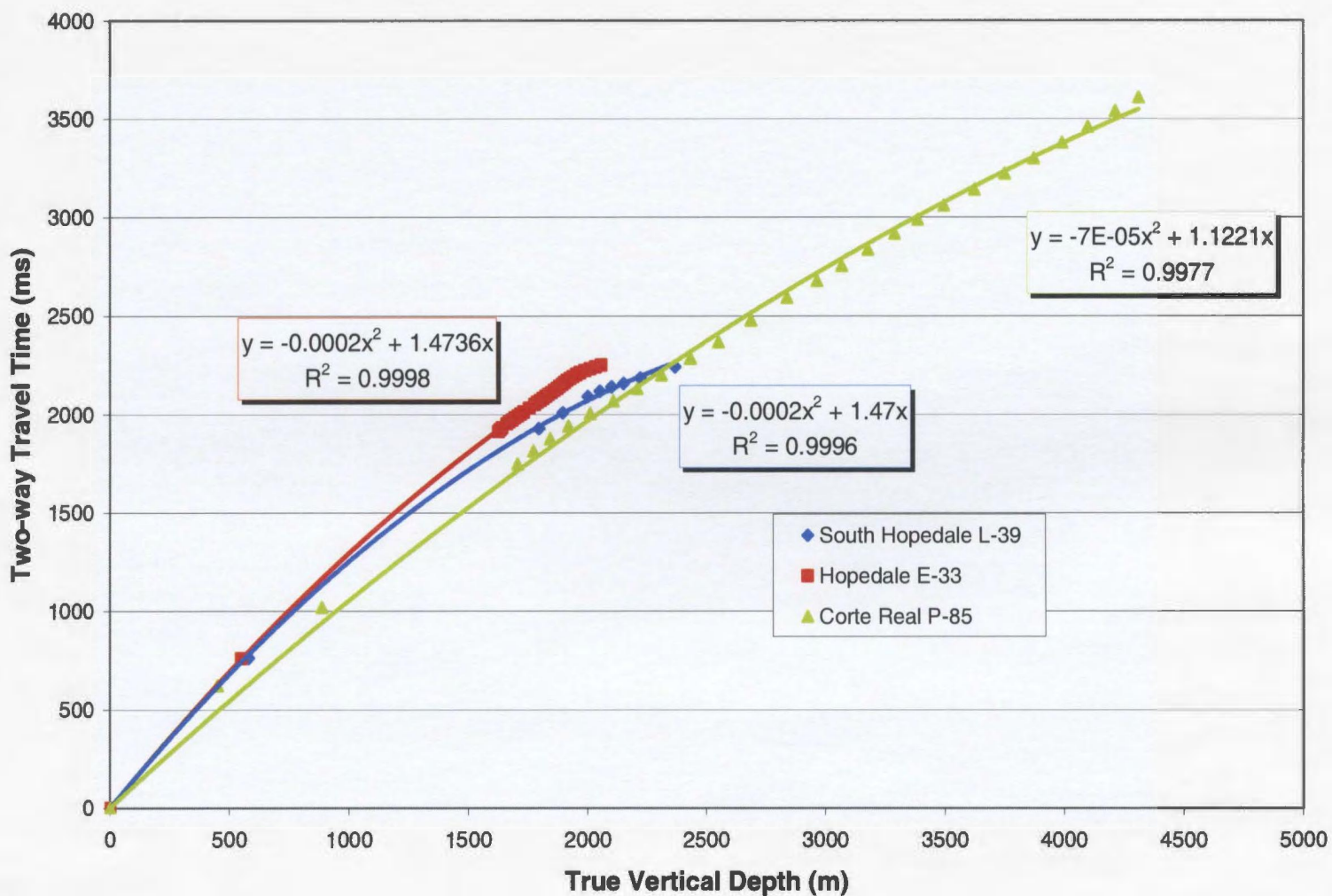


Figure 3.2 – Time-depth curves for wells in Group A and their respective time-depth functions. Created from data taken from well files in the C-NLOPB archive.

Time-Depth Curves for Group B wells

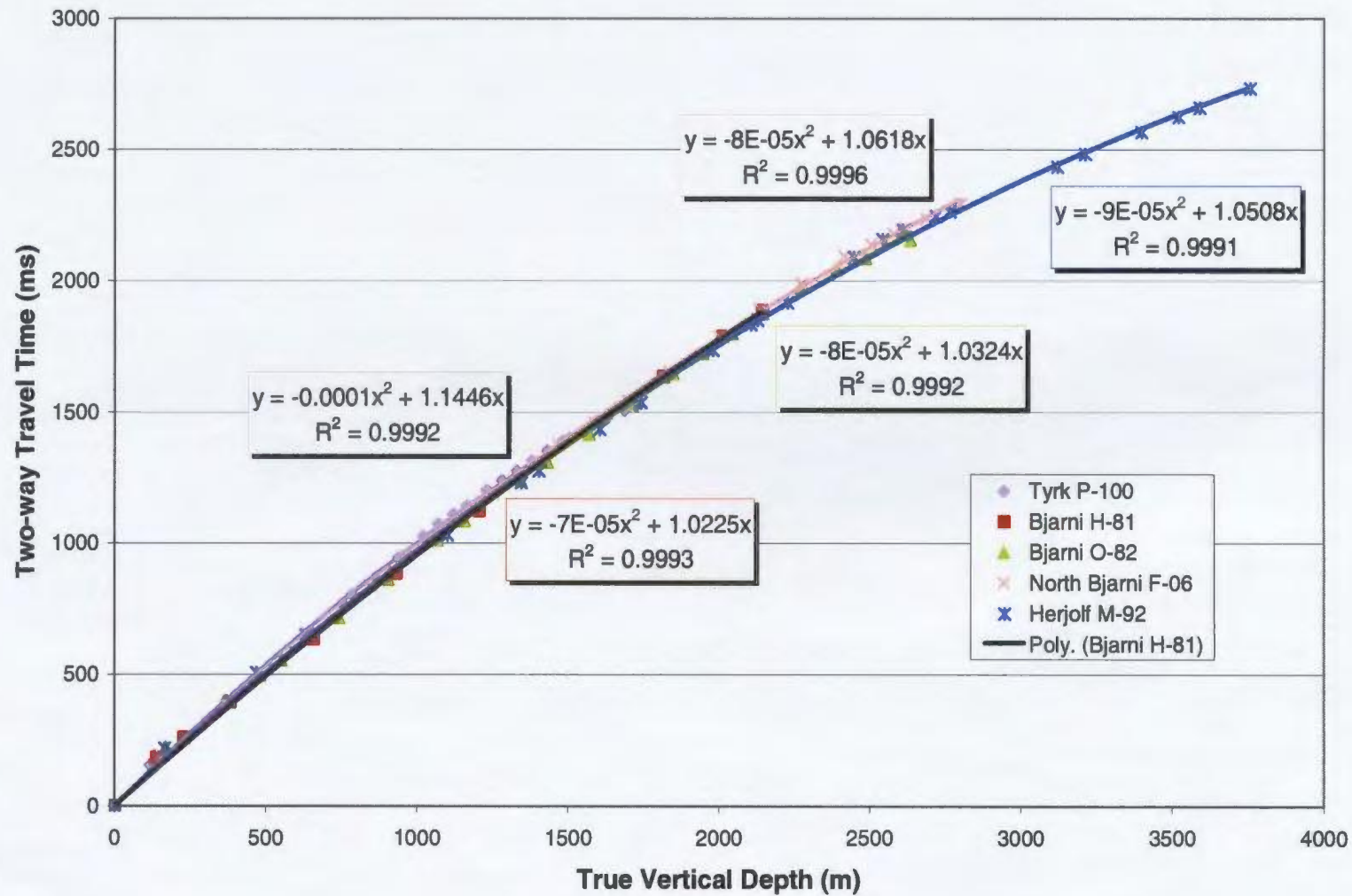


Figure 3.3 – Time-depth curves for wells in Group B and their respective time-depth functions.
Created from data taken from well files in the C-NLOPB archive.

Time-Depth Curves for Group C wells

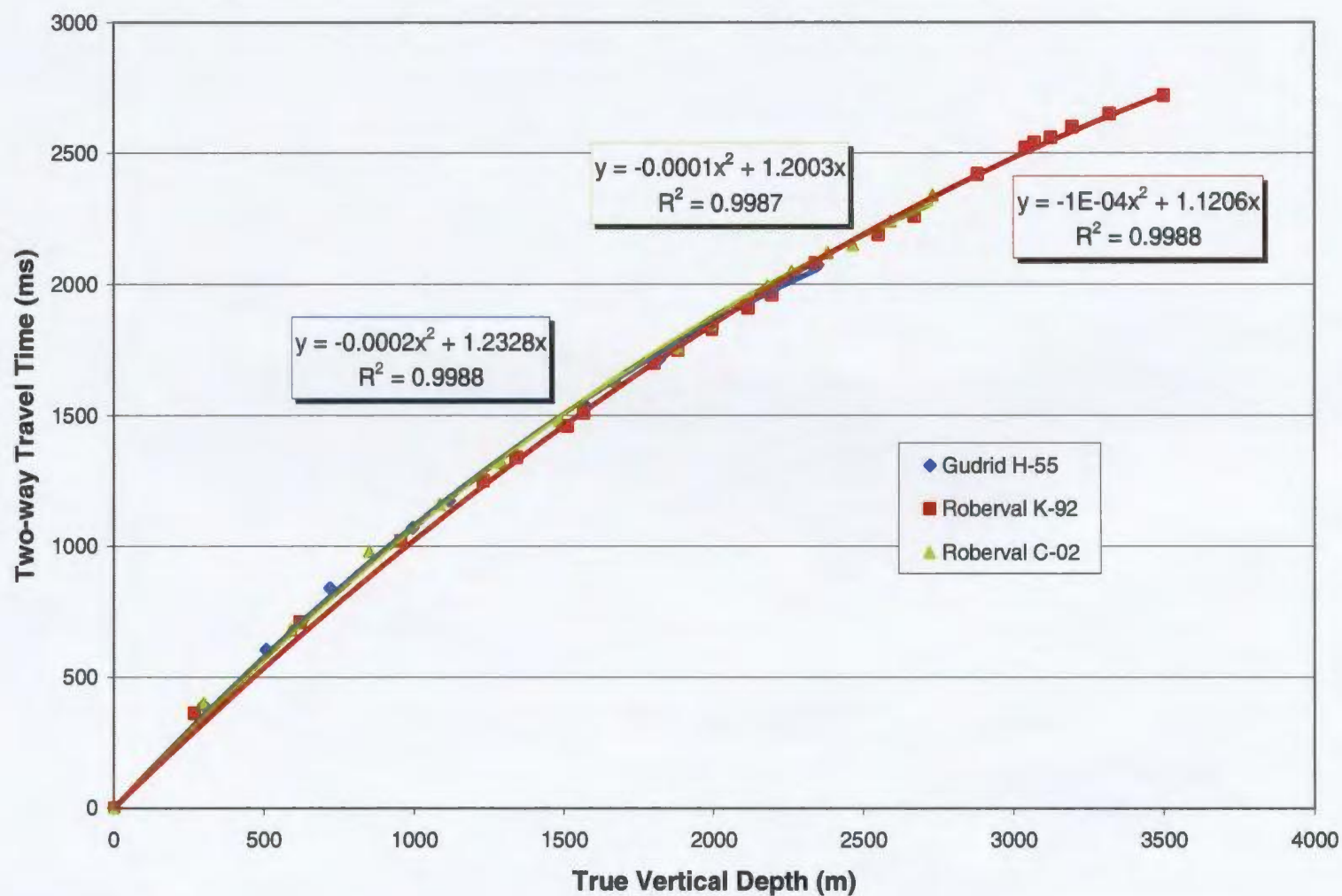


Figure 3.4 – Time-depth curves for wells in Group C and their respective time-depth functions. Created from data taken from well files in the C-NLOPB archives.

formation tops. Formation tops loaded into the Landmark[®] system are listed in Table 3.3. In general each seismic marker was fairly well-defined on the shelf and correlation between wells on seismic lines is fair to excellent. However, marker consistency diminishes under the shelf break where correlation between lines is poor. Beyond the shelf break the markers were also relatively well-defined. Figure 3.5 contains a schematic diagram illustrating formation age, formation names, lithology, horizon name, seismic sequence name and the quality and confidence of each of the markers (template for figure modified after Young (2005); lithostratigraphy modified after McWhae et al. (1980)). It also illustrates the indexing and color code used for the seismic markers.

The resolution of the seismic data and complexity of their distribution makes regional interpretation of the Freydis Member and Alexis Formation difficult and therefore neither has been interpreted for this thesis. The base of the post-Mesozoic sedimentary fill (base of Bjarni Formation) has been defined as the seismic basement; the deepest seismic event that can be regionally resolved. Therefore, it may or may not be the true pre-rift basement but may instead be the top or an intra-Alexis Formation event. The seismic basement may also include Paleozoic carbonate rocks that contain proven reservoirs at certain drilling locations. Also, due to contamination by water bottom multiples the top Saglek Formation marker was not mapped.

Well	Water Depth	Saglek	Mokami	Kenamu	Cartwright	Markland	Bjarni	Alexis	Carbonates	Basement
Bjarni H-81	153.2	222.0	724.5	1333.5	1820.0	1975.0	2150.5	2255.5		
Bjarni O-82	154.9	262.0	758.0	1360.0	1857.0	2062.0	2285.0			
Corte Real P-85	450.0	600.0	1355.0	3379.0	3379.0	4060.0				
Gudrid H-55	311.6	402.5	722.0	1676.0	2179.0	2391.5			2663.5	2804.0
Herjolf M-92	165.8	239.0	773.5	1402.0	1963.0	2211.0	2614.0	3751.0		4048.5
Hopedale E-33	562.6	613.0	840.0	1009.0	1593.0	1697.0	1948.0		1976.0	2000.0
N. Bjarni F-06	162.0	262.0	857.0	1480.0	2059.0	2289.0	2423.0			
Roberval C-02	276.0	375.0	703.0	1690.0	2196.0	2483.0				2803.0
Roberval K-92	268.5	340.0	725.0	1815.0	2355.0	2679.0	3080.0	3188.0	3544.0	
South Hopedale L-39	591.6	630.0	812.0	1073.0	1462.0	1547.0	2007.0			2220.0
Tyrk P-100	128.8	372.0	649.0	761.0	1084.0	1183.0	1194.0	1523.0		1706.0

Table 3.3 – List of wells and formation tops in the study area taken from the C-NLOPB Schedule of Wells (2003). These are the picks that were loaded into the LandMark[®] software for seismic sequence interpretation purposes. Depths (metres) are below rotary table (RT).

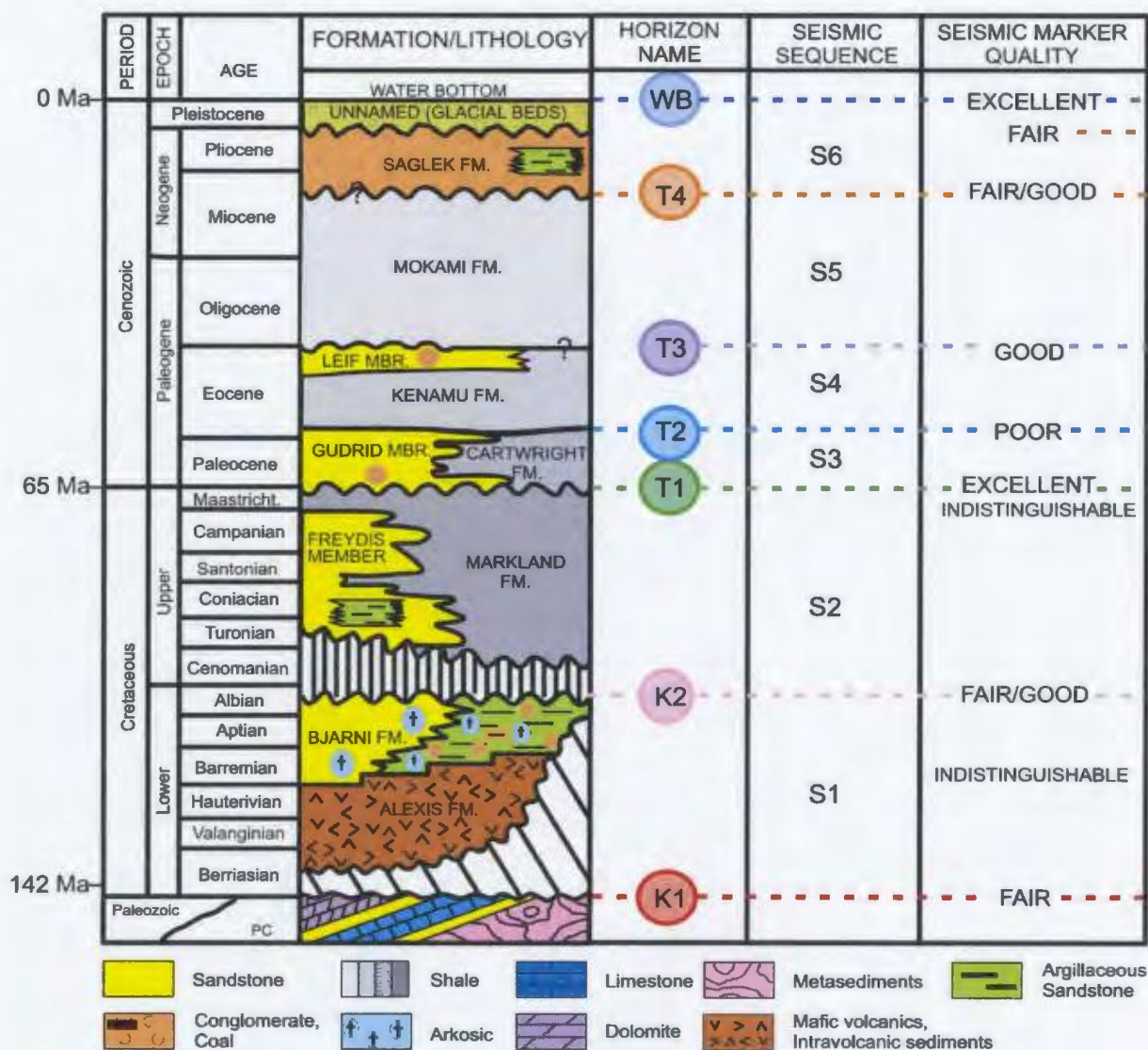


Figure 3.5 – Schematic diagram illustrating the age, formation names, lithology, horizon number, horizon name, depositional sequence name and the quality and confidence of each of the markers (template for figure modified after Young, 2005; lithostratigraphy modified after McWhae et al., 1980; ages after Gradstein et al., 2004).

3.3 Seismic Data Quality and Horizon Picking

Due to geological and bathymetric complexity there are several interpretation obstacles that are consistent throughout the dataset. Firstly, the sharp gradient change at the shelf edge and slope makes imaging beneath it challenging. Not only does this make interpretation through the shelf edge and upper slope difficult but the correlation of events beyond this point is seriously hindered because there are no wells in the deep water to help with the horizon correlation. Figures 3.6 & 3.7 illustrate the quality of the seismic markers beneath the shelf. Figure 3.6 shows an area where the data is relatively good whereas Figure 3.7 shows a section of poorer data beneath the shelf break typical of the data within the study area and elsewhere on the Labrador margin.

Another problem encountered with the data was the presence of peg-leg multiples of different reflections due to a pervasive hard water bottom. The seabed itself has created multiples which are displayed within the younger formations making interpretation of the Mokami and Kenamu Formations difficult in places (Figure 3.8). Unfortunately removal of these multiples is beyond the objective of this thesis so another method of dealing with them during the interpretation had to be used. Five more horizons were created; Water Bottom Multiple 1, 2, 3, 4 and 5. This was achieved by simply picking the seabed throughout the data set and taking the WB horizon and adding it to itself once, twice, three times and so on. These false horizons could be displayed when needed and averted during interpretation. With these horizons displayed it assisted in determining real events from the multiples. Similar multiple issues were evident with another strong reflection - the seismic basement. Its water induced peg-leg multiples are strong especially when the basement is shallow.

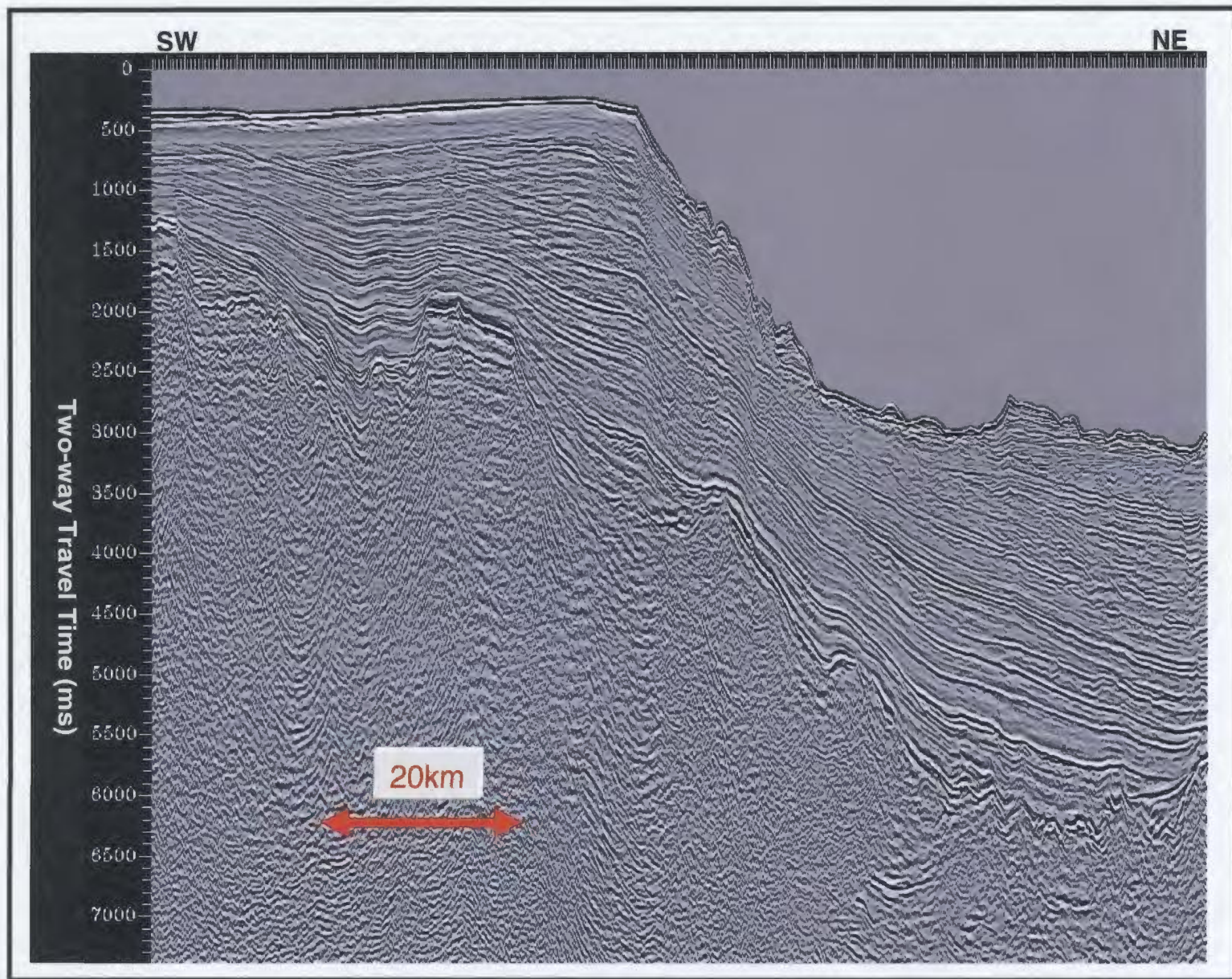


Figure 3.6 – Dip seismic section illustrating good reflection resolution below the shelf break and slope.

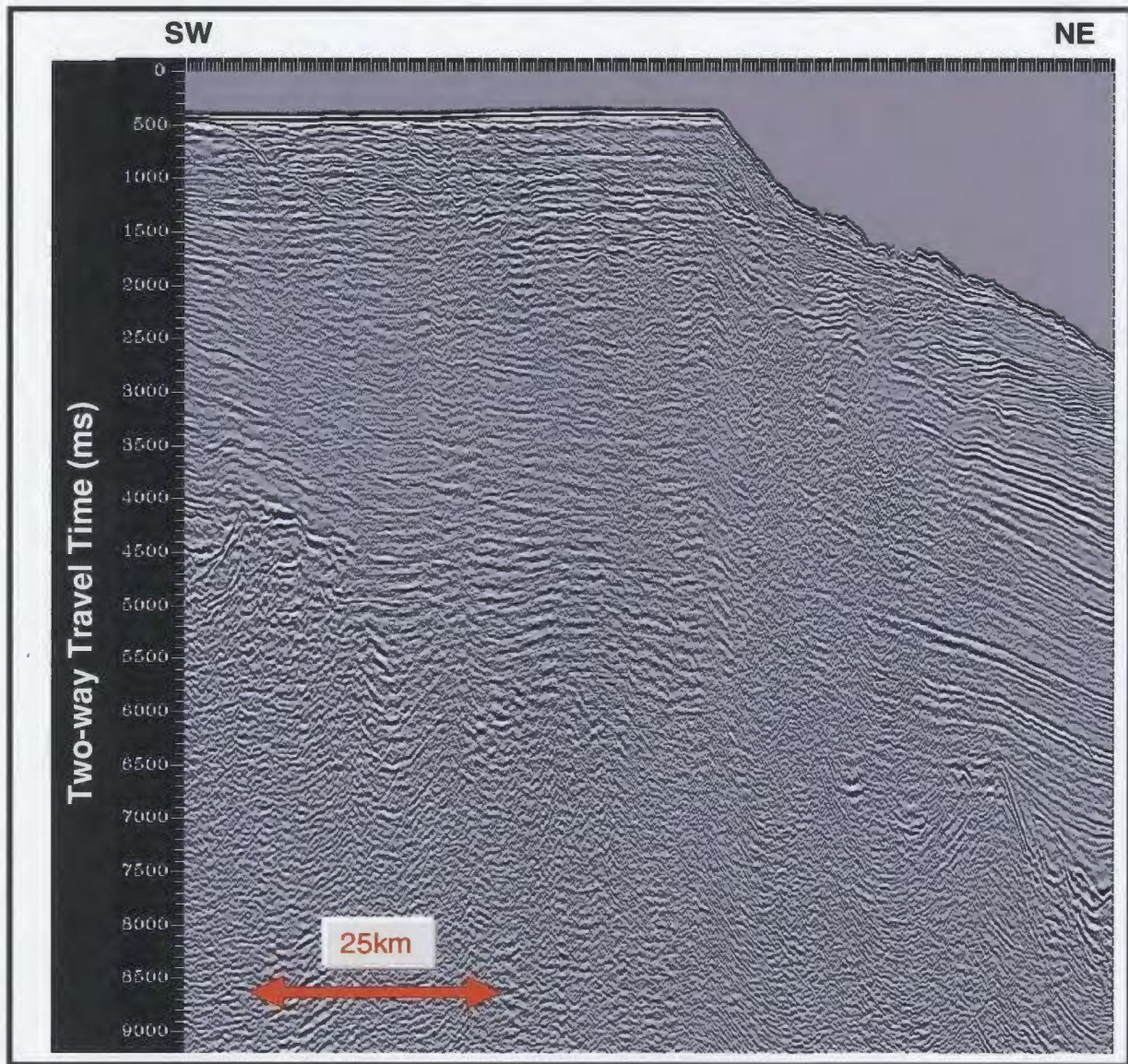


Figure 3.7 – Dip seismic section illustrating typical data quality below the shelf break within the study area. Significant loss of resolution and contamination by water bottom multiples of seismic reflectors is visible under the continental slope.

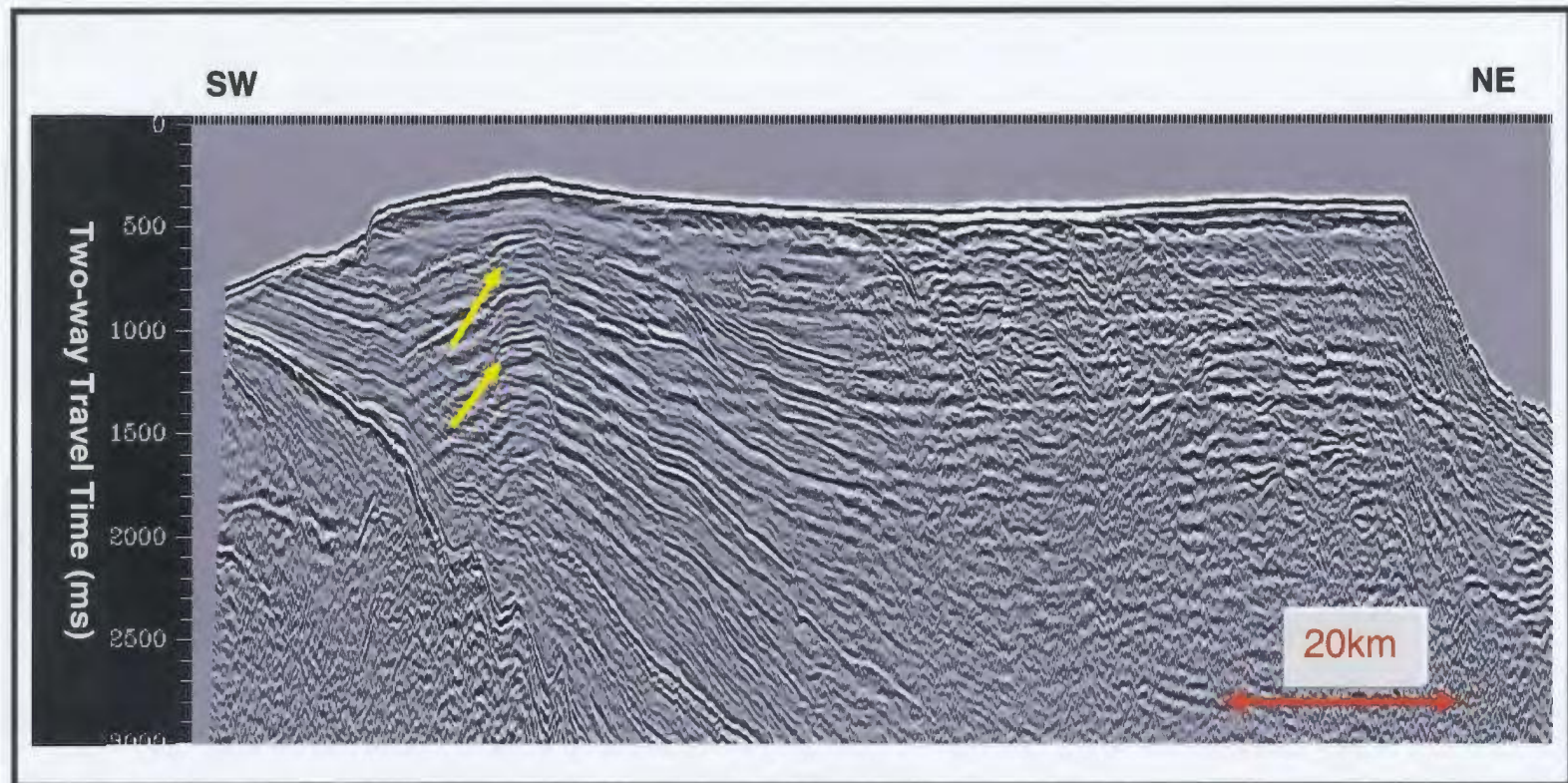


Figure 3.8 – Typical dip seismic section along the shelf and inner channel along the Labrador coast. Arrows are illustrating areas with crossing reflectors. Truncated reflectors at the water bottom are primary reflectors. Areas like this can be difficult to interpret since distinguishing between true reflectors and multiples can be difficult.

Finally, within the study area there is a sub-area of poor data quality below the shelf break and into the deep water where no reflectors were able to be mapped. This may be due to the presence of disseminated gas in non-consolidated and semi-consolidated sediments. In places the data are overmigrated due to difficulty in estimating primary velocities making horizon picking extremely difficult. This region has been noted as a "no data" zone. An example of the data quality in this area can be seen in Figure 3.9 and a regional map of the study area illustrating the no-data zone can be seen in Figure 3.10.

3.4 Seismic Sequence Analysis

Seismic stratigraphy was first formally introduced by Vail (1977) of ExxonMobil. Vail recognized that many reflectors in seismic data were generated as a result of bedding surfaces and not that of time-transgressive facies boundaries. He also noted that seismic data can be divided into seismic facies with distinct seismic patterns and characteristics. These different characteristics may be related to depositional environments as well as lithology, especially when well information is also available.

Seismic stratigraphy has 3 components: 1. sequence analysis; 2. seismic facies analysis; and 3. attribute analysis. Sequence analysis involves separating seismic sections into different seismic units based on relative sea-level changes (this being either a change in eustatic sea level, sediment supply, subsidence or uplift or some combination of these factors) whereas facies analysis involves determining the specific lithology of each unit. Attribute analysis is the determination of different seismic attribute characteristics for each of the units. This thesis will primarily concentrate on sequence

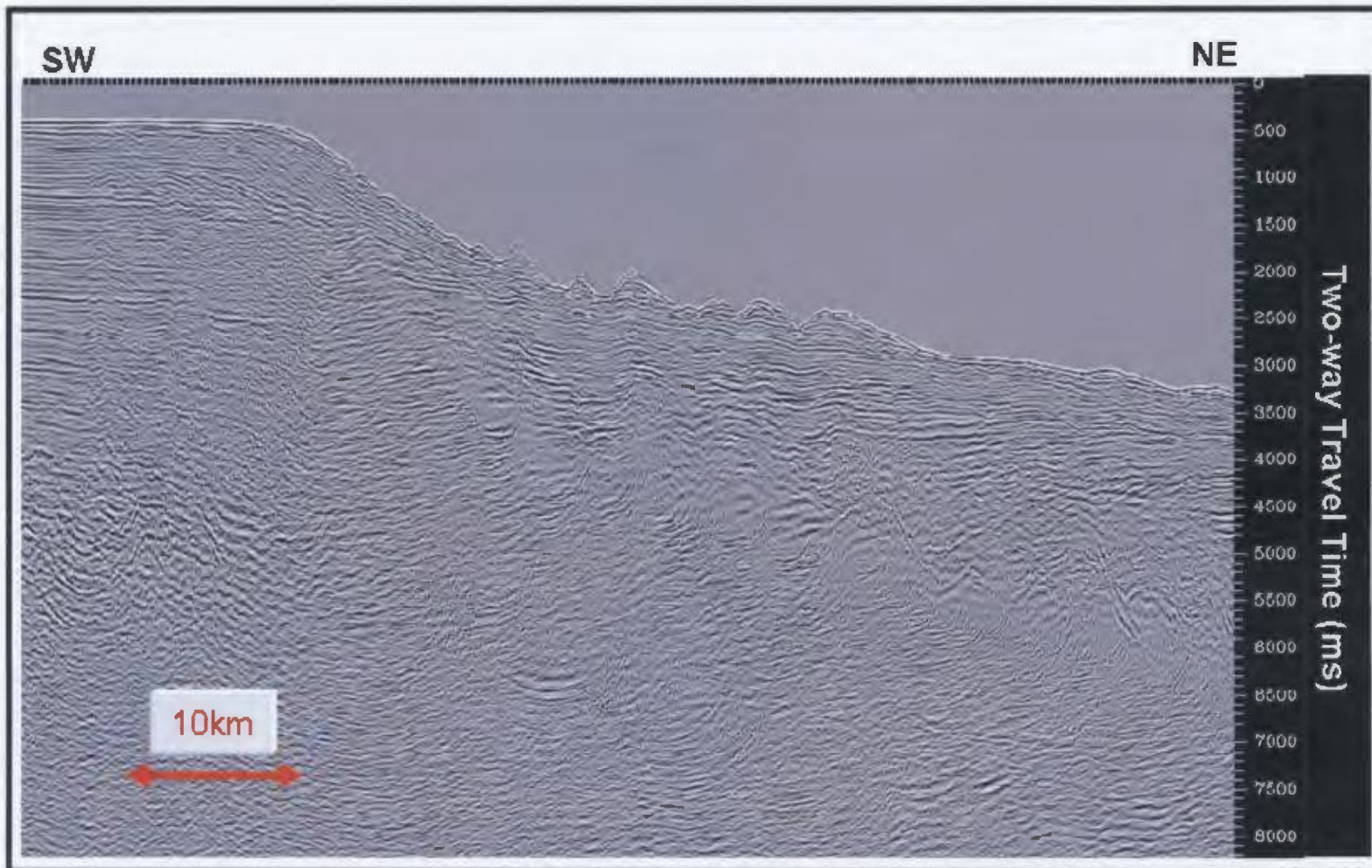


Figure 3.9 – Dip seismic section illustrating the quality of data typical of lines in the south-east portion of the study area. This low resolution data makes interpretation very difficult and therefore very little interpretation could be done in this area.

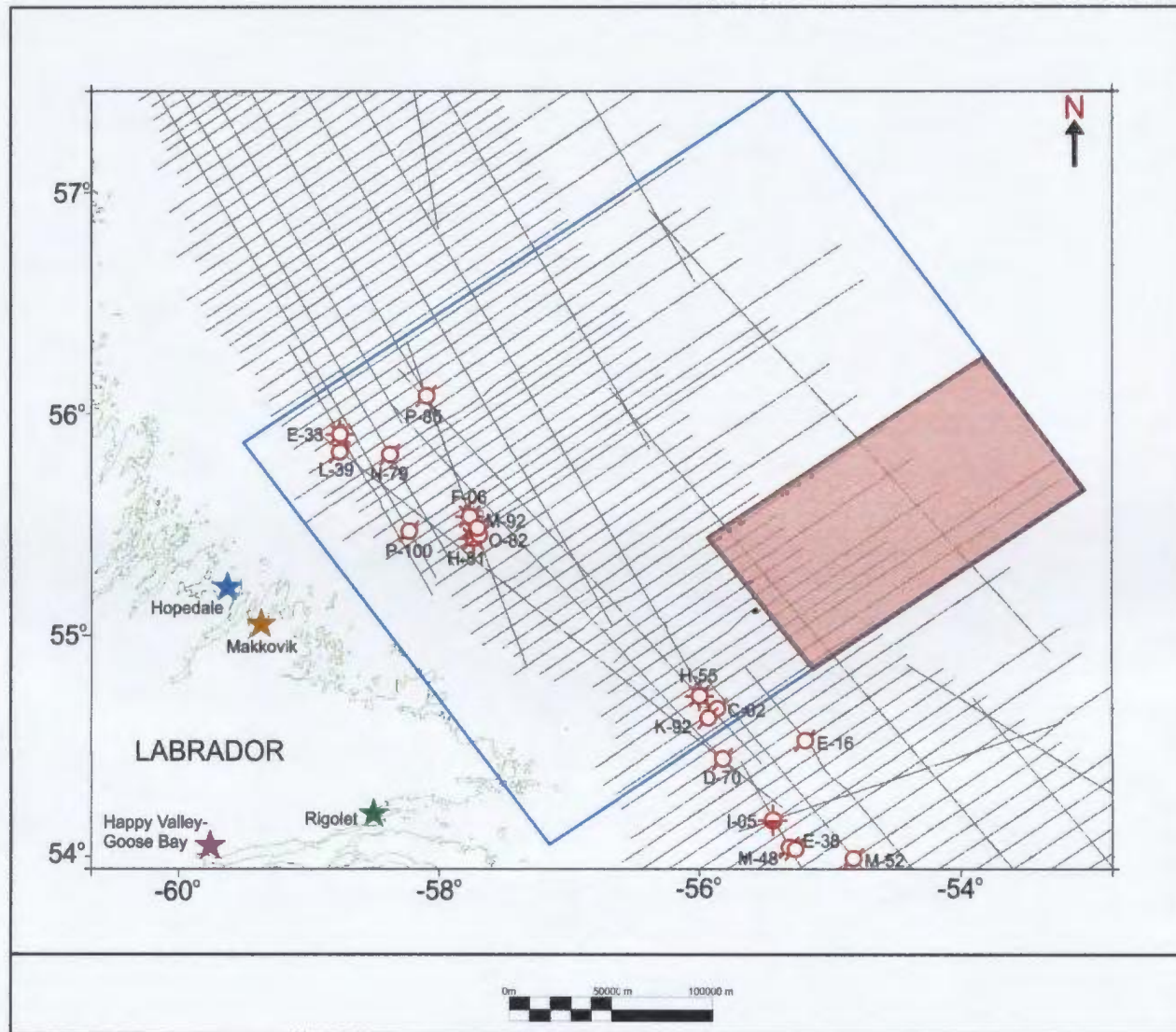


Figure 3.10 – Base map of the study area (blue) illustrating the area where the data is of poor quality and therefore interpretation in this region is limited (red rectangle). Coordinates in NAD83.

analysis (sequence stratigraphy) since the facies can be correlated through well logs and well cores and the 2D seismic data does not allow for areal attribute analysis.

Sequence stratigraphy in this region is dependent of marine accommodation space which is governed by relative sea level (influenced by both eustatic sea level and subsidence/uplift). The basic principles of sequence stratigraphy state that if there is no accommodation space an area of sediment bypass results. If there is negative accommodation space, erosion occurs and if there is positive accommodation deposition will occur. The following discussion has been summarized from Coe et al. (2002).

An individual sequence is made up of numerous parasequences and is defined by one cycle of change in equilibrium between accommodation space and sediment supply. These changes in the balance are caused by changes in eustatic sea level, subsidence/uplift, sediment supply or any combination of these. Each major sequence can then be divided into four systems tracts, representing one specific point along the sea level rise and fall cycle. Each of the four systems tracts is composed of at least one parasequence set but each of the systems tracts may not necessarily be preserved or even developed.

Figure 3.11 illustrates the four systems tracts and their relation to relative sea level changes. The first of these systems tracts is the highstand systems tract (HST). This is defined as the sediment package which is deposited between the maximum rate of relative sea level rise and the maximum relative sea level. This produces aggradational to progradational parasequence sets. When relative sea level reaches its maximum there is a sequence boundary (unconformity) which will mark the base of the sedimentary package deposited during falling relative sea level.

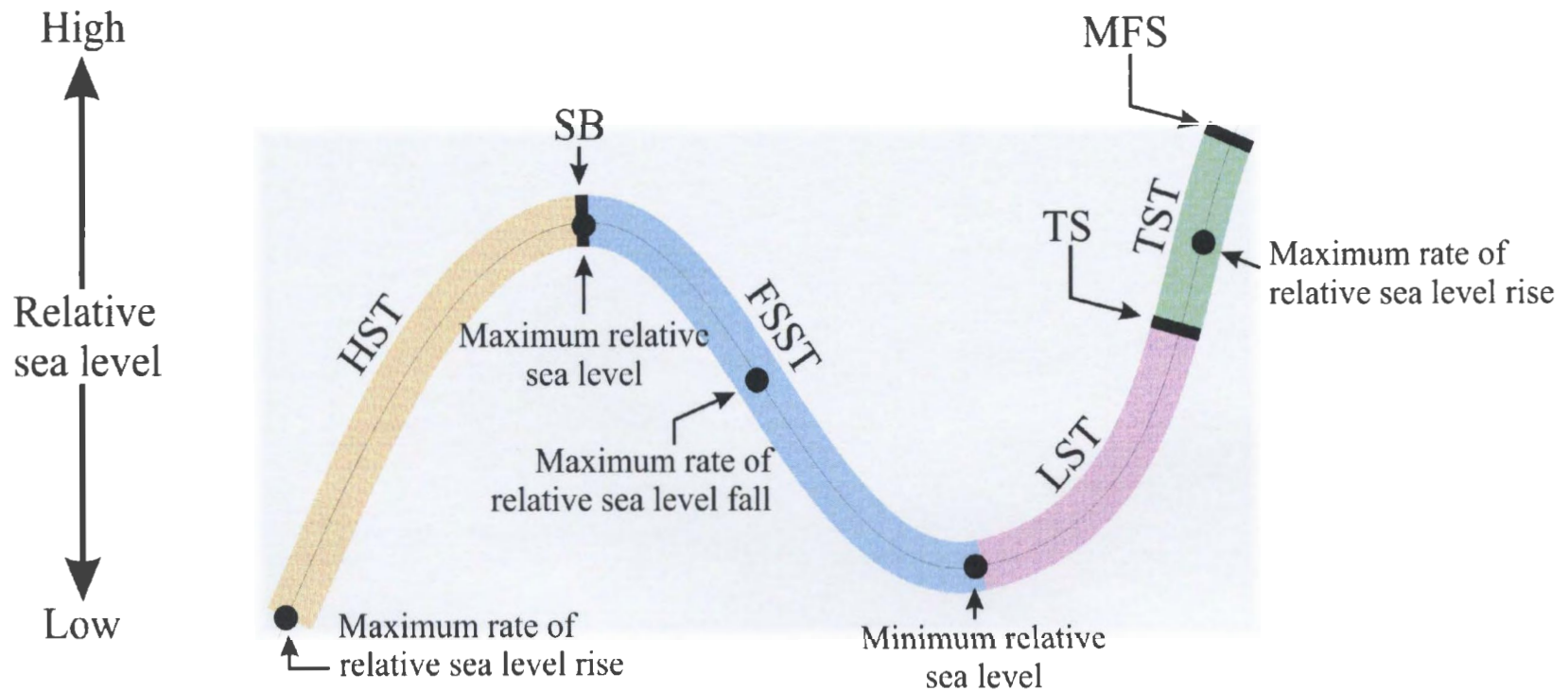


Figure 3.11 – Illustration of the four systems tracts defined in sequence stratigraphy. HST – highstand systems tract; FSST – falling stage systems tract; LST – lowstand systems tract; TST – transgressive systems tract; SB – sequence boundary; TS – transgressive surface; MFS – maximum flooding surface. Figure modified after Coe et al., (2002).

As the rate of relative sea level falls the second systems tract, the falling stage systems tract (FSST), begins to form. This is the package of sediment deposited between maximum and minimum relative sea level. This is caused by relative sea level fall and an increase in erosion which causes a greater supply into the sea from rivers.

After relative sea level fall reaches its minimum there is no change in accommodation space. As relative sea level begins to rise a small amount of accommodation space is created composing of progradational to aggradational parasequence sets. This is the third systems tract referred to as the lowstand systems tract (LST). This is the sediment that is deposited between the minimum relative sea level and the significant increase in accommodation space.

At the end of the LST there becomes a time where the rate of sediment supply is less than the amount of accommodation space being created. At this time, a transgressive surface (TS) will be created and marks the base of the fourth systems tract: the transgressive systems tract (TST). These sediments are deposited when the rate of sediment supply is less than the rate of increase in accommodation space and are retrogradational. Finally, the maximum flooding surface (mfs) occurs between the maximum rate of relative sea level rise and the maximum sea level.

These four systems tracts produce clinoforms which are recognizable in seismic reflection data. These seismic reflectors are usually chronostratigraphic surfaces. Sequence boundaries are identifiable on seismic data where the underlying strata are partly absent whether it be removed by erosion or no deposition. The termination of the reflectors known as erosional truncation can often be seen in the seismic data.

Figure 3.12 illustrates the different types of erosional truncation often visible in reflection seismic data. Toplap is a reflector termination which underlies the sequence boundary as it changes from an unconformity (proximal) to a correlative conformation (distal). Toplap is often confused with onlap which is the truncation visible when sediments are deposited on top of an erosional surface. Finally, downlap geometries are visible along the upper surface of maximum flooding surfaces where it overlies clinoforms. These different types of reflector termination can help distinguish sequence boundaries (erosional truncation and toplap below the surface and onlap on the top of the surface), transgressive surfaces (onlap) and mfs (downlap of the overlying sediments).

Six depositional sequences and seven sequence boundaries are defined in this study based on seismic character, upper and lower boundaries and association to lithology and formation tops identified in well logs. Their descriptions are followed with typical seismic sections defining the seismic sequences and boundaries from bottom to top of the basin (older to younger events). Figure 3.13 shows the location of some of the seismic lines but due to the confidential nature of this data, the location of all the seismic sections have not been included in the documentation.

3.4.1 K1 Sequence Boundary: Top Basement Marker

The K1 sequence boundary is interpreted as the Top of the Basement. The marker is very strong and continuous in the nearshore, shallower part of the basin. Based on the character of the reflection it is still difficult to seismically define the nature of basement. The mafic volcanics of the Alexis Formation (basaltic lava flows) have similar

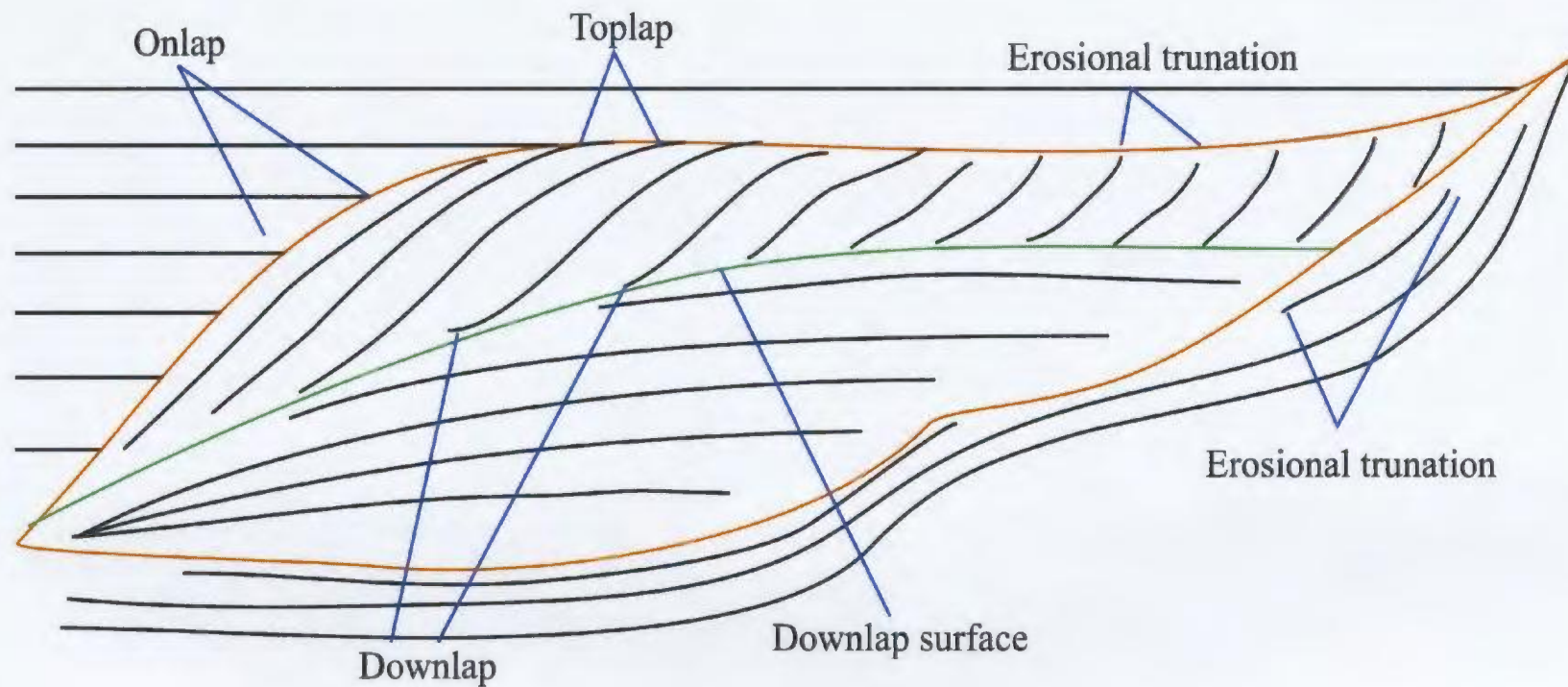


Figure 3.12 – Schematic diagram illustrating the different types of erosional truncation that are often evident in reflection seismic data. The orange lines represent sequence boundaries while the green line represents a maximum flooding surface (MFS). Figure modified after Coe et al. (2002).

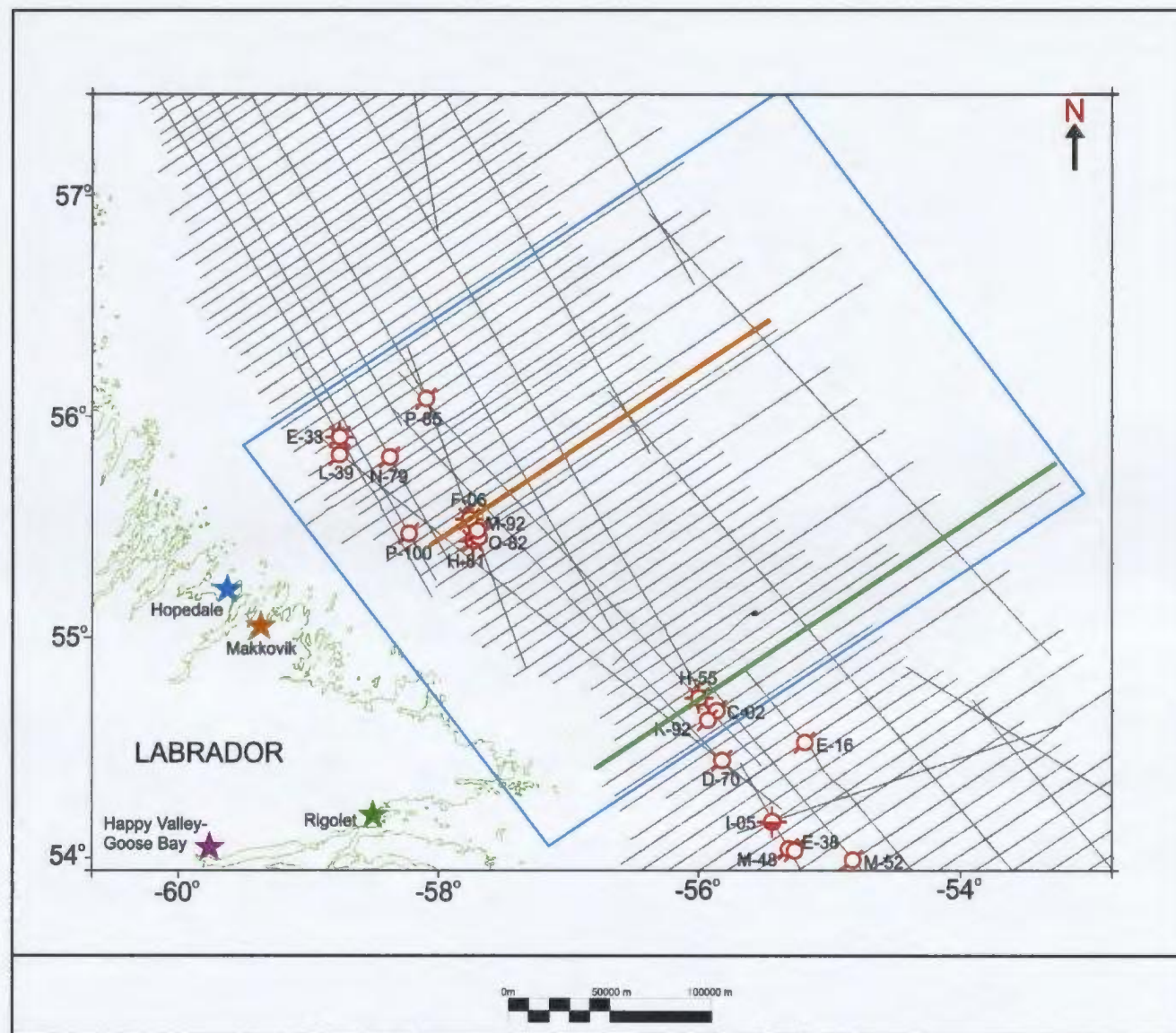


Figure 3.13 – Location map of two significant seismic sections. The red line shows the seismic line passing through the North Bjarni F-06 well (Figures 3.14 and 3.16) and the green line represents the seismic line passing through the Gudrid H-55 well (Figures 3.15 and 3.18).

seismic properties as the granites and gneisses of the Precambrian basement below, therefore making it difficult to distinguish between them. Moreover, Lower Paleozoic carbonates were drilled on several high blocks where they survived as erosional outliers on top of Precambrian basement and have similar seismic properties. In this study, the basement horizon refers to the seismic basement; that is, the deepest event resolvable in the seismic data which may or may not be true prerift basement. No attempts were made to discriminate between Lower Paleozoic carbonates and Precambrian rocks.

The K1 horizon varies in quality throughout the interpreted grid. On the shelf edge it is easily defined since it exists as a prominent peak with an interval exhibiting chaotic character beneath it. In deeper water the marker becomes harder to follow because it becomes very weak. In general, the picking confidence of this horizon is fair throughout the study area. Within the basement there is little internal reflectivity; in places multiples and peg leg multiples are visible.

The K1 horizon is segmented by numerous normal faults creating successions of horst and graben structures. This is visible especially on the shelf edge where horizon picking confidence is greatest (Figure 3.14). The K1 horizon, as defined by either the Alexis Formation or Precambrian basement, has been penetrated by nine of the twelve wells in the study area: Bjarni H-81, Tyrk P-100, Herjolf M-92, Roberval C-02, Roberval K-92, Gudrid H-55, South Labrador N-79, South Hopedale L-39 and Hopedale E-33 wells. In the seismic interpretation, the lower S1 sequence boundary is horizon K1 and is denoted by the colour red.

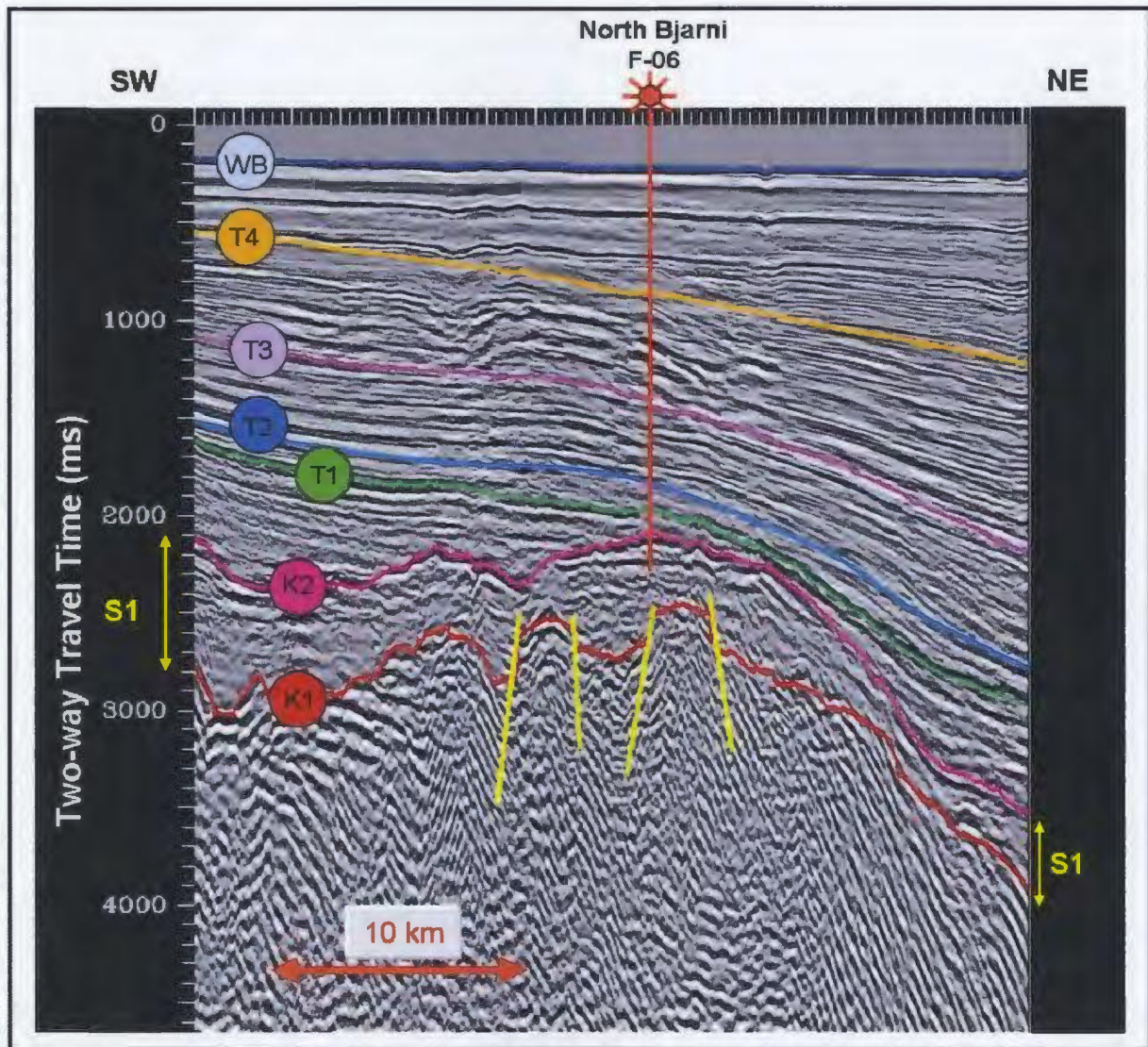


Figure 3.14 – Dip seismic section illustrating the typical seismic character of the K1 horizon as well as the relationship of the S1 seismic sequence to horizons K1 and K2. S1 seen at the North Bjarni F-06 location shows an obvious flat spot developed below the K2 horizon. Overlying markers and seismic sequences are also shown.

Figure 3.14 shows a representative dip seismic section within the basin and illustrates the typical character of the K1 sequence boundary.

3.4.2 Seismic Sequence S1

Seismic Sequence S1 was identified in the entire study area. Using well ties the sequence was correlated to the Early Cretaceous sandstones of the Bjarni Formation. The package itself has little internal structure, in other words, low seismic reflectivity and in most places it is nearly transparent (Figure 3.14). Internal reflectors are difficult to recognize but where they are visible they appear to be non-parallel, relatively chaotic and occasionally dipping. This sequence is bounded at the base by the K1 sequence boundary (horizon K1) and bounded at the top by the K2 sequence boundary (horizon K2).

The S1 sequence varies significantly in thickness throughout the study area. Generally it is thick in depositional lows (upwards of 1700 ms TWT) and thin on the horsts and ridges (<100 ms TWT). In some areas, S1 onlaps or is truncated before reaching the top of the horst blocks. The sequence is therefore absent on certain basement highs as was seen in the Gudrid H-55 (Figure 3.15) and Roberval C-02 wells. In other areas S1 thins below the resolution of seismic data and often its interpretation along the crestal areas is difficult.

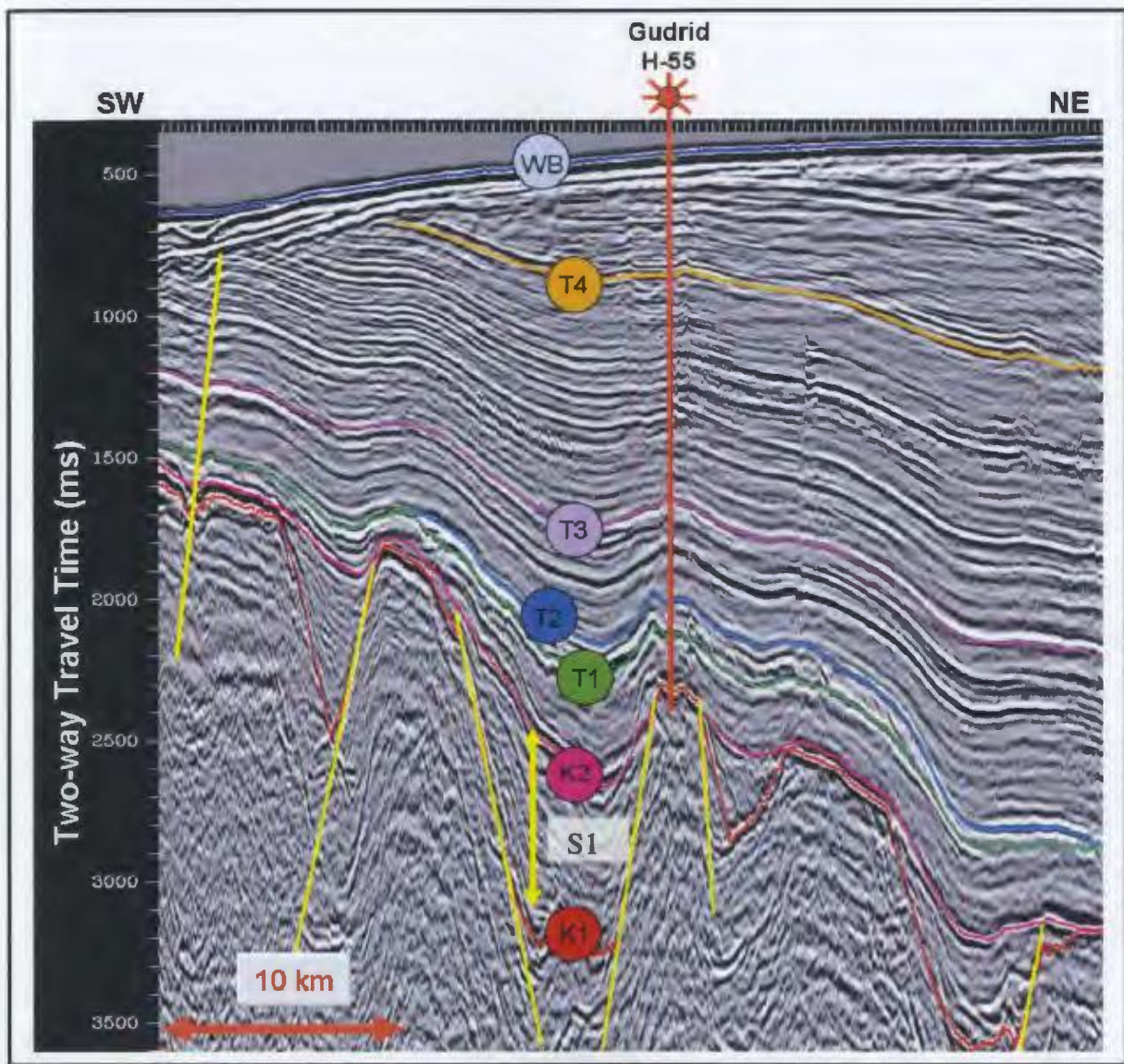


Figure 3.15 – Dip seismic section illustrating the S1 seismic sequence (Bjarni Formation) filling the half grabens on both sides of the Gudrid high. Bjarni Formation (S1 seismic sequence) is missing on the horst block at the Gudrid H-55 well due to erosion or non-deposition.

In general, there is little faulting occurring in S1, except for major faults marking the edges of horsts and rotated blocks. S1 encompasses both sandstones and shales of the Bjarni Formation, deposited within a continental environment (Umpleby, 1979; McWhae et al., 1980). The sequence continues on the outer shelf, slope and into the deeper water where it thins beyond seismic resolution and eventually ceases to exist (Martin et al., 2006). The confidence in the upper sequence boundary pick K2 varies along the lines.

The following wells have terminated in or have cut entirely through Seismic Sequence S1: North Bjarni H-81, Bjarni H-81, Bjarni O-82, Tyrk P-100 (Bjarni equivalent), Herjolf M-92, Roberval K-92, South Labrador N-79 (uncertain), South Hopedale L-39, and Hopedale E-33.

3.4.3 K2 Sequence Boundary

The K2 Sequence Boundary has been interpreted as the post-rift unconformity or Avalon Unconformity (Late Albian or pre-Late Cretaceous unconformity, McWhae et al., 1980) thus marking the upper boundary of the Bjarni Formation (S1). On interpreted seismic sections it is coloured pink and is noted as horizon K2. The K2 sequence boundary is a relatively strong reflection due to a significant change in lithology from shale to sandstone dominated. Confidence in picking the horizon is fair to good.

On the shelf it has variable relief and sometimes dips quite steeply along the shelf edge. As with most of the sequence boundaries, K2 is difficult to interpret beneath the shelf break. Tracking confidence decreases beyond the shelf edge. This horizon has a regional distribution, extending into the deep water (Martin et al., 2006) and is penetrated by the following wells: North Bjarni H-81, Bjarni H-81, Bjarni O-82, Tyrk P-100 (Bjarni

equivalent), Herjolf M-92, Roberval K-92, South Labrador N-79 (uncertain), South Hopedale L-39, and Hopedale E-33.

The unconformity character of the K2 sequence boundary is illustrated by the downlapping of overlying reflections on the K2 horizon and truncation of lower reflections (Figure 3.16).

Locally the K2 horizon terminates at basement horst structures. The K2 sequence boundary generally trends similar to the K1 sequence boundary and separates depositional sequence S1 from depositional sequence S2. The sequence above usually contains parallel or downlapping reflections with variable reflection amplitudes.

3.4.4 Seismic Sequence S2

S2 is bounded at the bottom by the K2 sequence boundary and at the top by the T1 sequence boundary. S2 lies directly on the Alexis Formation/Precambrian basement (K1 horizon) whenever S1 is absent. The sequence is composed of parallel to sub-parallel reflections which are higher frequency on the innermost part of the shelf and lower frequency towards the deep water. The sequence thins over basement highs and thickens within the grabens. Within the package, reflectors are weak except close to the upper and lower sequence boundaries. The basal K2 sequence boundary is an unconformity as described above.

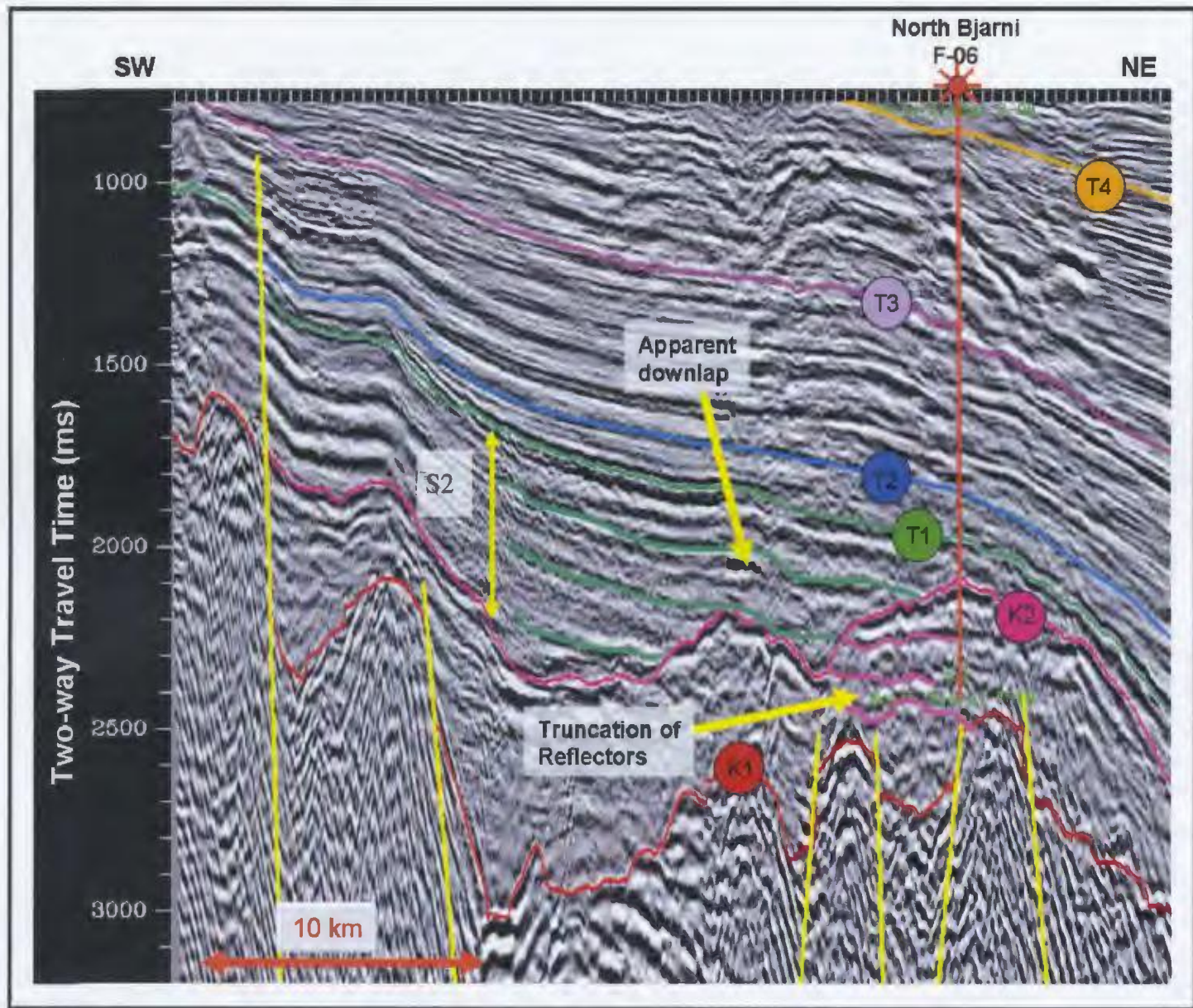


Figure 3.16– Dip seismic section illustrating seismic reflectors within S2 (denoted by green) which downlap onto the K2 sequence boundary. Truncation of reflector under K2 boundary (denoted by pink) is also observed.

Seismic sequence S2 has been interpreted as the Markland Formation through well correlation. The Markland Formation consists almost entirely of marine shales, except for a sandstone member that is present mostly in the nearshore and close to major basement ridges known as the Freydis Member (McWhae et al., 1980). The S2 reflectors downlap onto K2 as seen in Figure 3.16. Seismic Sequence 2 is interpreted as a highstand deposit indicated by the shale deposits as well as downlap of reflectors against the K2 Sequence Boundary.

Seismic sequence 2 is present throughout the entire study area including in the deep water. The thickness of the sequence differs throughout the area being nearly absent in the south-western portion of the block and thickening to about 1000 ms TWT towards the north-east. In the northern part of the study area this seismic sequence is affected by numerous faults (Figure 3.17).

All of the wells within the study area have intersected the S2 sequence illustrating the regional extent of the Markland Formation. One well, Corte Real P-85, terminated within the Markland shales due to mechanical problems and did not reach its Bjarni sandstone target.

Although the Freydis Member is a local component within the Markland Formation and was drilled at a couple of locations, its identification on seismic lines is difficult. Also, the member is absent from most wells and according to McWhae et al. (1980) it is only present in those wells near the Late Cretaceous paleoshoreline where it has been deposited in down-faulted lows and pinchouts which were not likely drilled. The Freydis sandstone within the S2 sequence has been identified in Skolp E-07 and

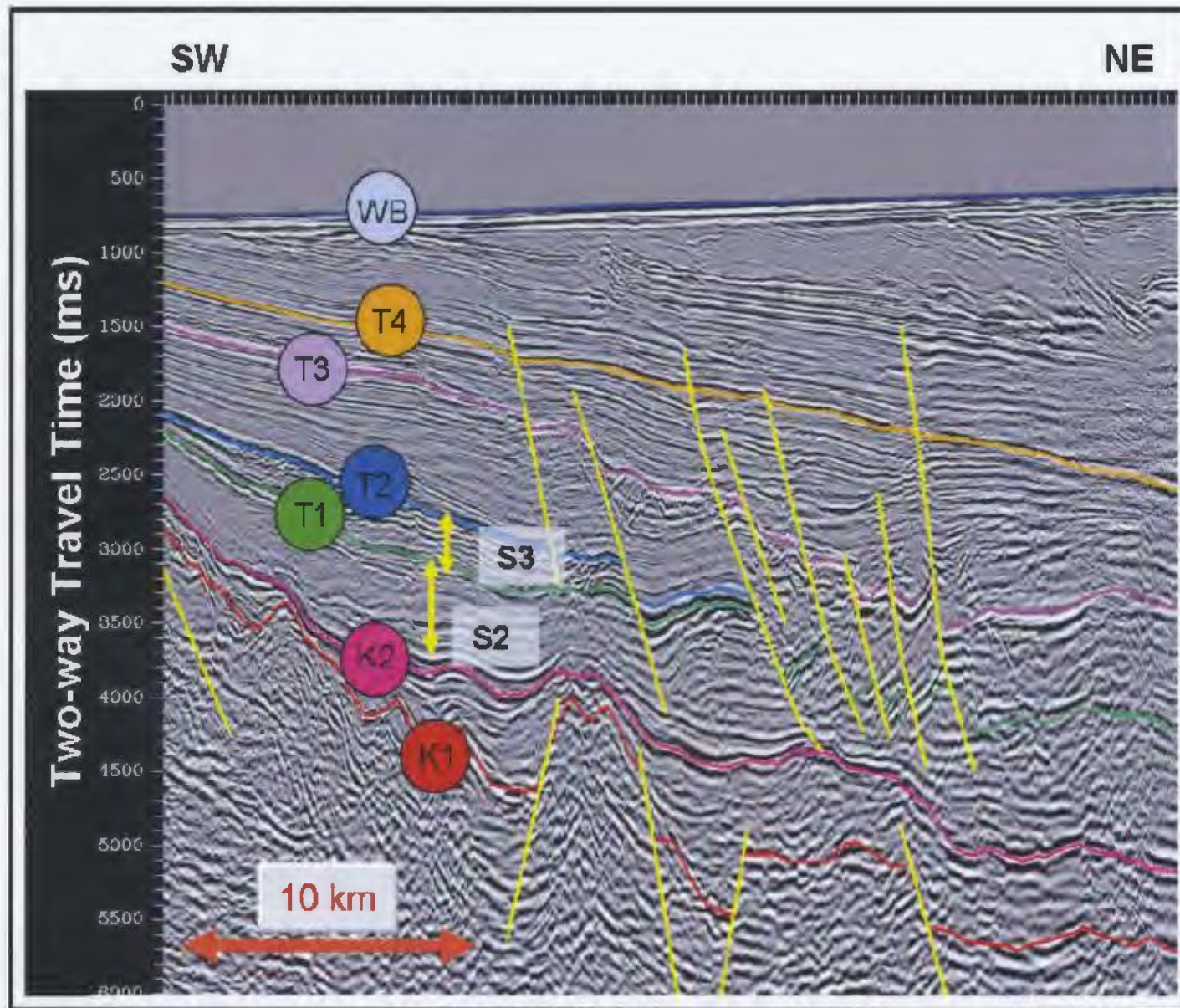


Figure 3.17 – Dip seismic section showing a family of down-to-basin faults cutting through S2, and seismic sequences S3, S4 and S5 on the shelf.

Freydis B-87 wells, neither of which is in the current study area.

3.4.5 T1 Sequence Boundary

The T1 horizon is interpreted as the unconformable reflector marking the upper sequence boundary of the S2 sequence representing the Markland Formation. T1 corresponds to the Base Tertiary or the Bylot Unconformity/Disconformity (McWhae et al., 1980). This is an excellent seismic marker and is the strongest and most continuous event in the study area and therefore most confidently picked of all the sequence boundaries.

The T1 horizon is relatively shallow on the near shelf and dips significantly on the outer shelf and in the deep water. It separates the underlying Markland shale (S2) from the Cartwright Formation (S3). It is present within the entire study area both in the shallow regions of the shelf as well as in the deep water. The T1 marker has been intersected by each of the wells in the study area including the Corte Real P-85 well, where it was the deepest sequence boundary to be penetrated.

Figure 3.18 shows a dip seismic line with the T1 sequence boundary shown in green. Although faulting within the post-rift sedimentary successions on the shelf is reduced, there are several fault sets which cut through the T1 horizon (Figure 3.17). The T1 sequence boundary is indicated by the colour green.

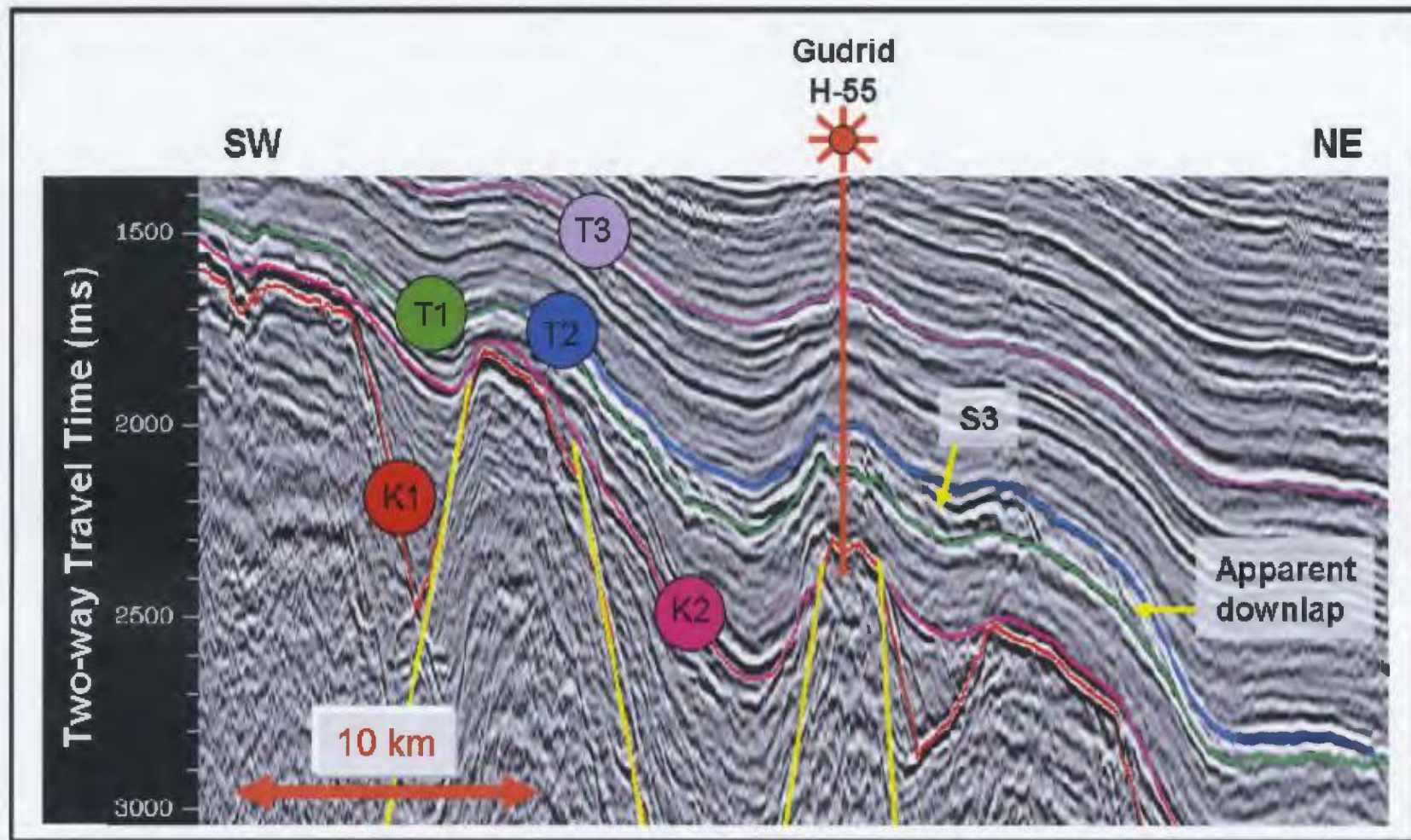


Figure 3.18 – Dip seismic line through the Gudrid H-55 well showing seismic sequence S3 and its relation to the T1 and T2 sequence boundaries. Notice the apparent downlap of several reflectors within S3 onto T1.

3.4.6 Seismic Sequence S3

Seismic Sequence S3 has been correlated to the Gudrid Member/Cartwright Formation through well correlation. The corresponding geological interval to S3 was deposited during the Paleocene and consists of the Paleocene-aged Gudrid sands and the distal shelf deposits – the Cartwright shales. The Gudrid Member is thought to be deposited as a turbidite deep sea fan on the continental slope and rise. This seismic sequence is limited by the T1 and T2 sequence boundaries. The base of the S3 sequence is easily defined because the T1 sequence boundary is a prominent seismic marker. Regional mapping of this unit is still difficult due to the poor reflective quality of the upper sequence boundary. The S3 sequence is conformable with the overlying seismic sequence S4 although it sometimes shows tolap.

The thickness of this unit varies significantly throughout the study area but never reaches time-thicknesses greater than 200 to 300 ms TWT. The seismic line which passes through the Gudrid H-55 well shows a typical example of the S3 sequence (Figure 3.18). This seismic sequence is thin and has significant internal character. It appears to downlap onto the T1 sequence boundary in places (Figure 3.18) but more often has parallel internal reflections which mimic the shape of the underlying sequence boundary. There is evidence of faulting segmenting S3 as shown in Figure 3.17.

The Cartwright Formation was penetrated by each of the wells in the study area whereas the sands of the age equivalent Gudrid Member were identified only in Corte Real P-85, Gudrid H-55, Roberval C-02, Roberval K-92, South Hopedale L-39 and Tyrk P-100 wells. It appears that S3 is present on the entire shelf but is difficult to map beyond the shelf break.

3.4.7 T2 Sequence Boundary

The T2 sequence boundary is much more difficult to identify than the other sequence boundaries which are interpreted and described. On displayed seismic sections T2 is coloured blue.

This sequence boundary is interpreted to be the top of the S3 sequence containing both Gudrid sandstone and Cartwright shale intervals and has been penetrated by each of the wells in the study area. It is a conformable surface separating the overlying S4 sequence from S3 and was part of the syn-drift sequence. This conformable contact separates the Paleocene from the Eocene sedimentary sequence. As discussed in the previous section, the T2 sequence boundary is locally quite difficult to track and is only easily identifiable on the shelf, where it is a relatively strong reflector (Figure 3.19). Beyond the shelf break it appears to be absent due to downlapping onto earlier surfaces.

In general it dips towards the north-east and mimics the shape of the underlying sedimentary sequences. It has a low regional gradient and has minimal structural relief. The T2 sequence boundary has been cut by the same fault family as seen in Figure 3.18 (T2 sequence boundary is the blue horizon). The overall quality of this seismic marker is considered poor and therefore the interpretation confidence for this horizon is low.

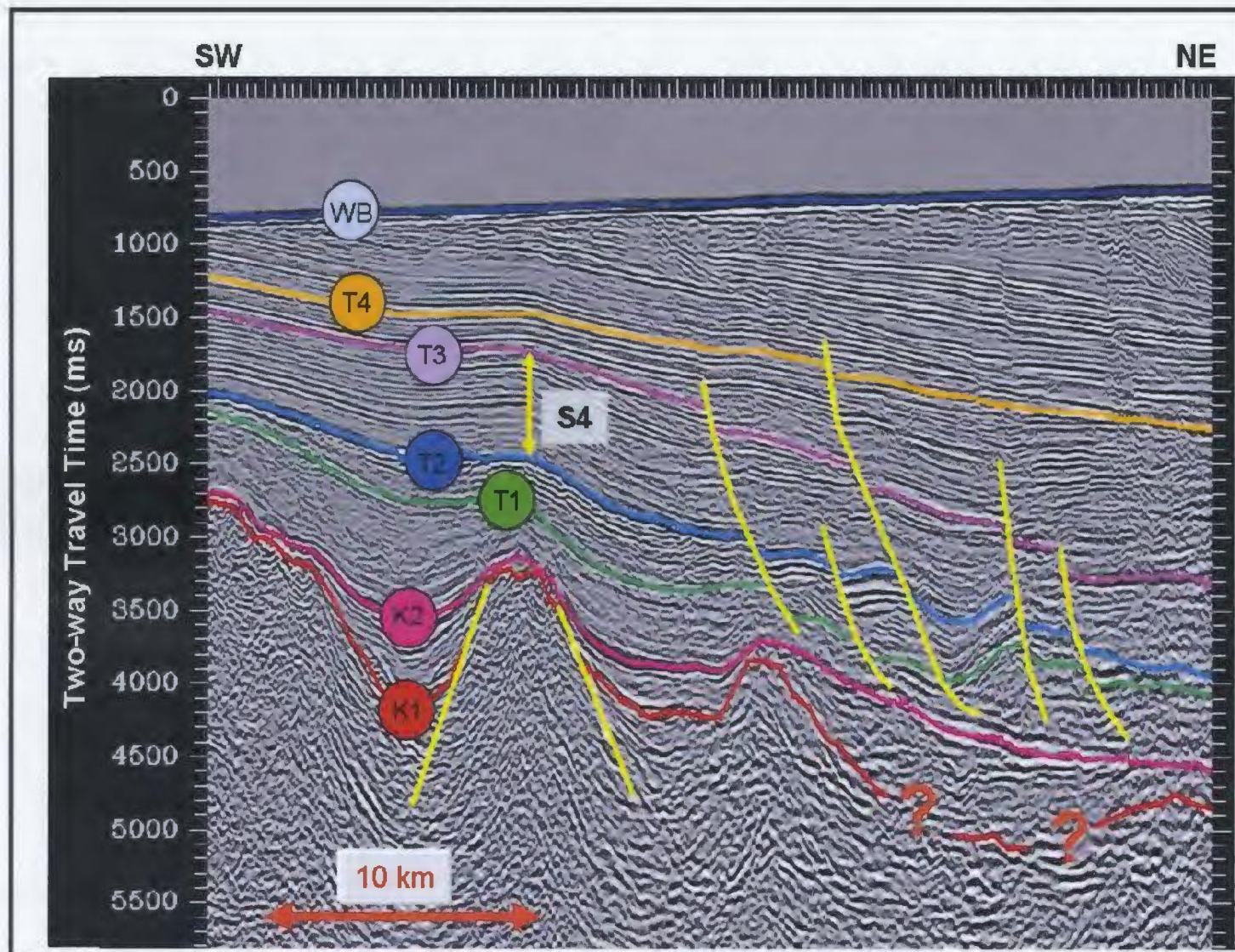


Figure 3.19 – Dip seismic section showing the typical characteristics of the depositional sequence S4.

3.4.8 Seismic Sequence S4

Seismic Sequence S4 was interpreted on all seismic sections and was correlated at several well locations to the Kenamu Formation. This formation was deposited in a highstand marine environment during the Eocene and consists of a brown-grey sandstone with interbedded siltstone and fine sandstone. This formation also includes the sandstones of the Leif Member. The upper boundary of this seismic sequence is the T3 sequence boundary (Baffin Bay Unconformity, McWhae et al., 1980). Its lower boundary is the T2 sequence boundary where S3 exists. Whenever S3 is absent the S4 sequence is basally bounded by the T1 horizon. The interpretation confidence of these bounding reflectors is usually good and correspondingly the definition of S4 is also good.

Seismic Sequence S4 has laterally persistent, moderate amplitude reflections. On the shelf, the reflectors are parallel, with moderate yet consistent amplitudes. There is significant thickening of the unit from 200 ms TWT in the south-west end of the lines to 900 ms TWT in the north-east end of the lines. As suggested by its penetration in each of the wells in the study area, this is a widespread depositional sequence. The sequence also continues into the deeper water where its thickness becomes more constant.

Faulting in this depositional sequence is minimal but present nonetheless. Figure 3.19 shows a small fault family cutting through numerous depositional successions, one of which is S4. This figure also shows the typical seismic character, as described above, of this unit and its location relative to other depositional sequences.

3.4.9 T3 Sequence Boundary

The T3 sequence boundary marks the upper boundary of the S4 sequence and was dated as Late Eocene-Early Oligocene from biostratigraphic analysis (Bell et al., 1989). This marker coincides with the Baffin Bay Unconformity (McWhae et al., 1980) and thus separates the syn-drift sediments of the Kenamu and Cartwright Formations from the overlying post-drift sediments of the Mokami Formation (Enachescu, 2006b). In seismic sections it is represented by a purple marker and is denoted as T3.

The T3 sequence boundary was penetrated by each of the wells in the study area therefore illustrating its regional presence. It extends through the entire basin from the nearshore to the deep water. The quality of the marker is relatively consistent throughout the basin (except below the shelf break in areas of poor data quality) and is considered a good quality marker when compared with other seismic markers in the basin. Mapping of this reflector was fairly confident even beyond the shelf break yet sequence boundaries T3 and T4 are often obscured by water bottom multiples on the shelf edge. The T3 sequence boundary dips along the shelf edge but has little structural relief. The dip of the reflector is steeper at the shelf break but becomes increasingly gentler in the deep water (Figure 3.20). In deepwater regions it has been interpreted as a strong peak. Seismic data in this area show no supporting evidence (such as downlapping) to suggest that the horizon is a prominent unconformity (Martin et al., 2006) and shows onlap (Figure 3.20).

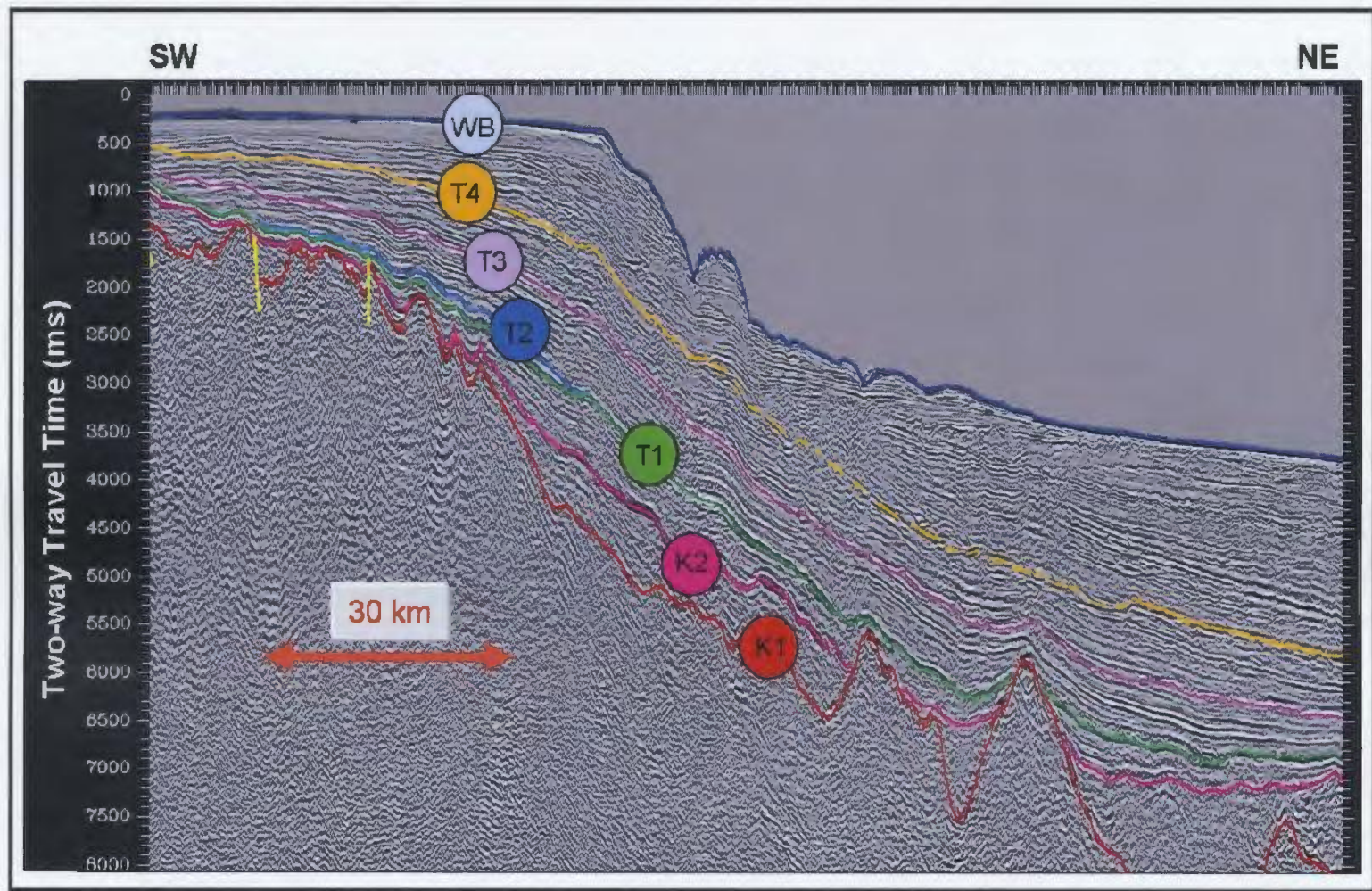


Figure 3.20 – Regional dip seismic line showing the extent of the T3 seismic boundary coloured in purple.

The T3 sequence boundary is affected by a major fault family (Figure 3.19). This is one of the most significant fault groups in the area and appears to have cut most of the Tertiary sedimentary sequences.

3.4.10 Seismic Sequence S5

This seismic unit is defined at the bottom by the T3 sequence boundary (top of the Kenamu Formation or Baffin Bay Unconformity) and at the top by the T4 sequence boundary (base of Saglek Formation). Seismic sequence S5 has been interpreted as containing the Mokami Formation and was deposited during the Oligocene and Early Miocene. When intersected by wells this formation consists entirely of marine shale and is a relatively thick succession. The correlation confidence of the T3 and T4 markers is fair to good, and this suggests that the depositional sequence S5 is reasonably defined in the study area.

This seismic unit varies in time-thickness throughout the study area. On the shelf edge it is relatively thin amounting to about 200 ms TWT in places. It begins to thicken in the NE direction and becomes more uniform in thickness close to the shelf break where it reaches thicknesses of 500 ms TWT. On the shelf it is difficult to describe the internal character of this package since it frequently contains water bottom and peg leg multiples. In places it appears to contain primarily sub-parallel reflectors with minimal structural relief. In the deeper regions beyond the shelf break the seismic unit becomes chaotic and internal reflectors become exceedingly difficult to see. This seismic sequence marks the beginning of post-drift sedimentation and is a highstand depositional sequence.

A representative seismic section showing S5 can be seen in Figure 3.21. Seismic sequence S5 is a continuous seismic unit present throughout the basin. It is penetrated by each of the wells in the study area. The T4 sequence basal boundary was primarily interpreted on the GSI 2003 and 2004 vintage data. The maps generated using this interpretation are believed to be a true representation of the unit since there are only a few small-scale structural features at the level of this marker.

There is also evidence of faulting in S5. Figure 3.22 shows faults cutting through the S3, S4 and S5 sequences. There are similar fault structures shown in the deep water which also cut through the S5 sequence.

3.4.11 T4 Sequence Boundary

The T4 sequence boundary marks the top of seismic sequence S5 and contains the Mokami Formation. The T4 marker is the uppermost seismic horizon with geological significance that was mapped during this study. The T4 horizon is coloured orange on interpreted seismic sections. It separates the underlying Mokami Formation from the conglomeratic (on the shelf) Saglek Formation of Late Miocene to Late Pliocene age. This horizon is regionally a fair to good marker. On the shelf it represents a large acoustic impedance contrast and would probably have a high amplitude but it is often obscured by sea bed multiples thus making it occasionally difficult to pick. Likewise, the

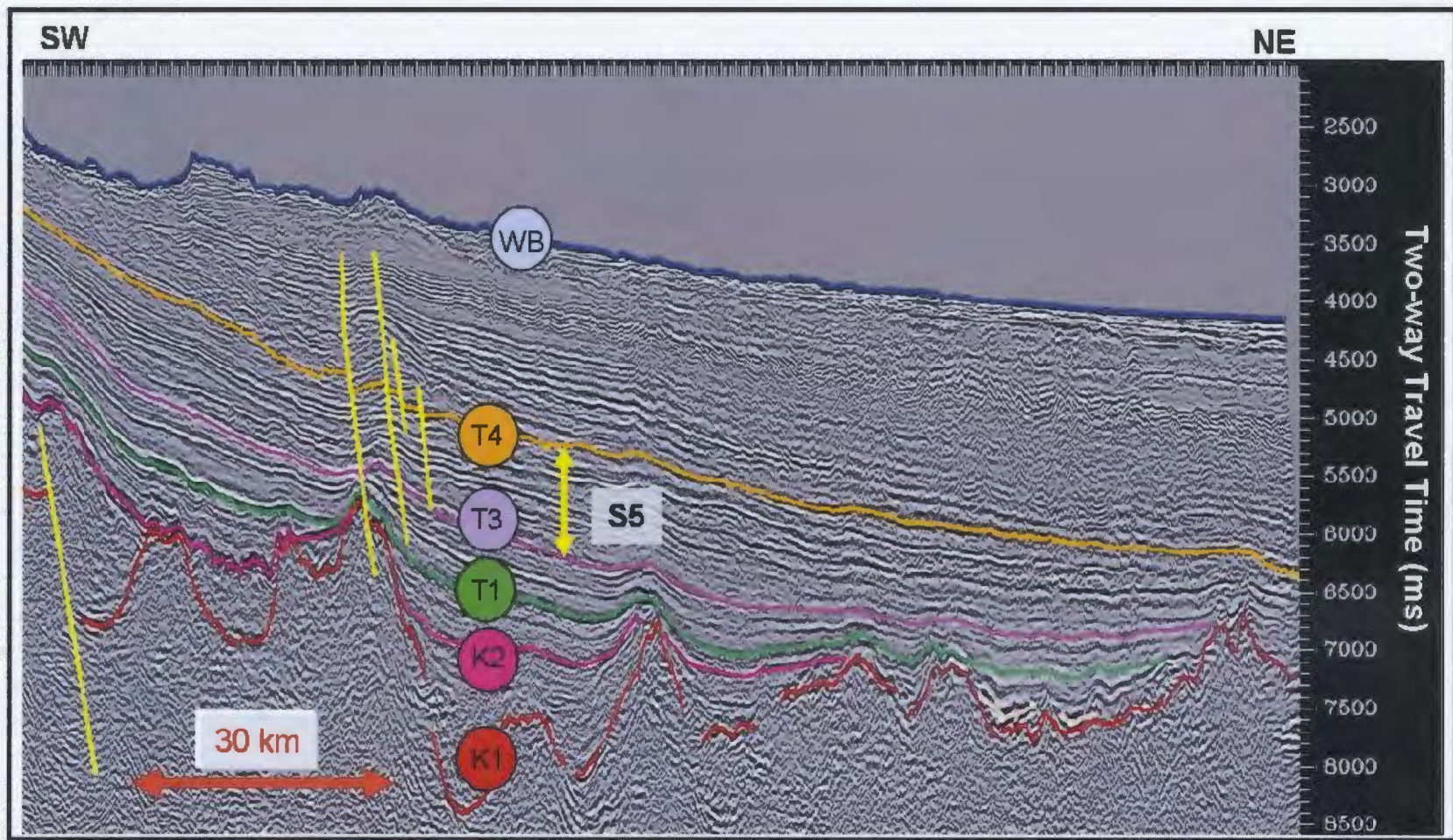


Figure 3.21– Dip seismic section illustrating the typical characteristics of depositional sequence S5.

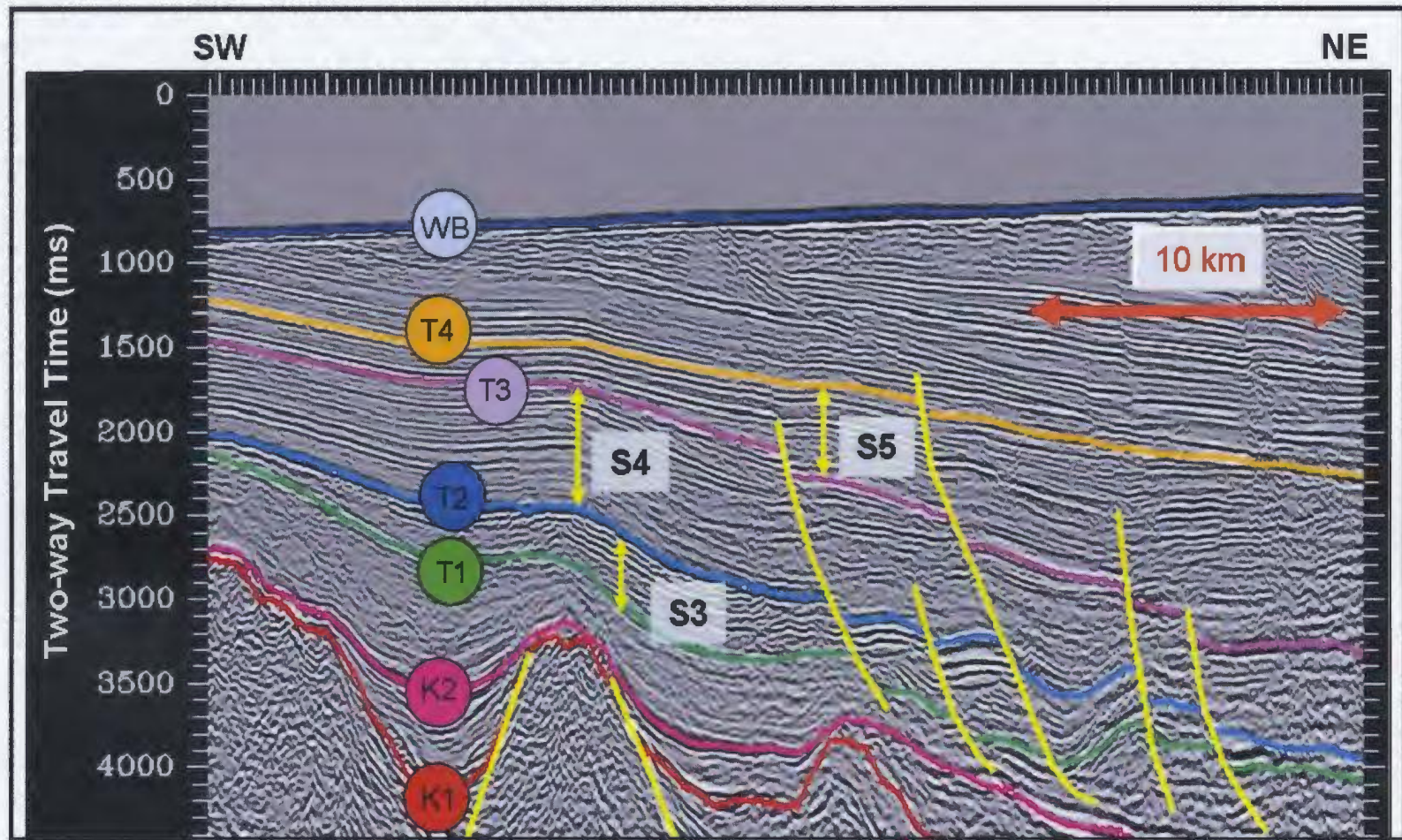


Figure 3.22 – Dip seismic section which shows several faults cutting through seismic sequences S3, S4 and S5. Also note the T3 sequence boundary in purple and the T4 sequence boundary in orange.

horizon is difficult to interpret through the shelf break and therefore interpretation into the deep water is less certain.

This sequence boundary has little local structural relief and gently dips basinward. It is uncertain from the seismic data whether or not this marker is an unconformity, as is described in all published lithostratigraphic charts (McWhae et al., 1980). In spite of not having strong seismic arguments, this horizon remains described here as an unconformity, representing most likely a depositional hiatus rather than a strong erosional episode.

This sequence boundary is cut by several faults which extend from the T4 sequence boundary into the T1 sequence boundary (Figure 3.21 and Figure 3.22, above). Every well in the study area encountered this sequence boundary and this regional seismic interpretation shows T4 to be a wide-spread depositional surface.

This sequence boundary has only been interpreted on the GSI 2003 and 2004 data since the 2005 data was made available while work on the thesis was in progress. The 2005 lines were used only to confirm the interpretation when fault or horizon aliasing were presumed.

3.4.12 Seismic Sequence S6

Seismic sequence S6 is bounded on the top by the seafloor and at the base by sequence boundary T4. The sequence includes the Saglek Formation and unnamed glacial beds and its age range is from Late Miocene to Late Pliocene/ Pleistocene. The Saglek Formation contains mostly porous, conglomeratic sandstone. This depositional sequence is quite thin towards the shelf and greatly thickens out in the deep water

indicating what is interpreted to be a major phase of thermal subsidence in the basin accompanied by pronounced easterly tilting.

The major issue with this depositional sequence is that it contains further sequence boundaries and sub-divisions that significantly thicken out into the deeper water. These subdivisions do not have associated age or lithostratigraphic nomenclature; none of these younger sub-divisions has been interpreted. Most of these seismically recognized sub-units become important on the slope and in deepwater and may be important when considering drilling hazards for deep water drill targets. Alternatively, these sub-units may contain sandstone turbidites and constitute viable drilling targets on the upper and lower slope. The stratigraphy of the Labrador shelf was defined through well cuttings, cores and logs and since all the wells were drilled on the shelf, the deep water deposits were never reached or formally described. Figure 3.23 shows a relatively good quality sequence boundary T4 pick through the shelf break and into the deep water. Above T4, several younger sequence boundaries exist which have no formal lithostratigraphic correspondence and were traditionally described as unnamed slope and deep water deposits and glacial beds.

This seismic sequence is present throughout the entire study area and likely exists within all of the Labrador Sea. It varies in time-thickness from tens of milliseconds (TWT) closer to the Labrador shoreline to as much as 2000 ms TWT on the lower slope. In the deep water, S6 forms a significant portion of the sedimentary cover of the extended basement blocks, transitional crust, exhumed mantle and oceanic crust (discussed below).

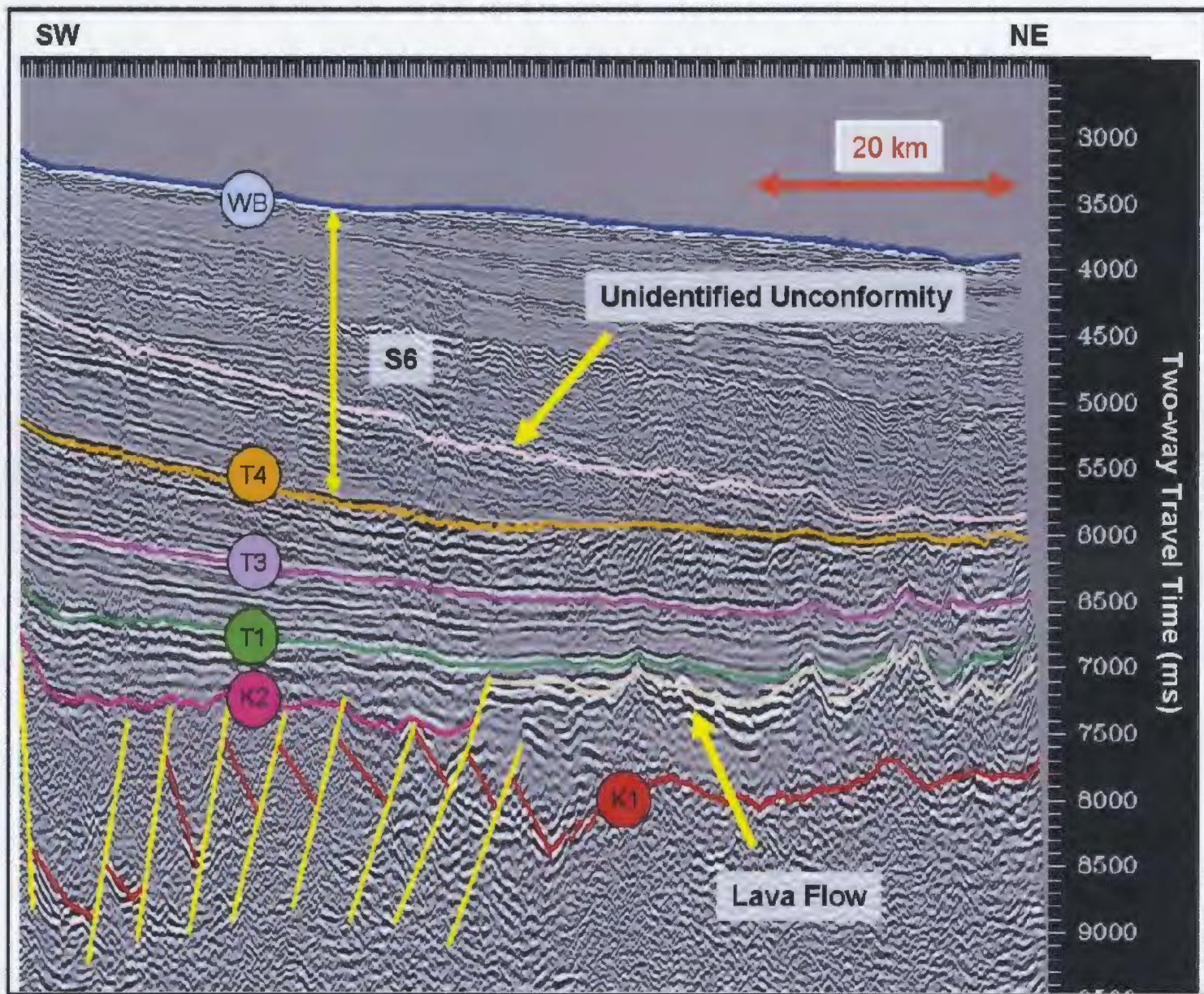


Figure 3.23 – Dip seismic section illustrating the S6 sequence as well as at least one unidentified unconformity within S6 (light pink marker).

Internally it contains mostly parallel reflections as well as strong markers representing previously unnamed sub-sequence boundaries. Clearly the sequence can be further subdivided in several units that internally have their own individual characteristics. These sub-sequences show the manner in which the continental shelf was built and progressed seaward during basin deepening and tilting but their description is beyond the scope of this study. An illustration of just one of these sub-sequence boundaries can be seen in Figure 3.21.

The S6 seismic sequence is always underlain by S5 and is bounded at the top by the present-day water bottom. It may be argued that the top of the Saglek Formation should constitute the sequence boundary T5 and should be regionally interpreted, but unfortunately, the unconformity that separates the Saglek Formation from the overlying glacial beds is again difficult to distinguish in seismic data due to its low amplitude as well as interference from sea bed multiples. This sequence has been penetrated by each of the wells in the study area thus illustrating its widespread deposition. The Saglek Formation will therefore be included in seismic sequence S6 along with the presently unnamed sub-units and glacial beds. The sequence also includes young slope deposits that greatly thicken on the slope and in the deep water and in some areas contain dense normal (gravity) faults.

3.4.13 WB Horizon (Water Bottom)

The uppermost horizon that was interpreted was the water bottom. In seismic sections it is denoted WB and its colour is dark blue. The water bottom is marked by a very strong continuous horizon which has very high amplitude and represents a large

acoustic impedance contrast between the water above and the unconsolidated glacial deposits below. This horizon was very easy to map and was interpreted on all of the 2003, 2004 and 2005 data which were acquired, therefore making it an excellent quality marker. This horizon shows little local structural relief but denotes a relatively flat shelfal area, a steeply dipping shelf edge and a relatively flat deep water component. Examples of the quality of this marker can be seen in Figures 3.14, 3.15, 3.17, and 3.19-3.23, 3.25.

Figure 3.24 shows a bathymetry map based on the interpretation of the WB horizon. On this map there is an evident coastal bathymetric low evident which is called the Labrador Marginal Trough and was created during the glacial period. From the bathymetry map other regional features can be seen within the study area. These features are, from north to south, the Nain Bank, the Hopedale Saddle, the Makkovik and Harrison Banks, the Cartwright Saddle and the Hamilton Bank. Figure 3.24 illustrates these modern bathymetric features as well as shows where the previously drilled wells are located with regards to these features.

3.4.14 Serpentinized Peridotite Ridges (PR)

There are two additional interpreted markers on the Labrador shelf which are not included in the classic lithostratigraphy chart (McWhae et al., 1980) probably because this chart was defined from shelf well information and seismic data and the structure of the continental slope and rise was less known at that time.

One of these horizons has been interpreted to be serpentinized peridotite ridges. Serpentinization is the process by which pre-existing pyroxene and olivine, which is

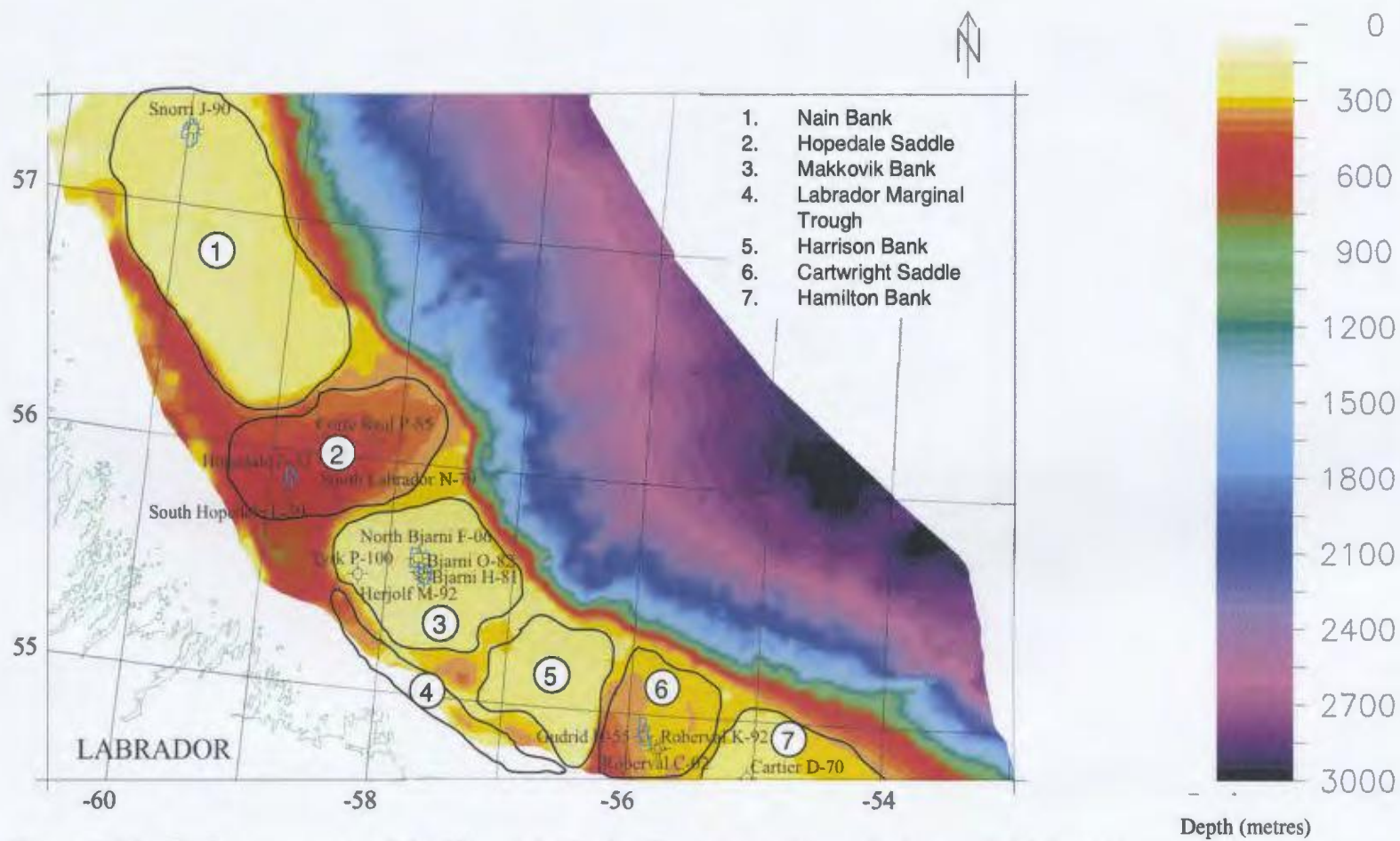
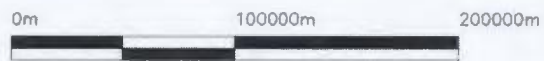


Figure 3.24 – Bathymetry map of the Hopedale Basin illustrating relevant bathymetric highs and lows. Annotations are: 1 = Nain Bank, 2 = Hopedale Saddle, 3 = Makkovik Bank, 4 = Labrador Marginal Trough, 5 = Harrison Bank, 6 = Cartwright Saddle, 7 = Hamilton Bank.



typically found in igneous ultramafic rocks such as peridotites, undergo metamorphism and hydrothermal processes to form a new metamorphic rock called serpentinite (Blatt and Tracy, 1996). During the drilling of ODP Leg 210, Site 1277, it was reported that there is a wide zone of apparent transitional crust. At drill site 1277 they encountered the basement and recovered basalt flows along with serpentinitized peridotite, sediments and gabbro proving their presence east of the Grand Banks. Louden (2002) and Louden and Lau (2002) illustrate the seismic character of these serpentinitized peridotites along the Labrador margin and describe it as a prominent marker which marks the top of the high-velocity serpentinitized mantle. The velocity of this zone has been determined to be 6.4-7.7 km/s from refraction seismic data (Chian et al., 1995) and likely produces significant seismic signature. This interpreted exhumed continental mantle area can be seen on consecutive seismic lines and is considered as the continent-ocean transitional zone.

Seismic indication of serpentinitized peridotite bodies rising above the Cretaceous sedimentary sequences appears at the end of the longer survey lines, that is, the ones from the 2003 and 2004 surveys. In places it accompanies the distinct lava flows (next section) and appears to underlie either the lava flows (where they exist) or S2.

This PR interval is seismically similar to the seismic basement (upper boundary defined as K1). There is little internal structure and choppy reflectors with conflicting dips can be seen in areas where serpentinitized ridges were detected. It differs from the seismic basement in that it forms sharp ridges, sometimes rising abruptly above the Cretaceous layered sediments appearing like mounds rather than the typical horst and graben features which define the extended continental basement. Therefore it could be argued that it is the PR horizon structure and not the seismic character which defines this

seismic unit. Regional mapping of this unit is tentative and based only on reflection seismic character. It is also difficult to present a detailed regional map due to lack of seismic coverage of the area where serpentized peridotite ridges are present.

The age of this unit is unknown from well penetrations but it is assumed that it is older or the same age as the overlying Markland Formation (S2). Consequently it can be estimated to be early Late Cretaceous in age. The composition of this formation is unknown (due to lack of drilling) yet Chalmers and Pulvertaft (2001) using magnetic and seismic data, and Loudon (2002), Enachescu et al. (2006) and Sibuet et al. (2007) by comparison to deepwater features in front of the Grand Banks and Iberia margins, have proposed that it is serpentized peridotite and makes up a larger continental-ocean transitional crust than previously thought.

Figure 3.25 shows a seismic line which images several serpentized peridotite ridges in the deepwater of the Hopedale Basin. The line illustrates the seismic character and position of this unit within the previously defined seismic sequences.

3.4.15 Lava Flow (LF)

Although not included in the lithostratigraphy chart (McWhae et al., 1980), there is evidence of yet another prominent seismic unit with an associated top marker (LW) present in the deep water, at the end of the longer seismic lines (2003 and 2004 vintage). This top marker is interpreted as the lava flow marker that defines a large domain (Enachescu et al., 2006; Enachescu, 2006b). It has been interpreted as a lava flow since it

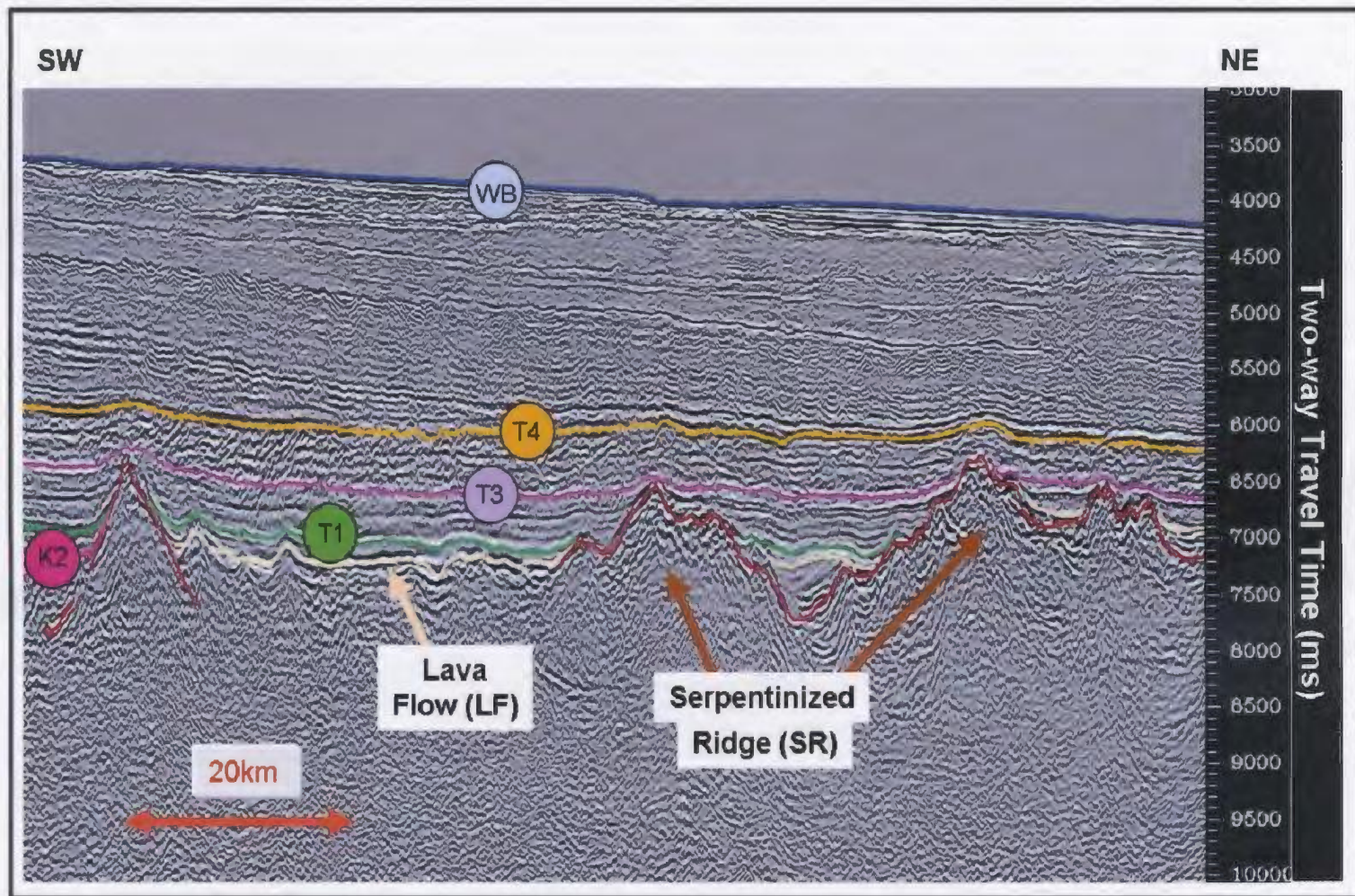


Figure 3.25 – Dip seismic section showing the interpreted serpentinized peridotite ridge sequence and its relation to the other horizons which have been interpreted in the study area.

has a large areal distribution with several strong reflections illustrating a large change in acoustic impedance. It should be noted that other researchers have interpreted this unit as true oceanic crust basalts (Srivastava, 1978 and Srivastava and Roest, 1999).

Unfortunately the 2005 data do not extend as far into the deep water to allow detail mapping of the horizon. The seismic marker LF has very strong amplitude and is characterized by a strong peak-trough-peak pattern. The LF reflector is relatively flat and parallel to the overlying sedimentary layers. There is some structural relief on the LF marker and the reflector is segmented in places probably indicating multiple lava flow sheets.

The basinward extent of this horizon is unknown. It was mapped on the 2003 and 2004 data and at the very end of some of the 2005 vintage data. It is a discontinuous marker in that it onlaps and terminates at large peridotite or basalt ridges. On some seismic lines it is less prominent than on others, yet its character is unmistakeable. It appears to be overlain by S2. Its seismic properties differ greatly from S1, which disappears before reaching the LF domain. Directly below the LF marker the geology is unknown. It appears to be both extended and intruded continental basement or tectonized serpentinitized peridotite mantle with occurrences of distinct serpentinitized ridges.

Seismic mapping of this horizon is difficult due to the limited amount of data recorded that far into the deep water. Nonetheless the areal extent of the lava flow domain and its internal fracturing is important when researching the geodynamic evolution of the Labrador Sea. Figure 3.26 shows the typical seismic character of the

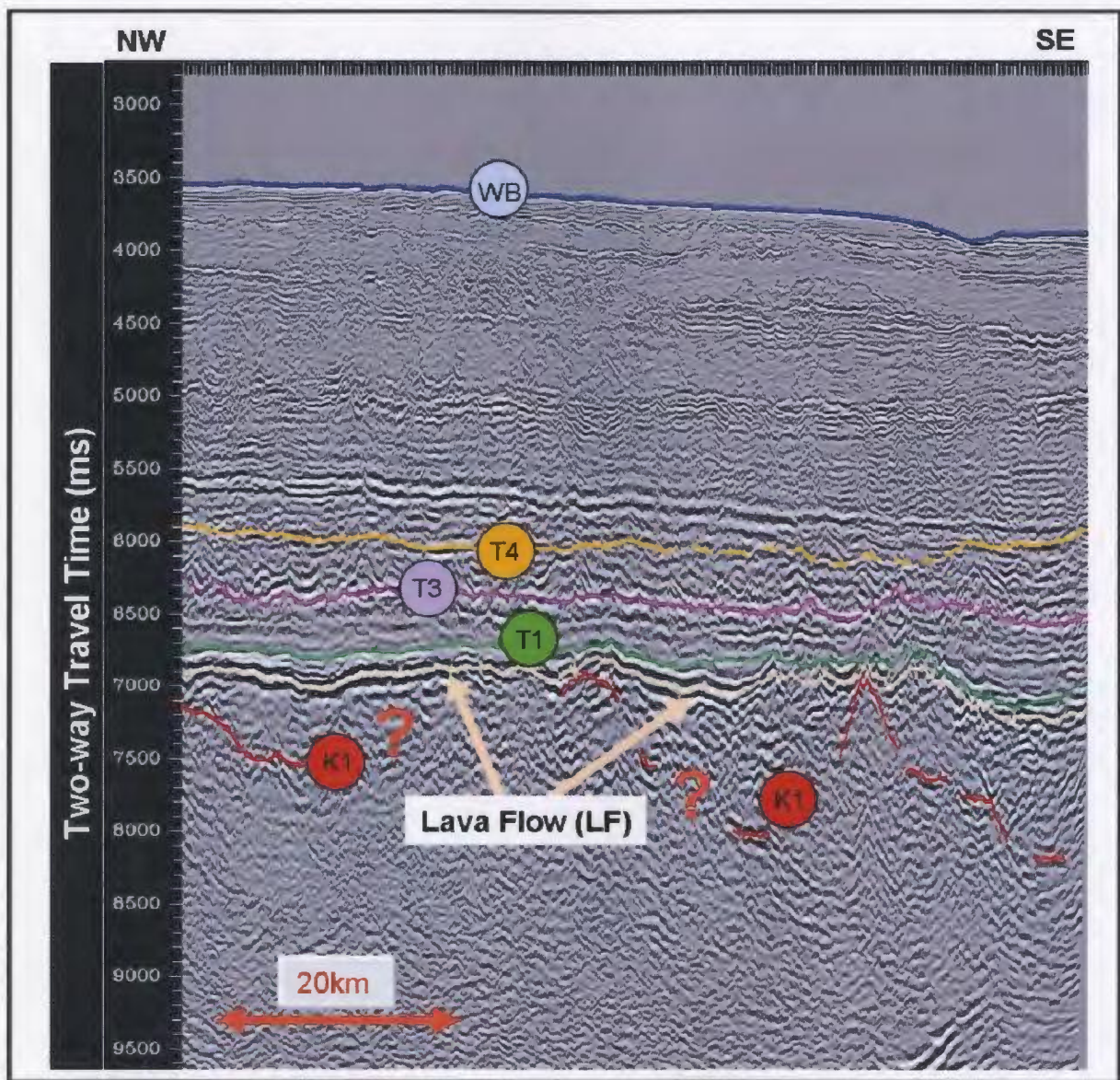


Figure 3.26 – Strike seismic section showing the typical seismic characteristics of the interpreted lava flows and its relation to other seismic horizons and sequences within the study area.

interpreted lava flows and their relationship to the overlying sediments and the underlying serpentized mantle. Please note that this is a strike line and not a dip line.

Chapter Four: Kinematic modelling of a representative Hopedale Basin dip profile

4.1 Purpose

This chapter has the following objectives:

- a.) Using the seismic 2D grid, identify structural and stratigraphic features within the basin, correlate them with various stages of geodynamic evolution for the Hopedale Basin and synthesize sequences into a simplified tectono-stratigraphic chart for easy reference;
- b.) Depth convert a representative seismic line passing through the Hopedale Basin to build a typical depth model in a dip direction, to view basinal structural features in depth and to divide the seismic section into the following major seismic units: 1. prerift basement, 2. synrift sequence, 3. syndrift sequence, 4. postdrift sequence (final subsidence stage), and 5. transitional crust (exhumed mantle, serpentinized ridges and lava flows).
- c.) Using the depth converted seismic section each of the seismic sequences will sequentially be removed starting with the youngest deposits (postdrift) and finishing with the oldest deposits (synrift). After each removal the depth section will be flattened on the upper sequence boundaries. This is known as a kinematic model. A kinematic model is a step-by-step reconstruction of the basin during each stage of geological evolution thereby illustrating the circumstances under which each of the major stratigraphic sequences was deposited. This will be conducted for the succeeding stages of basin evolution: synrift, postrift, syndrift and postdrift. No attempts were made to

estimate the effect of intrabasinal basement erosion or to balance the cross-sections as this was beyond the scope of this thesis.

d.) Finally, to use all of the acquired information to generate ideas and concepts regarding the geodynamic evolution of the Labrador Shelf during rifting, after rifting and during the subsidence stage while gaining insight into the establishment of the Hopedale Basin's petroleum system.

4.2 Depth Conversion and Kinematic Modelling - Methods

To enable the proper modelling of the Hopedale Basin a representative seismic section was selected - the dip line passing through the North Bjarni F-06 well. This line was chosen for the following reasons: 1) it adequately represented the structural style within the study area; 2) the presence of the North Bjarni F-06 well on this line provided the geologic identification of the seismic horizons (well ties); 3) the seismic quality on this line was fair to good allowing reasonably confident interpretation along the line; 4) this seismic line continues farther into the deep water beyond the ending of the majority of the seismic lines collected in 2005; and 5) all significant horizons were interpreted on this line.

This line was interpreted using the processes and correlations described in Chapter 3. The horizons were gridded using X and Y spacing of 2000 metres and a search radius of 15 kilometres (due to the spacing of the data) in SeisWorks®. The gridding algorithm in SeisWorks® searches the horizon for control points that fall within a radius of each node (15 000 metres) and computes an average two-way travel time

value for the node. The values for TWT are weighted according to their proximity to the node. Next, the seismic traces and the time horizons were converted into depth. To do this, the Depth Team Express® (DTE®) program within the Landmark® suite was used. DTE® does not read horizons but instead understands gridded surfaces so the horizons were gridded in ZMap®. Next, the well picks were loaded into DTE® based on interpreter preference (where multiple interpreters had entered different picks). The C-NLOPB well picks listed in Table 3.3 were used. Also, the time-depth information and newly gridded surfaces were loaded into DTE®.

Once all relevant information was loaded, it was necessary to assign well picks to gridded surfaces. Landmark® is unable to understand the correlation between well tops and interpreted horizons therefore this relationship was defined. DTE® then interpolated interval velocities (from the time-depth information) between consecutive well picks and applied this velocity to all regions between the gridded surfaces assigned to those well picks. In my study area, this method has one significant limitation: there is limited well data on the shelf and no well data in the deep water therefore making depth conversions difficult. Average interval velocities between well picks were applied to the data for the entire survey, regardless of location. There are likely errors in the values calculated for the deeper water depth regions due to ignoring compaction of sediments from the overlying water column. Once this procedure was completed, the velocity model was created.

With this depth model, the seismic line, as well as the horizons, were converted to depth using TDQ®. This program is an application which simply applies the velocity

model created in DTE® and converts horizons or seismic traces from time to depth or from depth to time, whichever is required. Each horizon was converted to depth separately while all the seismic traces along the line were converted simultaneously. The newly created depth seismic section and depth horizons were viewed in SeisWorks® by opening a new Depth Session.

With the depth section, the synrift, postrift, syndrift and postdrift sedimentary sequences were identified as well as areas with exhumed mantle, serpentinized ridges and lava flows. This section was then coloured in CorelDraw® to better illustrate the various tectono-stratigraphic sequences. Next the depth seismic section was displayed in SeisWorks® and it was flattened on each of the upper horizons defining major tectono-stratigraphic sequences. These successive seismic sections were then imported into CorelDraw® and colour-coded to form four panels representing the end of synrift, the postrift, the syndrift and the postdrift geodynamic stages.

4.3 Tectono-Stratigraphy

In this section the distinctive structural and stratigraphic features of each evolutionary stage will be described and illustrated including basement involved faulting (Section 4.3.1). The geodynamic stages will then be compiled into a tectono-stratigraphic chart that will include ages of particular tectono-stratigraphic sequences with supporting evidence from the structural and stratigraphic features.

4.3.1 Basement Tectonics

During intracratonic rifting the prerift basement which consists of Precambrian metamorphic rock and lower Palaeozoic carbonates was extended, causing numerous faults and rotated basement blocks.

Balkwill et al. (1990) has characterized the faults as northwest-striking master faults created during rifting. A map of the basement along with significant master faults created from the GSI data can be seen in Figure 4.1. These master faults seen on this map are several kilometres long and are comparable to those shown by Balkwill et al. (1990) as well as Balkwill (1987) and Bell et al. (1989). Balkwill (1987) states that each of the master faults are linked to one another by shorter, orthogonal transfer faults that are difficult to image and directly identify in the GSI dataset but they can be inferred by the offset of the master faults. These master faults dip both landward and seaward although the seaward dipping faults usually prevail, resulting in the creation of rotated basement blocks and half grabens (Balkwill, 1987).

When the map in Figure 4.1 is compared to previously published maps, there are subtle differences possibly due to the quality and density of data which was available during the time of mapping. The most significant similarities are the presence of the long, northwest-striking, down-to-the-east master faults which are linked to presumed shorter northeast-striking faults (Balkwill et al., 1990). When compared to the basement structure map created by Balkwill et al. (1990) and Balkwill (1987) the main master faults appear relatively in the same locations as seen in Figure 4.1. The new basement

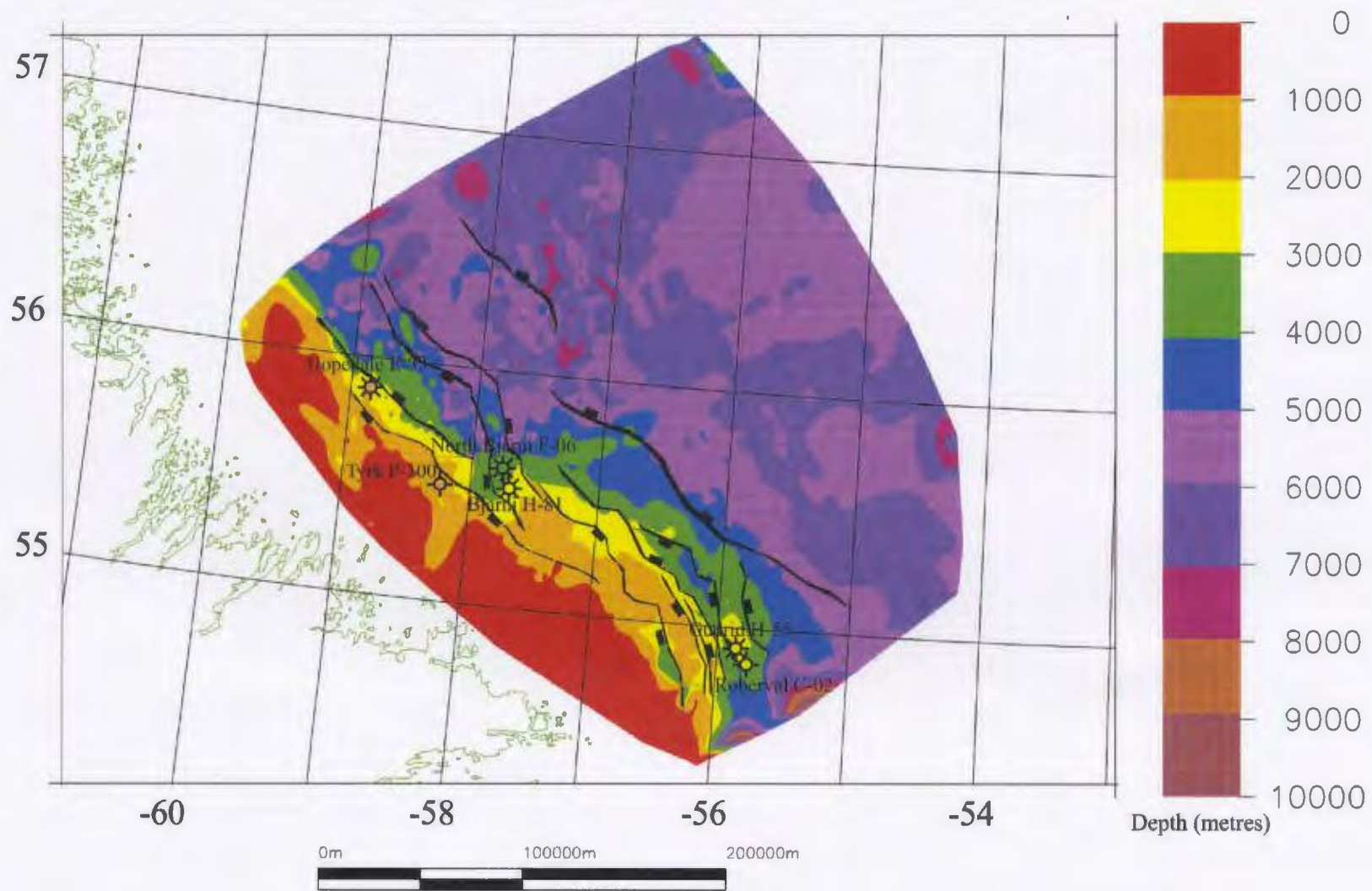


Figure 4.1 – Depth structure map of the seismic basement (K1 horizon) in the study area. Black lines represent fault planes and tick marks show direction of normal faulting.

map created from this study shows several other less important faults not included in the map produced by Balkwill et al. (1990). Balkwill et al. (1990) and Balkwill (1987) including the minor northeast striking faults as described in the text which are not seen in Figure 4.1.

When compared to the basement structure map in the Labrador Basin Atlas (Bell et al., 1989) there are more noticeable differences. In the region of the study area Bell et al. (1989) show significantly longer northeast-striking faults than described by Balkwill (1987) and Balkwill et al. (1990). In some regions, these northeast-striking faults are considerably longer than the main master faults. Mapping of long northeast trending faults with any degree of confidence was difficult. In contrast, most of the master faults shown in the atlas are consistent with those shown in Figure 4.1.

Interestingly, the master faults shown in the southern part of the Bjarni area basement map coincide with fault mapping currently being done by Stead (M.Sc, in progress) which has been conducted on the same GSI data set. Many of the faults mapped in this thesis continue south into the study area of Stead (in progress).

Overall, the general trend of the faults shown in Figure 4.1 coincide with those mapped and published by other authors in the past 20 years. These faults were created as a result of rifting during the Early Cretaceous and greatly influence the structure of the basement as well as the overlying postrift sediments. Some of these faults extend higher into the basin's sedimentary infill while others remain confined to the basement and synrift sedimentary sequence.

4.3.2 Evolutionary Stages and Structural Features

The geodynamic evolutionary stages have been denoted as in Figure 4.2. The Hopedale Basin is characterized by the presence of typical extensional structures such as rotated blocks, horst and grabens and normal listric faults that affect the basement or reside only within the sedimentary successions; some are major features while others are minor. Unexpectedly, compressional features are also present (Enachescu et al., 2006). The following section will describe some of these major features visible on numerous seismic lines or, in some cases, through most of the study area. The heading numbers coordinate with the stage numbers used in Figure 4.2. The following offers a brief description about each stage:

1. **Prerift** – Prior to the start of the intracratonic rifting the area was occupied by a large platform containing mainly Precambrian metamorphic basement pertaining to the Grenville, Nain and Churchill provinces (e.g. Taylor, 1979 and 1981). At some places, during a lower Palaeozoic period of basin formation, carbonate successions (limestones and dolomites) were deposited and then folded or tilted during the Appalachian orogeny. Peneplaning of the Precambrian and Palaeozoic formations followed. Any structural features or remnants of the Palaeozoic carbonate formations are difficult to resolve with available geophysical data and the sparse exploration drilling in the basin.

In this study the prerift stage includes all the metamorphic, volcanic and sedimentary formations that were present prior to the onset of intra-continental rifting.

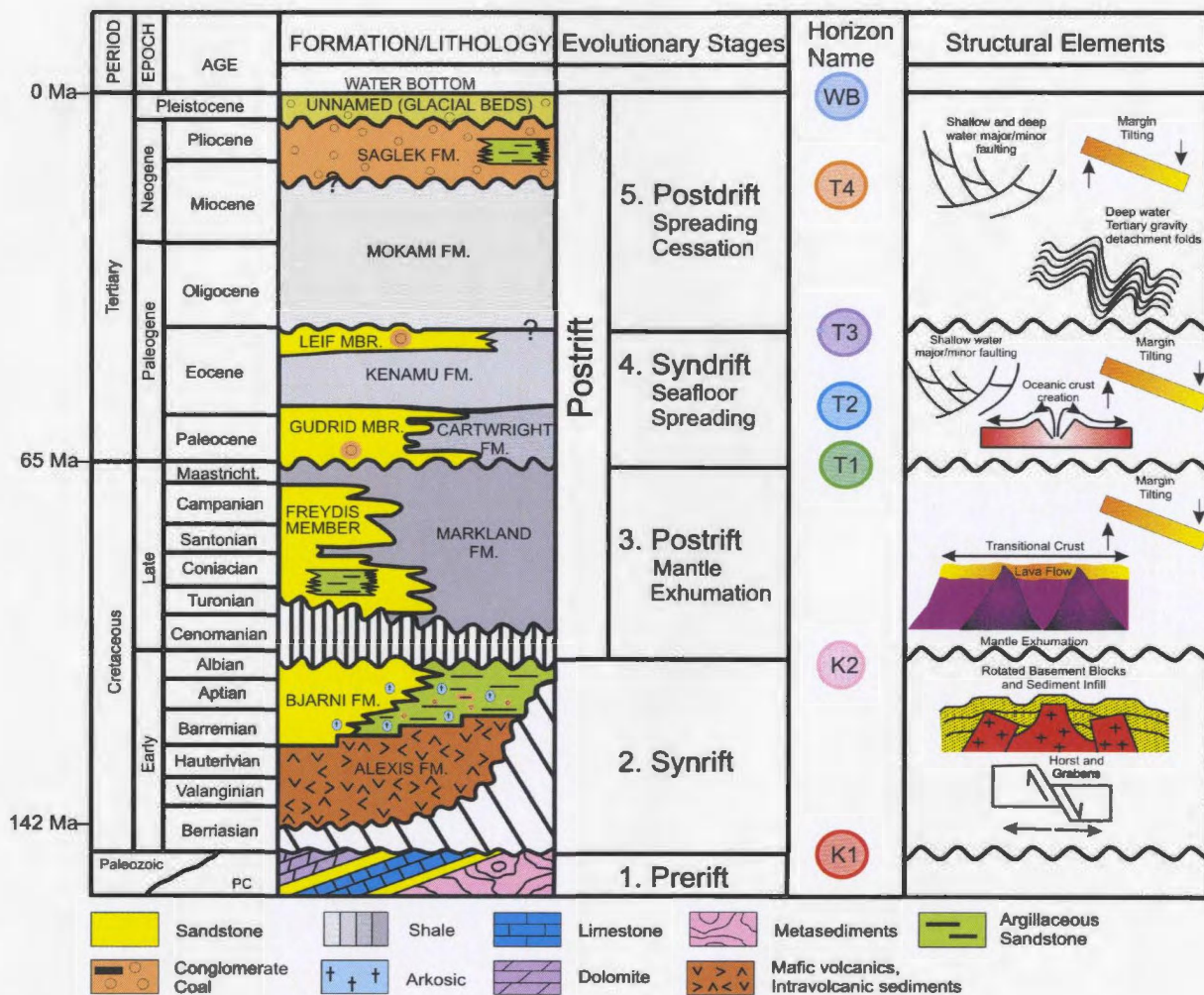


Figure 4.2 – Hopedale Basin tectono-stratigraphic chart. Modified after Figure 2.2 (McWhae et al., 1980, GSC). Geodynamic evolutionary stages after Enachescu (2006) and timescale from Gradstein et al. (2004).

They were partially peneplained during most of the Late Palaeozoic to early Cretaceous (or in places possibly Late Jurassic) time and presently form the basement of the Hopedale Basin.

2. **Synrift** – At the start of rifting, the prerift basement was affected by numerous normal faults and started stretching, creating rotated blocks and horst and graben features. As mentioned in Chapter 3, the prerift formations are included in the economic basement which is any formation older than Cretaceous. A basal volcanic episode that produced the Alexis Formation is included in this stage. Successive basaltic flows were emplaced along the major crustal faults segmenting the prerift basement. During rifting, erosion of the elevated rift shoulders or intra-rift high basement blocks produced the Bjarni Formation which filled in depositional lows created by the faulting of the prerift basement. The Bjarni Formation also drapes on top of some of the basement highs. Continuous movement along major faults deepened the sub-basins and troughs formed between basement highs (tectonic subsidence). The deposition of Bjarni sandstone is accompanied by both thick and thin-skinned faulting. The Bjarni Formation is thicker close to the basin margin and in several depocenters near the shelf edge and slope.

Based on these characteristics the synrift stage is defined as the time period when the Earth's crust and lithosphere are being pulled apart yet there is no oceanic crust being produced (Enachescu 2006a and personal communication); sedimentary sequences formed during crustal stretching are usually deposited within rotated basement blocks. According to previous studies synrift refers to the period of time from Berriasian (and

probably older in places) to mid Albian (McWhae et al., 1980; Balkwill, 1987; Balkwill and McMillan, 1990).

3. **Postrift (Mantle Exhumation)**: Continuous thinning of the crust during the rifting stage brought the continental mantle closer to the surface while some postrift subsidence allowed a marginal sea to settle in the sagged rifted area. The mantle was then brought to upper crustal position in a marine setting. Mantle denudation occurred probably in several spurts of soft mantle material, forming several ridges parallel with the rift axis. In places significant faults penetrate the exhumed mantle allowing contact with sea water and facilitating alteration of the peridotites (Chian and Loudon, 1994; Loudon, 2002; Enachescu, 2006b; Sibuet et al., in press). This alteration of the mantle material is known as serpentinization and was identified by drilling of analogous ridges offshore Iberia and east of the Grand Banks (Pinheiro et al., 1996; Reston et al., 2001; Whitmarsh and Wallace, 2001; Tucholke et al., 2004; Shillington et al., 2004). Possible serpentinized peridotite ridges are visible in some of the longer seismic sections from the Hopedale Basin.

These features categorize the postrift sequence; therefore postrift refers to the time period after the continental crustal extension ceases. The stage is followed by thermal sag in an intracontinental setting (failed rift) and by mantle exhumation or seafloor spreading when rifting is successful (Chian and Loudon, 1994; Enachescu, 2006b). In the Labrador Sea, the initial postrift stage occurred from Cenomanian (early Late Cretaceous) to Maastrichtian (Late Cretaceous) and is synchronous with mantle exhumation and formation of several lineaments of serpentinized peridotite ridges

interpreted from seismic data but yet unproved by scientific drilling (Chian and Loudon, 1994; Loudon, 2002; Enachescu et al., 2006 and Martin et al., 2006). This is the time period when the Hopedale Basin continental basement separated from its Greenland conjugate basement. The postrift continued to present day and for the Labrador Sea evolution, has been further subdivided based on the time of seafloor spreading into syndrift and postdrift stages.

4. **Syndrift (Oceanic Crust Emplacement)**: Although not evident on the seismic lines from the study area (but indicated by existing longer reflection lines and potential field data) there was oceanic crust emplacement between the Hopedale Basin and its Greenland conjugate area. The Labrador Sea was continuing to open during the Palaeocene to earliest Oligocene due to slow oceanic crust formation at the mid-ocean ridge (Chian and Loudon, 1994; Srivastava and Roest, 1999). Also during this stage there was major and minor faulting occurring on the Labrador continental margin due to progressing accommodation of basement blocks and incipient tilting of the margin. Other than this fault movement and some draping of the sedimentary layers on older topography there are few significant structural features present within the syndrift sedimentary sequence. The sequence shows marginal thickening from the shelf to the shelf edge.

According to Enachescu (2006 and personal communication) syndrift is the time period of oceanic crust creation (basalt layer emplacement) from a mid-oceanic spreading ridge. The name is extended here to the sedimentary sequence deposited on the continental margin during oceanic crust emplacement. Drifting in the Hopedale Basin

area occurred from the Paleocene to earliest Oligocene transforming the Hopedale Basin from an intracontinental to a plate margin basin (Enachescu, 2006b).

5. **Postdrift**: The Labrador margin underwent extreme thermal subsidence and significant seaward-thickening sedimentary successions were deposited during this stage. Several important structural features are present. Most intriguing are the deep water Tertiary gravity detachment folds that were identified primarily between the Hamilton and Harrison subbasins (Figure 4.3). According to Enachescu (2006b) this could be a result of shale gravity detachment and/or transtensional movements. Shale detachment folding has been identified in other areas and modelled by Alberty et al. (2006). Just beyond the shelf break there is a significant listric fault family that creates numerous fault-bounded rotated blocks (Enachescu, 2006b). On the shelf there are also minor faults present within Late Tertiary sediments. There are other structural and stratigraphic features evident within the postdrift sediments especially in the youngest Tertiary sediments that thicken at the shelf edge and in the deepwater.

These features are evident within the postdrift sequence. Enachescu (2006b and personal communication) defines postdrift as the time period when the formation of oceanic crust stopped in the Labrador Sea area due to oceanic ridge extinction, probably caused by a dramatic shifting of the generative mantle plume. The name is also given to the sedimentary sequence deposited within the Labrador margin and sea after oceanic ridge failure. This geodynamic stage occupies the time between earliest Oligocene and the present day. These evolutionary stages will be referred to throughout the remainder of this chapter.

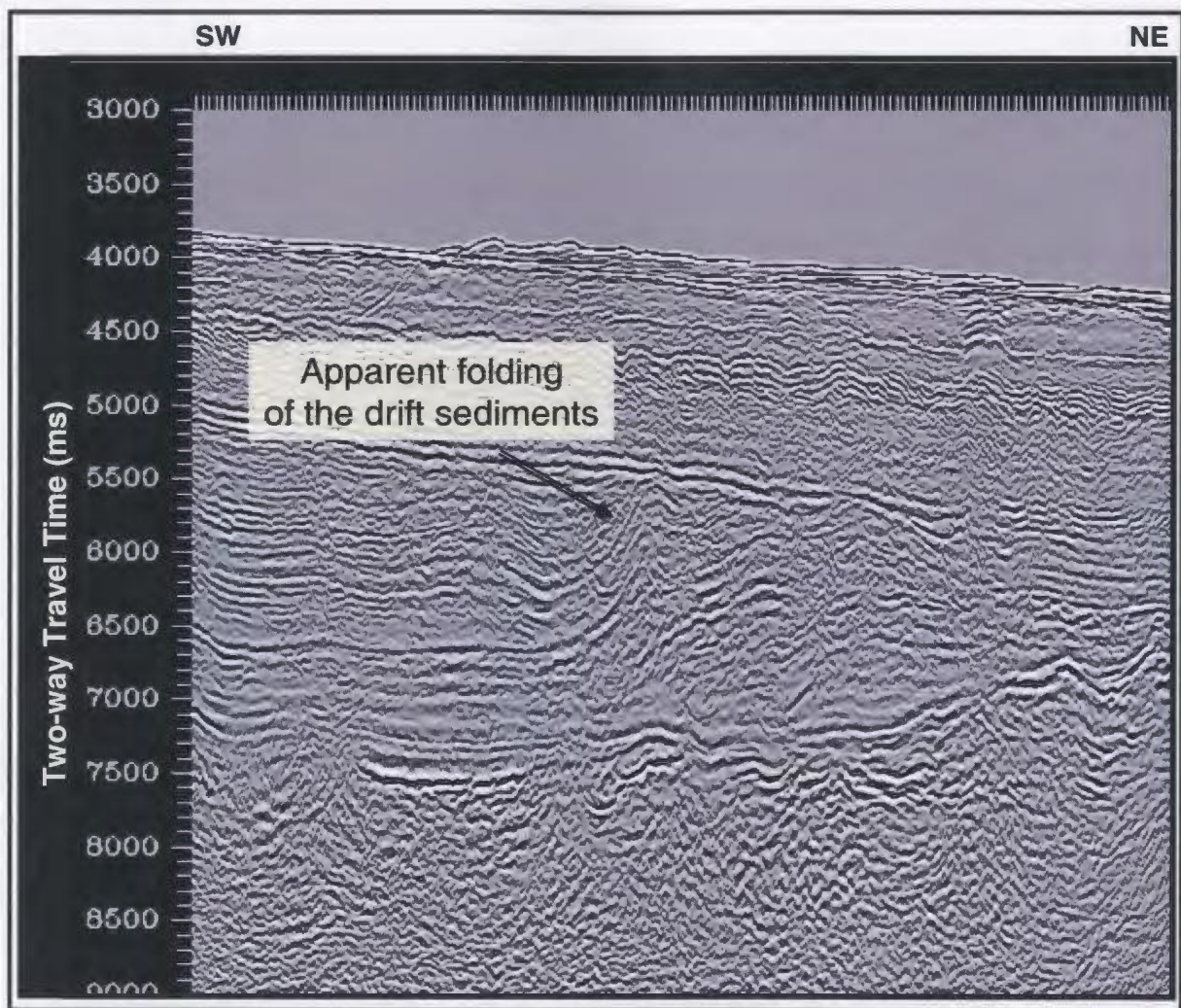


Figure 4.3 – Seismic section illustrating the postdrift Tertiary gravity folds present in the deep water section of the Hopedale Basin.

4.4 Kinematic Model

The kinematic model was based on one depth section crossing the North Bjarni F-06 well location. The section was first interpreted in two-way travel time. The seismic traces were then converted to depth using the method described in section 4.2. The seismic horizons were also converted to depth and overlain on the newly created depth section. The sections were then coloured based on the main geodynamic stages described in section 4.3.2 and the coloured depth-converted seismic section is displayed in Figure 4.4. This is a present-day representation of a depth cross-section through the Hopedale Basin.

The coloured units of the depth section represent the following:

Red - This unit on the seismic section approximately represents the economic basement which includes the prerift Precambrian basement and Palaeozoic carbonates. The upper part of this sequence is suffered brittle extension and appears segmented by numerous normal faults. Fault planes within the basement are only occasionally imaged by the seismic data but their extent at depth is uncertain. Interpreted normal faults are shown in black. At depth the basement sequence connects to the middle crust. Due to small reflectivity contrasts the base Alexis Formation seismic marker was not picked and this formation may be included with the prerift basement.

Yellow - Stratigraphically higher is the yellow section. This section illustrates the present-day thickness and distribution of the Bjarni Formation. The sandstone and shale of the formation were deposited during the rifting stage (synrift deposits).

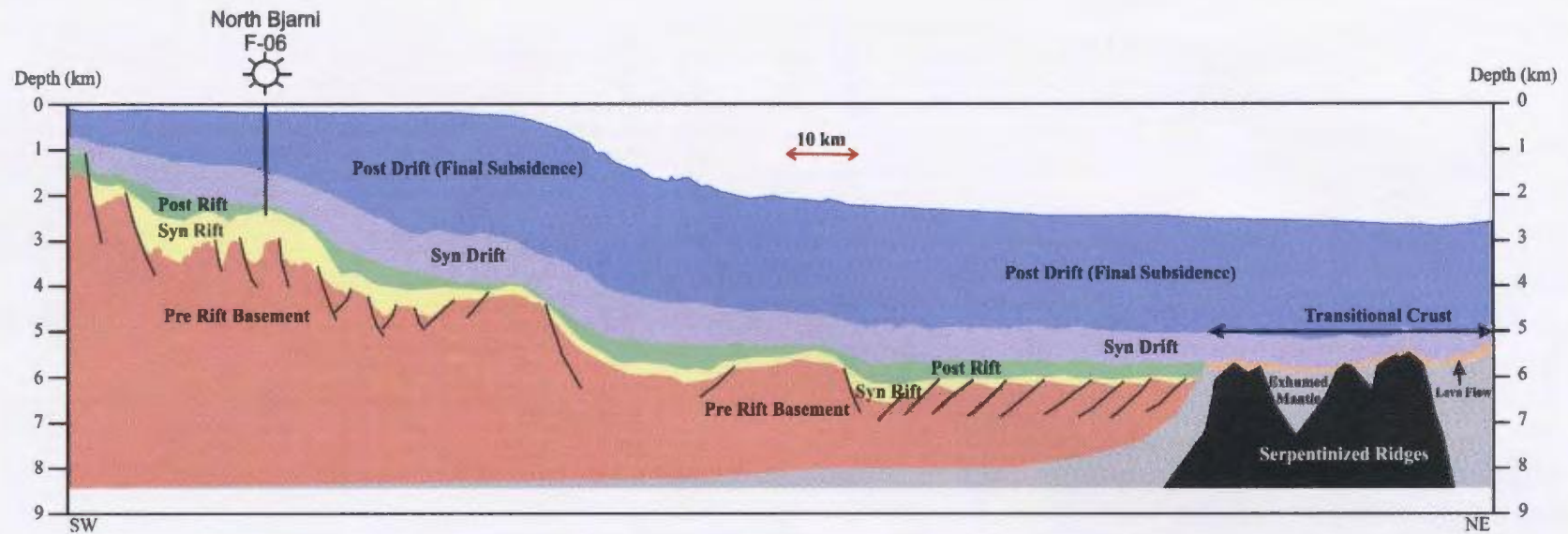


Figure 4.4 – Depth section near the area of the North Bjarni F-06 well. Red = prerift basement, yellow = synrift stage sequence, green = postrift stage sequence, purple = syndrift stage sequence, blue = postdrift stage sequence, grey = exhumed mantle, black = serpentized mantle (peridotite ridges), orange = lava flows.

Green - The postrift sediments overlying the Bjarni Formation (yellow) are represented by the colour green. This unit is made up of the Markland Formation and the Freydis Member.

Purple – The purple unit represents syndrift deposits. The formations included in the syndrift deposits are the Cartwright Formation, Gudrid Member, Kenamu Formation and the Leif Member.

Blue – This unit represents the postdrift sediments up to the present day seabed. This includes the shales of the Mokami Formation, the Saglek Formation and the currently unnamed glacial beds.

Orange – This thin section of orange represents the lava flows as described in Chapter 3. Enachescu (2006b) has referred to it as the igneous extrusive province and it has been included in the transitional crust region.

Grey – This section is mantle which has been pushed up below the stretched, thinned crust. The unit was densely faulted in places allowing the sea water to react with the underlying mantle peridotites thus creating serpentized peridotites (Chian and Loudon, 1994; Loudon, 2002).

Black – This represents the ridges of altered, serpentized mantle. The ridges form mounds that rise above or lie beneath the igneous extrusive layers.

With all stages of the geodynamic evolution of the area identified, it was then possible to successively remove each corresponding sedimentary sequence and reconstruct the paleo-depth section for each stage. These reconstructions do not include the transitional crust which was identified in the present day depth-converted section in

Figure 4.4. Also, erosion of rotated blocks was not accounted for, the section was not balanced and there was no accounting of paleobathymetry. This model is a first approximation for the tectonic and depositional history of the Hopedale Basin and further work would be required to improve this model.

Figure 4.5 illustrates a succession of possible geological models for the Labrador margin at the North Bjarni F-06 well location at the end of each of the geodynamic stages. Figure 4.5 (A) illustrates the basin towards the end of the rifting stage; approximately the end of the Early Cretaceous. At this time, intracontinental rifting of the Precambrian/Palaeozoic basement is in an advanced phase and the lateral stretching of the lithosphere had caused numerous normal faults to form to compensate for the extension. Rotated blocks and horst and graben structures were created as a result of dense normal faulting and the Bjarni Formation (synrift sediments) was deposited in relative structural lows (thicks) and onlapping and even draping the intrabasinal highs. Extension to the west appears to have been greatest since the relative throws along the faults appear greater than in the east. As well, the sediments in the west are relatively thicker than those in the east. Some faulting appears to have continued through most of the Early Cretaceous and into the Late Cretaceous as evident in Figure 4.5 (B). In the Late Cretaceous, following continental stretching an incipient thermal subsidence stage took place. This was accompanied by margin tilting. As a result the sea covered most of the rifted area, depositing fine clastics. These postrift sediments are marine shales of the Markland Formation and were deposited in the lows created by tectonic subsidence of the

SW

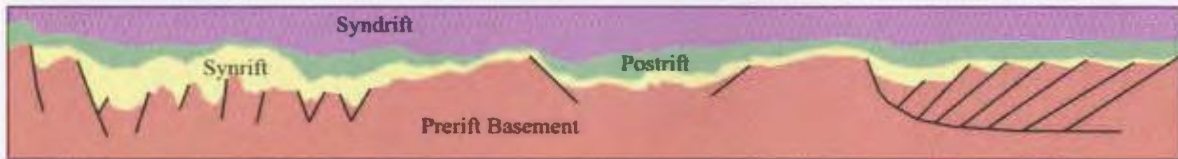
NE



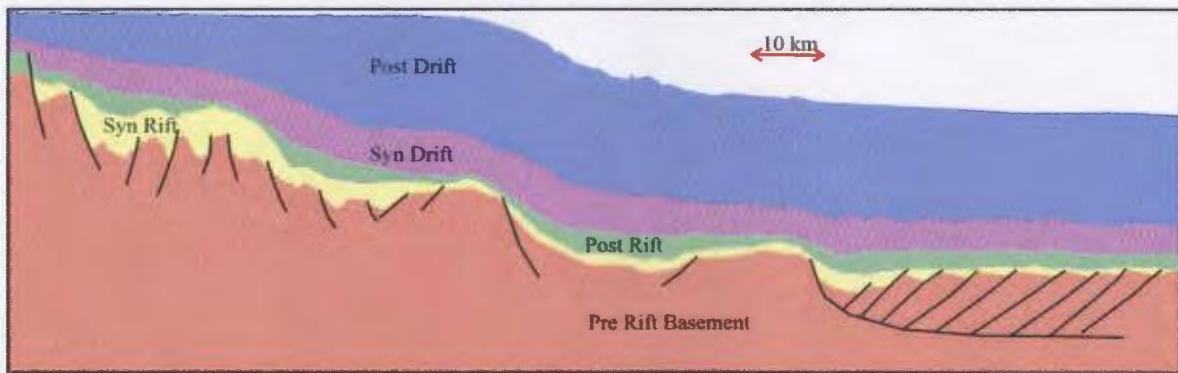
(A) Basin reconstruction towards the end of the Early Cretaceous. Appears to be greater extension towards the west with synrift deposits being thickest in this area.



(B) Basin reconstruction towards the end of the Late Cretaceous. Deposition of marine shales filled in lows caused by extension and continuous movement along basement faults and incipient thermal subsidence.



(C) Basin reconstruction towards the end of the Eocene. Thermal subsidence during this time was minimal and deposition of syndrift sediments was relatively uniform in thickness.



(D) Basin geometry at present. Thermal subsidence after oceanic ridge extinction was high therefore postdrift deposits are progressively thicker farther from the continent.

Figure 4.5 – Kinematic model of the Labrador Shelf in the region of the Hopedale Basin. In each figure red = prerift basement, yellow = synrift sedimentary sequence, green = postrift sedimentary sequence, purple = syndrift sedimentary sequence, blue = postdrift sedimentary sequence. (A) This figure represents the basin configuration at the end of rifting (total synrift deposits) at the end of the Early Cretaceous (mid to late Albian time); (B) This figure represents basin configuration at the end of the postrift (mantle exhumation) stage at the end of the Late Cretaceous (late Maastrichtian); (C) The third figure shows the basin configuration after syndrift, that is, at the end of sea floor spreading (late Eocene); (D) The last figure shows the basin configuration at present time after deposition of thick postdrift sedimentary wedges.

Bjarni Formation and by tilting. Sealevel was high during deposition of these sediments. The sequence is generally thin on the highs and thicker in the lows. It is apparent that movement along most of the basement faults has ceased because they do not cut through the postrift sediments. At the end of the Late Cretaceous sea floor spreading commenced and continued until extinction of the oceanic ridge in the Late Eocene. Figure 4.5 (C) illustrates the basin during this time.

During the drifting stage very little thermal subsidence took place although determining broader tilting or subsidence is difficult without paleobathymetric information. This is evident from the relatively uniform thickness of the syndrift sediments. Figure 4.5 (C) illustrates this by showing very little sag in the underlying postrift sediments. By the end of the Eocene all syndrift sediments were deposited. This includes the sediments of the Cartwright Formation, Gudrid Member, Kenamu Formation and Leif Member.

Finally, Figure 4.5 (D) shows the present day Labrador Shelf. The most significant aspect of this figure is the apparent massive thermal subsidence that occurred during the late Tertiary in the Hopedale Basin. The postdrift sediments of the Mokami and Saglek Formations show significant thickening. Thermal subsidence was greatest farther from the continent and therefore the sediments being deposited were thicker where the lows were deepest. This continuous subsidence and deposition during the postdrift stage resulted in the dramatic advancement of the shelf edge and the thick sequences of postdrift sediments located in the deeper water. It is evident that a significant thickness of the nearshore sedimentary layers was cannibalized and re-

deposited near the shelf edge and on the slope. In the deep water, this sequence is as thick as 2500 metres and is made of numerous subunits that are not present on the shelf. It is possible that with further work in the deep water region more Late Tertiary stratigraphic units can be defined and characterized.

The overall subsidence history and depositional sequences can be seen in Figure 4.6. This information coincides with that proposed by Enachescu (2006b).

4.5 Discussion

There are several interesting structural features present along the Labrador Shelf which add insight into its rifting history. One thing that is particularly intriguing is the apparent uneven extension of the area during the Early Cretaceous. This uneven stretching resulted in significantly thicker synrift deposits along the present day shelf. It also verifies the current interpretation of the deposition of the Bjarni Formation since the shelf break was a result of more recent thermal subsidence. The quality of older seismic data did not allow accurate mapping of the Bjarni Formation into the outer shelf, slope and deepwater following the postrift unconformity. New data allows interpreting the extension of Bjarni Formation mapping into the deep water. Consequently cross sections that were previously proposed illustrating the Bjarni Formation pinching out before it reached the deepwater (ex. Figure 2.4) are, according to the model of this study, incorrect. Enachescu (2006b) proposed that the Bjarni Formation is actually a widespread depositional sequence that was derived from both rift shoulders as well as local intrabasinal ridges.

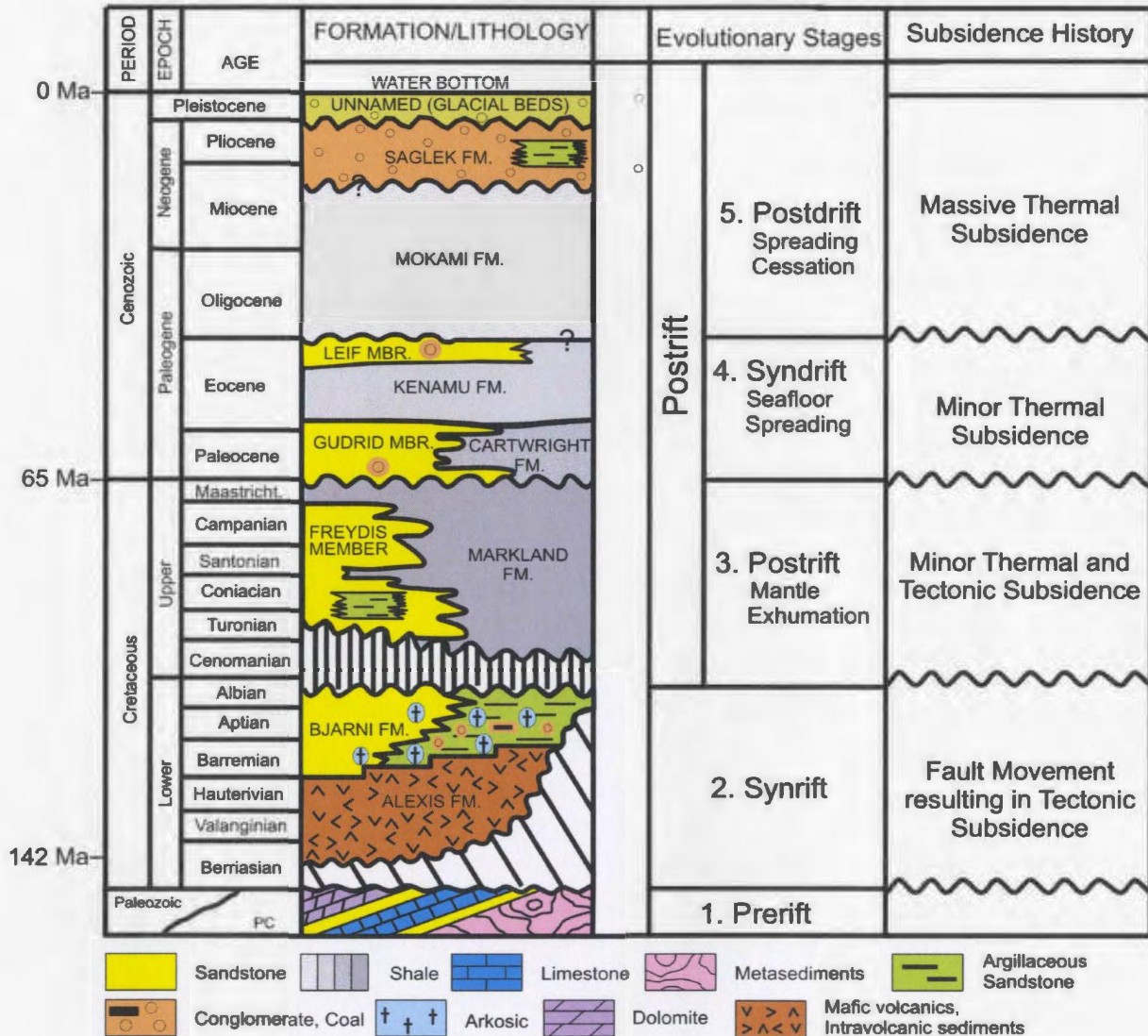


Figure 4.6 – Stratigraphic chart illustrating stratigraphic units, evolutionary stages and thermal and tectonic subsidence history of the Hopedale Basin (modified after McWhae et al., 1980 and GSC, 1987 and Enachescu, 2006). Ages after Gradstein et al. (2004).

Although there were no attempts to determine a stretching factor in the Labrador Sea, we can assume that it would be greater than 3.5 given information that is known about faulting in the area. According to Reston et al. (2001) and Chian and Loudon (1994) the presence of serpentinized mantle (ridges), such as what is shown here to be present along the Labrador Shelf, suggests that stretching must have been large enough to cause significant crustal thinning and mantle denudation. The stretching factor varies along the dip profile and also across the strike of the margin. Determining the precise stretching factor is outside the objectives of this thesis.

Several long seismic lines show a wide transitional crust that includes new oceanic crust, lava flows, exhumed mantle and serpentinized ridges. Slow spreading rates combined with faulting of the crust created this extensional transitional crust which has been described in other parts of the Newfoundland and Labrador offshore region (Chian and Loudon, 1994; Chian et al., 1995; Loudon, 2002). These longer seismic lines give good indication as to the boundary between continental and oceanic crust.

The thermal and tectonic subsidence history of the Hopedale Basin as determined from this study coincides with that of Enachescu (2006b) who said “significant faulting and tectonic subsidence took place during most of the Cretaceous and lasted in some areas, up to Paleocene time, interrupted by several episodes of thermal subsidence”. Tectonic subsidence appears to be most relevant in the Early Cretaceous while thermal subsidence is most significant in the Late Tertiary. It is obvious from this study that thermal subsidence was greatest after oceanic ridge extinction and thermal subsidence prior to that was minor. It was this final massive thermal subsidence that created the

shelf edge as is seen today when assuming a horizontal reconstruction datum for the earlier stages.

Transtensional movement within the Hopedale Basin is not as obvious as that seen in the Orphan Basin. Seismic sections from the Orphan Basin reveal large inversion structures; some reaching as high as the present-day seafloor (Enachescu et al., 2005). These large features present within the Orphan Basin were probably a result of pronounced multiple rifting events. The Labrador Shelf did not see these multiple events therefore any transtensional features would probably be minor in comparison. Unfortunately, one of the structural features which may indicate transtensional movements are only evident on the longer seismic lines which are less dense than the shorter, 2005 seismic lines. Nonetheless, it is evident that there is compressional folding of drift sediments in the middle of the study area but this may be due to gravity sliding rather than crustal tectonics.

The rifting and subsidence history of the Hopedale Basin makes it an ideal location for hydrocarbon generation. With significant faulting creating basement highs and lows, deposition of significant source and reservoir rocks and substantial subsidence burying sediments well into the oil and gas window, the Hopedale Basin is definite location for hydrocarbon exploration.

4.6 Conclusions

The kinematic modelling completed along the North Bjarni F-06 line resulted in important conclusions about the Hopedale Basin. Thus, in the Hopedale Basin:

1. Five stages of basin formation were interpreted: I) prerift, II) synrift, III) postrift (mantle exhumation), IV) syndrift (sea floor spreading) and V) postdrift;
2. Most of the extension took place in a continental setting during the Early Cretaceous;
3. There is widespread distribution of the Bjarni Formation, now preserved both in shallow and deepwater regions;
4. Most of the thermal subsidence took place in the Late Tertiary;
5. A large strip of transitional crust composed of exhumed mantle, serpentinized ridges and lava flows exists;
6. Several compressional features due to transtensional movements and/or gravity sliding are evident.

Chapter Five: Petroleum Systems

5.1 Introduction

Offshore Labrador has had a superior success rate when it comes to exploration drilling. The successful wells in a previous drilling campaign of 1973-1983 confirmed the presence of a source and reservoir rocks. Also, these discoveries show that there are structural trapping mechanisms formed at several stratigraphic levels, from the Palaeozoic prerift carbonates within the basement to overlying synrift and postrift sandstones present in several formations. Assuming that the wells in the area have sampled only a small portion of the vast Hopedale Basin and neighbouring Saglek Basin, it can be presumed that there are many more structural and stratigraphic plays with potential reserves that remain to be explored.

Previous seismic exploration and most of the scientific literature have been based on older vintage seismic data (up to 1982), most of it being unmigrated, lacking adequate multiple suppression and having poor resolution within the Cretaceous successions. The following chapter will examine petroleum prospectivity of the Bjarni area of the Hopedale Basin based on interpretation of the new 2003, 2004 and 2005 grid of GSI data. More data were collected in 2006 and 2007 but was not available for this study. The chapter is divided into sections based on the four main components necessary for a petroleum system: 1) source rocks and migration, 2) reservoir rocks, 3) seals and 4) traps.

To describe the petroleum systems of the Hopedale Basin several regional maps were produced and analyzed. These maps included general time and depth structural maps and maps of depth to hydrocarbon maturation. The first section, Section 5.1.1, will

describe the methods used to produce these depth maps from the horizons interpreted in Two-Way Travel Time (TWT). The following sections will describe the four main components of the Hopedale Basin's petroleum system.

5.1.1 Producing Depth Maps

Seven horizons (K1, K2, T1, T2, T3, T4 and WB) were interpreted in two-way travel time using SeisWorks®. To convert these time horizons to depth a velocity model was generated using Depth Team Express® (DTE®) - one of many programs within Landmark. DTE® creates velocity models by using the time horizons, well picks and well time-depth data. To create a depth model in Depth Team Express® the following procedure was used:

1. Loaded time horizons, relevant well picks (based on interpreter choice) and primary time-depth curves (if others are present);
2. Gridded the time horizons and made them into surfaces;
3. Assigned a time surface to its respective well pick name;
4. Saved the model;
5. Within TDQ®, opened the model and converted the time horizons into depth.

DTE® applies the depths of the picks at the well bores to the interpreted horizon and applies that interval velocity derived from the depth and time picks to the interval between the interpreted horizons. Unfortunately, with the lack of well data in the deep

water there are certainly errors in the depth conversion due to computer program or differential compaction.

Although this is a geographically large area, the data for all the wells were combined into a single model and all depth maps were generated from this model. More explanation regarding the DTE® model is contained in Chapter 4, Section 4.2.

The horizons were then gridded using a search radius of 15 000 metres. This search radius was necessary due to the wide line spacing of the 2D seismic data in the area. The X and Y spacing used during gridding was 2000 metres. To check the effectiveness of these parameters the original time horizons were gridded and contoured with the above parameters and then the map points from the newly gridded surface were converted back into a seismic horizon. Comparison of the original time horizon and the time horizon generated from the map points showed that the final map was an accurate representation of the interpreted time horizons.

Another quality control measure was used to validate the structure depth maps and depth model. After the maps were generated, the depths of the formations as represented by the contours were checked with the formation tops provided by the C-NLOPB Schedule of Wells (2003a). From this it appears that the depth maps are accurate at the well locations when compared with actual well data; a ± 10 metre error at the well bore is acceptable for this regional mapping project.

Also, water depths created by the model were checked with water depths calculated from the time taken to travel to the water bottom. Using an approximate seismic water velocity of 1450 m/s, the depth to the water bottom was determined (using

the relationship depth = velocity x time) and compared with the depths created by the model. This method illustrated that the depth model was adequately converting the water bottom time horizon into depth (± 5 metres). All the maps have been created in UTM Zone 21, NAD 83.

5.2 Source Rock

The shales of the Markland Formation have been thought to be the prominent source rock for the Hopedale Basin (McWhae et al., 1980; Balkwill and McMillan, 1990) and, more generally, the Labrador Shelf. More recently, Fowler et al. (2005) have proposed, and Enachescu (2006b) has reiterated, that the Bjarni Formation has significant interbedded shales with high organic content and therefore could be a significant source rock for the area. The following sections will discuss the Markland Formation as a possible source rock as well as introduce the Bjarni Formation as a potential source rock.

5.2.1 Markland Formation

The source rock in the area has always been believed to be the shales of the Markland Formation (McWhae et al., 1980; Balkwill and McMillan, 1990). To illustrate the Markland Formation distribution in the Bjarni area a regional interpretation of this formation was completed. The Markland shales were mapped in time and subsequently converted to depth using the time-depth conversion method as described in section 5.1.1. A regional depth structure map of the Markland Formation can be seen in Figure 5.1. This map shows several structural high trends along the shelf. The formation becomes

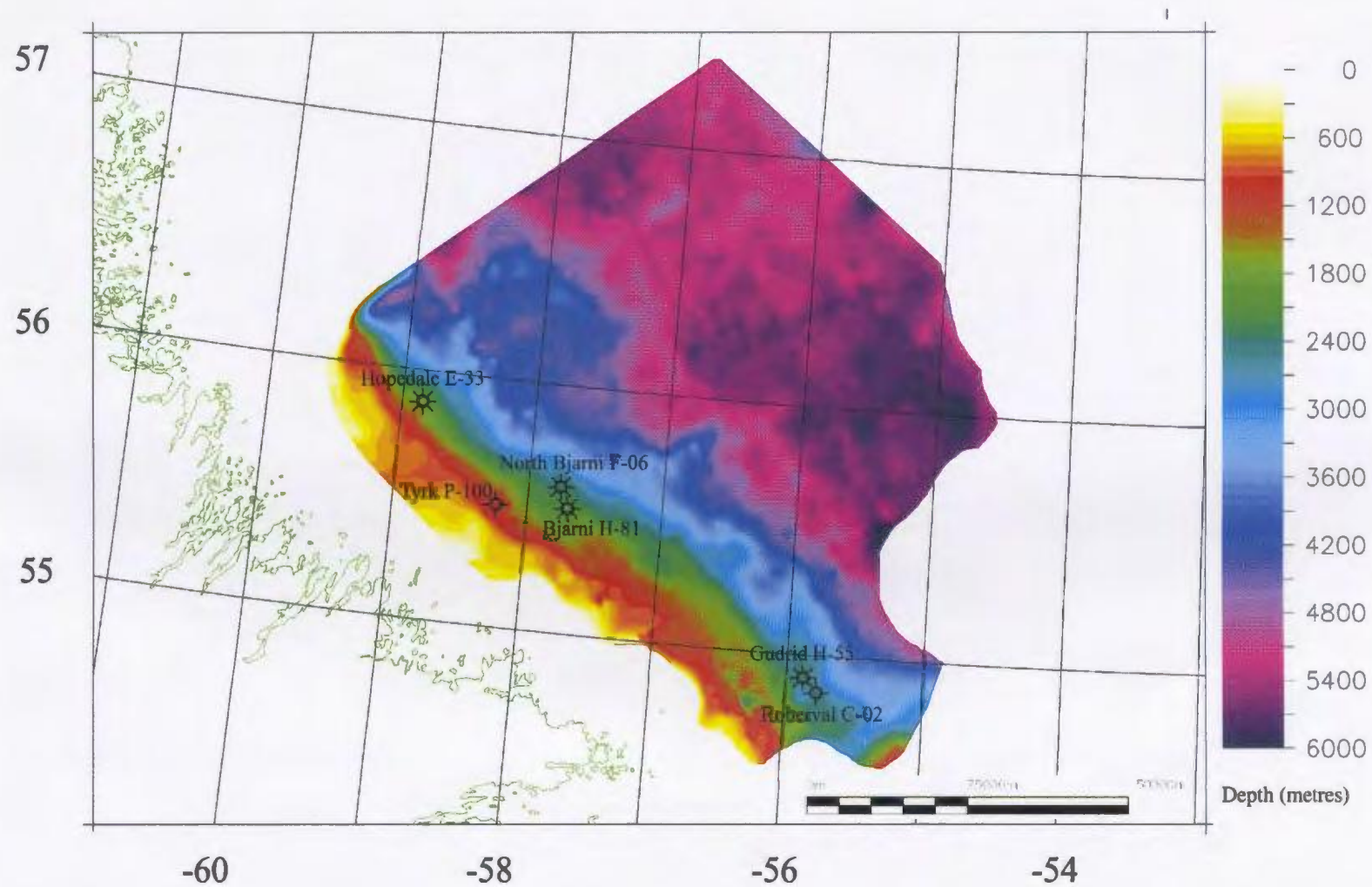


Figure 5.1 – Depth structure map of the top of the Markland Formation (horizon T1). The map was created in UTM Zone 21, NAD 83.

deeper on the slope and in the deep water. In the northwestern portion of the map the top of the Markland dips more gently than in other regions. The deepest structural lows reach depths of approximately 6 kilometres. The Markland Formation would be an ideal source rock due to its regional presence along the Labrador shelf. The shales, if acting as a source rock for the area, needed to be buried to a depth where the heat and pressure were high enough to generate hydrocarbons.

Dehler and Keen (1993) have used isopach maps of particular sediment packages to determine the tectonic and thermal subsidence of these packages. They have presented several maps that represent crustal and lithospheric thinning for the eastern continental margin. Using their predicted thermal history, they were able to estimate the organic maturity of the sediments within the basins and to present several other maps concentrating on the depth to organic maturity. These estimates are used in conjunction with borehole data to better understand the basin's thermal history.

Unfortunately, Dehler and Keen (1993) were unable to model the thermal history of the synrift sediments as a result of insufficient information with regards to the synrift subsidence history. Therefore their results are concentrated on early postrift sediments such as the Markland shales.

Keen and Beaumont (1990) and Dehler and Keen (1993) have suggested that there are numerous elements that affect the thermal history of an area:

- 1.) amount of lithospheric stretching – during the postrift stage heat flow into the sediments decreases due to the cooling of the lithosphere;

- 2.) subsidence of the lithosphere – increase in burial depth increases temperature;
- 3.) porosity – thermal conductivity of the sediments increases with depth because the porosity decreases.

According to Dehler and Keen (1993), in the area of the Hopedale Basin the depth to the top of the zone that reached thermal maturity appears to be between 3.5 and 4.5 kilometres which is consistent with the average value taken from maturation data from wells (Bell, 1989) and the average depth to maturation used in this thesis.

Data taken from the Labrador Basin Atlas (Bell et al., 1989) gives depths at each of the wells where the vitrinite reflectance (R_o) for the Markland shales is greater than 0.7% implying that when this value is reached the shales are buried deep enough to generate hydrocarbons. The information in Table 5.1 was taken from the Labrador Basin Atlas (Bell et al., 1989).

The depth to $R_o > 0.7\%$ ranges from 2000 metres at wells near the shore to >5000 metres at wells farther from shore. With this well information the average depth to hydrocarbon generation can be estimated. If we consider all the wells in the area, this average is 3323 metres but if we remove the two values described as unreliable data

Well Name	Depth BKB (m) $R_o > 0.7\%$
Roberval C-02	3493
Roberval K-92	3672
Gudrid H-55*	2432
Bjarni O-82	2245 ¹
Bjarni H-81*	3111
Herjolf M-92	3582
North Bjarni F-06*	3493
Tyrk P-100	4151 ²
South Labrador N-79	3580
South Hopedale L-39	2757
Hopedale E-33*	2256
Corte Real P-85	5098

¹may require revision ²very poorly constrained

Table 5.1 – Measured or projected depths to 0.7% R_o taken from the Labrador Basin Atlas (1989). It is important to note that two wells have unreliable values (Tyrk P-100 and Bjarni O-82). The asterisks (*) indicate the wells which are hydrocarbon bearing.

values (Bjarni O-82 and Tyrk P-100), the average depth to maturation is 3347 ± 800 metres. To satisfy the data, an average depth of 3335.0 metres will be used as the minimum depth of burial in order to generate hydrocarbons. Using this value in conjunction with the Markland depth map, a hydrocarbon “kitchen” map can be produced. By setting the minimum maturation level as 3335.0 ± 800 metres it is evident from the map where hydrocarbons should be generated within the Markland Formation. It is understood that this map is only a first approximation of the Markland “kitchen” area as I used an average depth value to maturation taking into consideration the wells in the study area. All the wells were drilled on structural highs and locations farther away from them are likely to be quite different in terms of maturation. It is also important to note that there is no agreed upon upper R_o limit to acknowledge where overmaturity may be present. From general information of gas generating source rocks, it is likely that where the Markland Formation is greater than 6000 metres it is overmature. Also, depth is only one indicator of maturity; temperature is also another factor that it is important when considering the maturity of hydrocarbons and temperature can significantly vary within an evolving rift system.

The kitchen map can be seen in Figure 5.2. Clearly the formation is mature in a very large area situated downdip from the wells drilled on the inner shelf. The map in Figure 5.2 shows that the abandoned gas wells within the study area lie outside of the region where maturity has been predicted but updip hydrocarbon migration from the eastern positioned half grabens is possible. These wells are North Bjarni F-06, Bjarni H-81, Gudrid H-55 and Hopedale E-33. The gas pay in the Gudrid H-55 well is contained

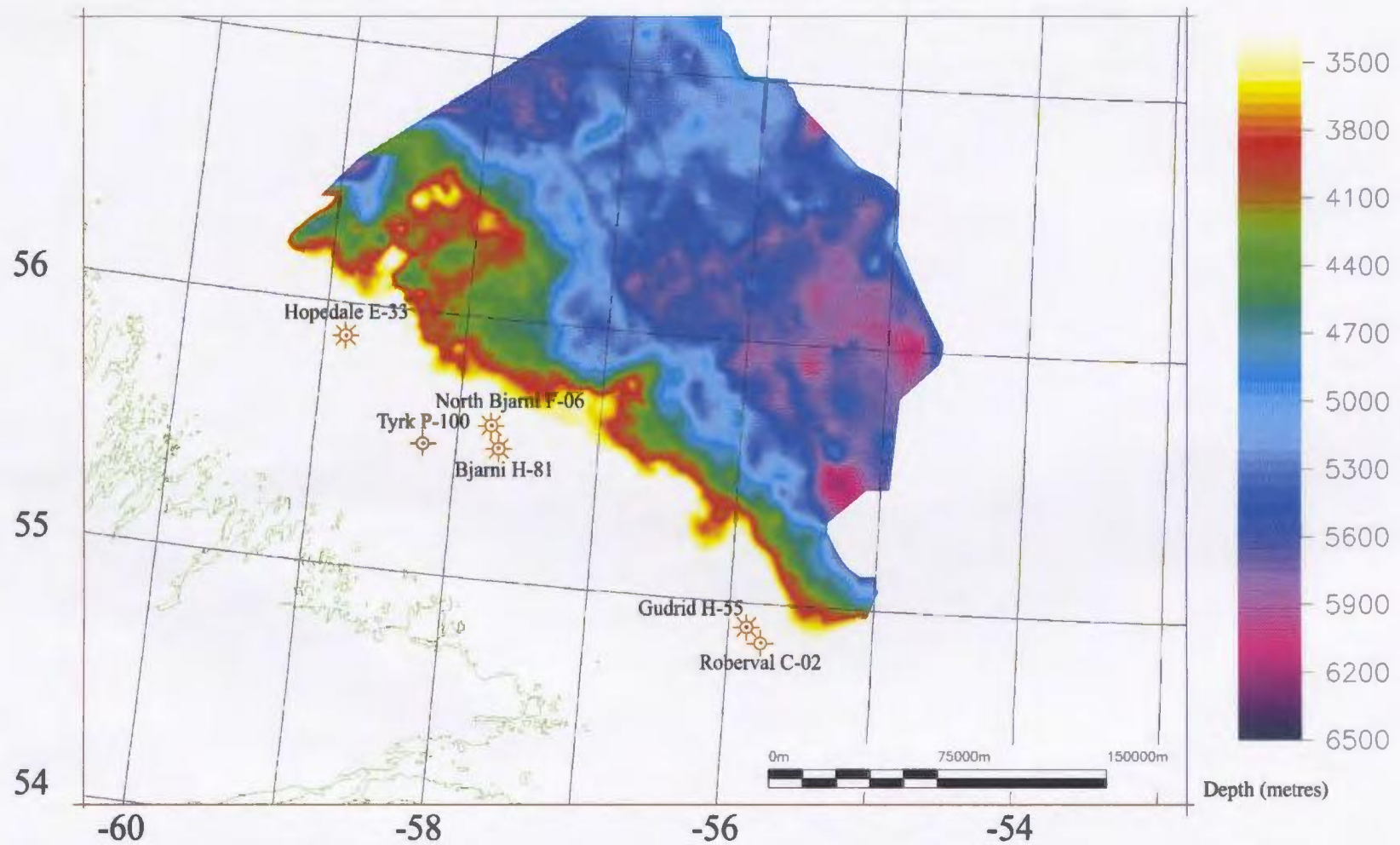


Figure 5.2 – Depth map of the top Markland Formation (T1 horizon) with an upper maturation limit of 3335.0 metres. Map shows the areas with Markland Formation below top of maturation window. The map has been generated in UTM Zone 21, NAD 83.

in the Palaeozoic carbonates in the region but generated in the Cretaceous shales. One of the wells, Hopedale E-33, has a depth to maturation significantly less than the average value used here of 3335.0 metres (Table 5.1). Even so, the Markland Formation is not buried to the appropriate depth at the Hopedale E-33 location and requires lateral migration. The other two wells have values closer to the average. The true average depth to maturation is difficult to identify since all of the wells were drilled on structural highs and therefore possibly yield a biased sample set compared to the actual average depth to maturation over the rest of the basin.

Issler and Beaumont (1987) suggest slightly different values for vitrinite reflectance relationship to source rock maturation. They propose that mature sediments occur at R_o values $>0.6\%$ as opposed to 0.7% stated in the Labrador Basin Atlas (1989). Also, they suggest that marginally mature sediments occur between $0.45-0.6\%$ R_o therefore burial depths need not be as great. This may be why none of the producing wells fall within the hydrocarbon “kitchen”. They also suggest that the depth to maturity increases oceanward. With the depth to the Markland Formation also increasing with depth it is likely that it still falls within the hydrocarbon window and the map illustrated in Figure 5.2 can still be regarded as a decent first estimate. Regardless, the area where the wells are drilled appears to be along the borderline of mature versus immature source rocks. This map indicates that if the Markland Formation is the actual source for the respective wells, the presence of hydrocarbons at these locations may be a result of long-path lateral migration of hydrocarbons from eastern deeper troughs.

There has always been debate regarding the location of the hydrocarbon source rocks in this area. McWhae et al. (1980) believed the associated hydrocarbons are products of local generation whereas Powell (1979) questioned whether or not the hydrocarbons were a result of long distance migration. The map in this study suggests that the marine Markland shale is widespread on the outer shelf and slope where little drilling was done and that any potential plays in these areas should encounter mature (and possibly overmature) Markland source rock.

5.2.2 Bjarni Formation

According to past research, GSC reports and papers, the Markland shales were believed to be the main source rock for the Labrador shelf (McWhae et al., 1980, Bell et al., 1989, Enachescu and Fagan, 2005). More recent geochemistry studies performed by the GSC show that the source rock for the Labrador shelf is within the Lower Cretaceous Bjarni Formation (Fowler et al., 2005). Issler and Beaumont (1987) also believed that the Lower Cretaceous Bjarni Formation contains shales capable of generating oil. The North Leif I-05 well (outside the current study area) contained waxy crude which was thought to be generated from terrestrial types II and III kerogens found within the Bjarni Formation (Issler and Beaumont, 1987). Recent geochemistry and organic petrography analysis performed by Fowler et al. (2005) shows that the Bjarni Formation shales are rich in type III terrestrial organic content.

Using the same average minimum depth to hydrocarbon generation of 3335.0 metres a “kitchen” map for the top Bjarni Formation was also produced (Figure 5.3).

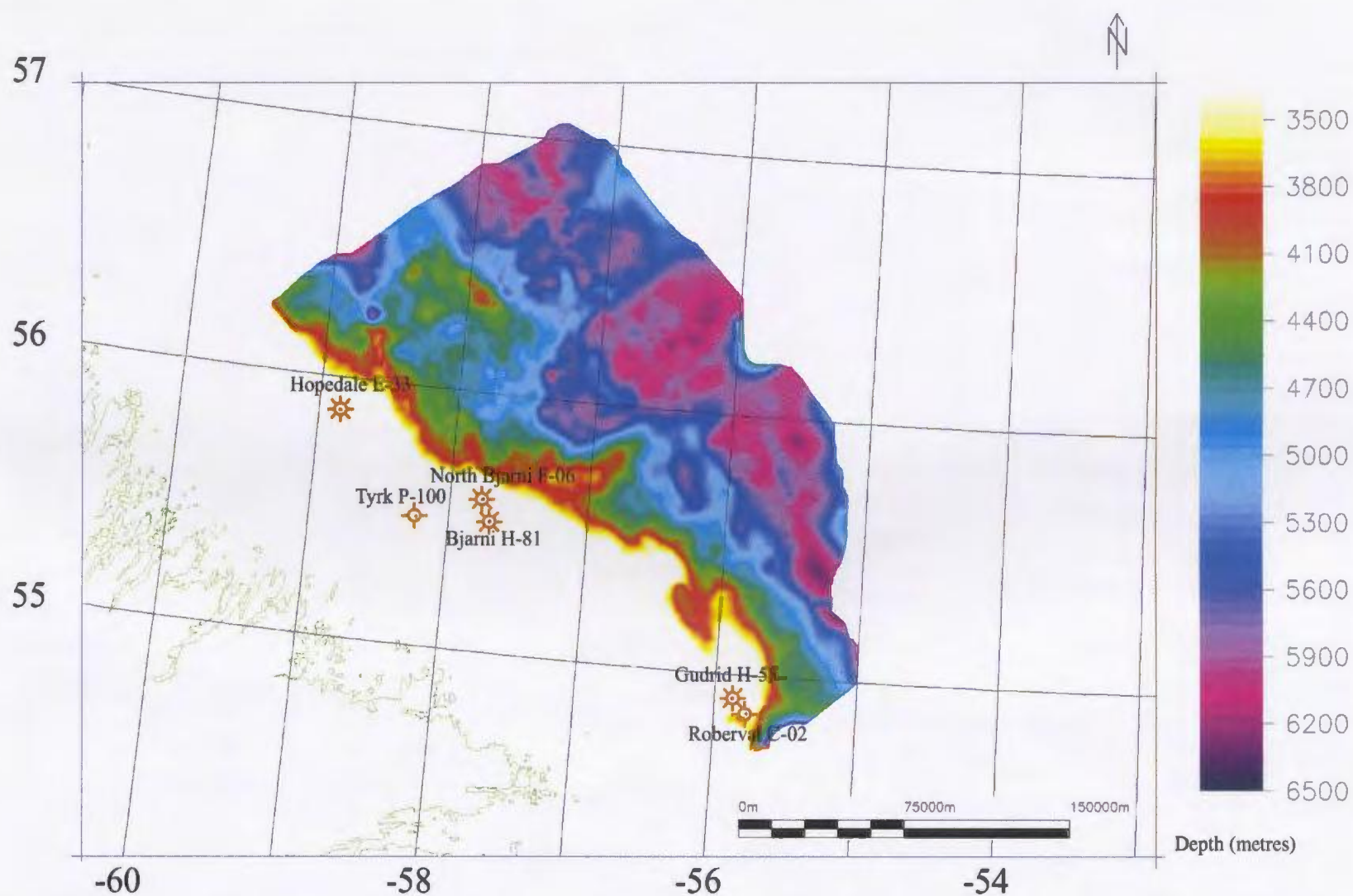


Figure 5.3 – Depth map of the top Bjarni Formation (K2 horizon) with an upper maturation limit of 3335.0 metres. This map indicates a large hydrocarbon kitchen for the shales of the Bjarni Formation. The map has been generated in UTM Zone 21, NAD 83.

This map has some similar characteristics to the Markland Formation depth map. It follows comparable trends and has a slightly deeper region in the southeast portion of the study area. The Bjarni Formation is stratigraphically lower than the Markland Formation therefore the 3335.0 metre contour lies laterally closer to the wells with proven hydrocarbons. Interestingly, using this average value, none of the drilled wells fall in the Bjarni Formation hydrocarbon “kitchen” either. The actual depth to maturation at the Hopedale E-33 well is significantly lower than the average and therefore this well does fall within the Bjarni Formation “kitchen”. As per the Markland Formation “kitchen” map, this map illustrates that there is probably lateral migration of the hydrocarbons into the structurally higher regions on the shelf or the R_o value of gas release may be too high at 0.7% and should be lower at approximately 0.6%. At 0.6% R_o the actual depth to maturation is also lower and this makes the North Bjarni F-06 well possibly fall within the “kitchen window” map. However, lateral migration has to be considered to explain gas charging from the Bjarni Formation for most of the large discoveries within the Hopedale Basin.

Overall, regardless of which rock formation sourced the hydrocarbons present on the Labrador Shelf, lateral migration from the eastern half grabens must be considered. The two kitchen maps also suggest that a large area exists towards the shelf edge and deepwater which should encounter mature source rocks and ultimately hydrocarbons as opposed to locations drilled along the inner shelf such was the case with the Tyrk P-100 well. It has to be mentioned that shales occupy mostly the lower part of the half grabens on the shelf and that they are not equally distributed within the Bjarni Formation. The

map in Figure 5.3 has to be used only as a regional indicator of source maturation.

Detailed maps of the distribution and depth of the shales of the Bjarni Formation should be produced when analyzing individual hydrocarbon plays.

5.3 Reservoir Rock

Several reservoir rocks were encountered at different stratigraphic levels by the wells drilled offshore Labrador. For this study, focus was on the sandstones of the Bjarni Formation and the Cartwright Formation (Gudrid Member). Seismic resolution constraints and time limitations precluded mapping other reservoirs in the study area. The following sections will discuss the Bjarni and Gudrid reservoirs but for completeness, the other potential reservoir rocks in the area including the Leif Member of the Kenamu Formation, the Freydis Member of the Markland Formation and the Palaeozoic carbonates will be briefly discussed.

5.3.1 Bjarni Formation

The Bjarni Formation was deposited during the intra-continental rifting of the Labrador Sea and typically fills in lows created by rotated basement blocks while also draping over some of the highs. It is evident from previous drilling that high blocks may or may not be overlain by Bjarni Formation. This was demonstrated at the Roberval C-02 well location which did not encounter Bjarni sandstones. Figure 5.4 shows the general structure of the Bjarni Formation as far as its extent into the deep water. When compared

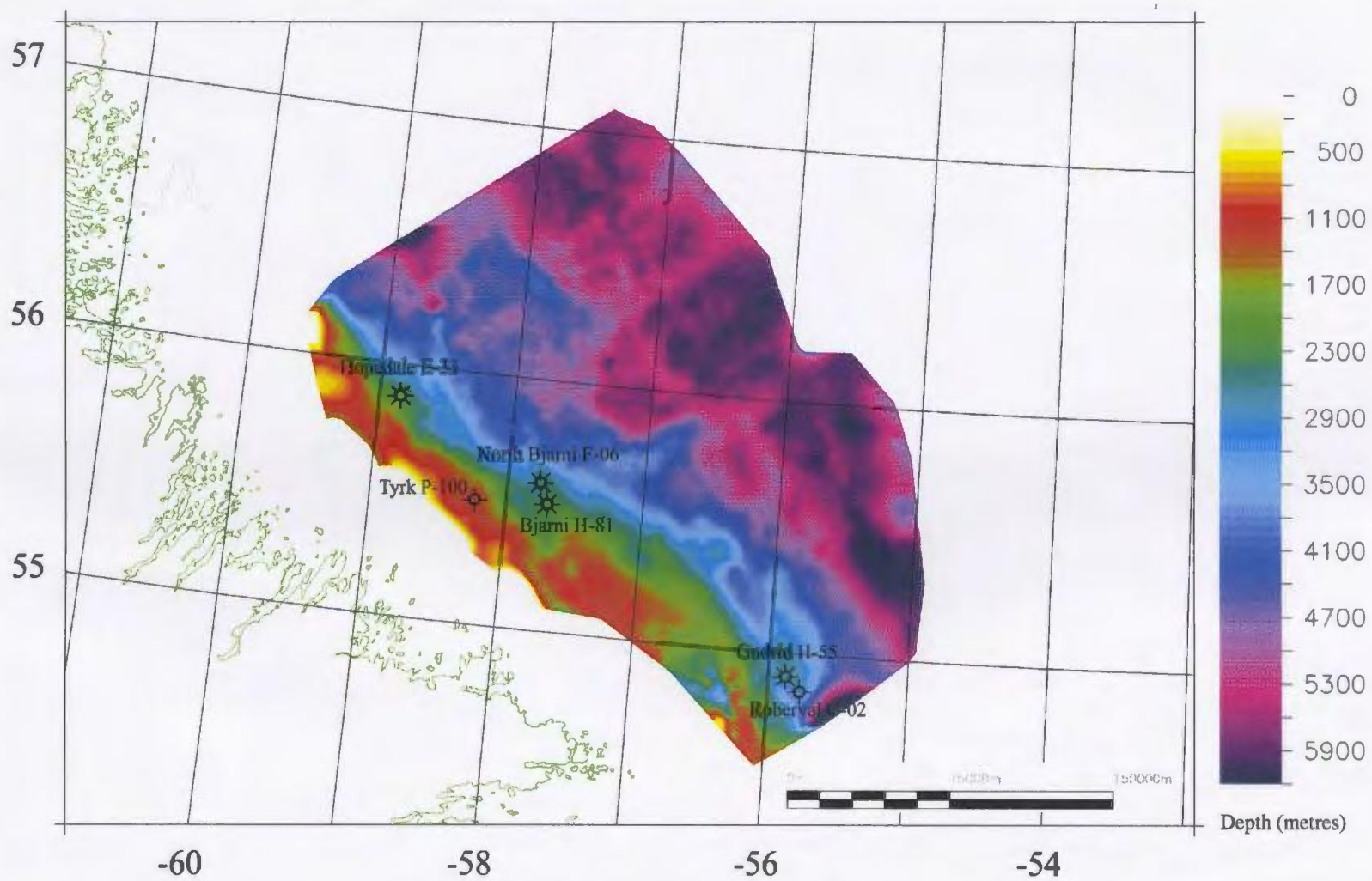


Figure 5.4 – Depth structure map of the top of the Bjarni Formation (K2 horizon). The map was created in UTM Zone 21, NAD 83.

to other structure maps (Figure 5.1) it is obvious that the Bjarni sandstones terminate beyond the shelf edge and does not extend as far into the deepwater as the postrift sediments. If the Bjarni Formation is considered a potential source rock as well as a reservoir for the area, this would imply the presence of numerous structural and stratigraphic plays on the outer shelf and deep water.

According to the Properties of Gas Bearing Reservoirs (C-NLOPB, 2003b) the Bjarni Formation has good to high porosity. In the North Bjarni F-06 well the porosity was 19% while the Bjarni sandstones within the Bjarni H-81 and Hopedale E-33 wells had porosity values of 20% and 11% respectively. These high porosity values make the Bjarni Formation an ideal oil/gas reservoir sandstone. It has also been tested in several wells including Bjarni H-81, Bjarni O-82, Hopedale E-33, North Bjarni F-06, North Leif I-05 and Snorri J-90. The initial flow in these wells ranged from 170 000 m³/day to 401 860 m³/day. Tests also revealed oil from the Bjarni Formation in the North Leif I-05 well. These tests as well as the Bjarni reservoir's wide lateral extent also give hope for further discoveries in the basin.

5.3.2 Gudrid Member of the Cartwright Formation

The Gudrid Member of the Cartwright Formation was encountered by wells on the inner shelf. Its mapping into the deep water becomes difficult due to low seismic resolution and lack of tie points. From older studies and the interpretation of recent seismic lines, it appears that the marker associated with the sandstone pinches out instead of being deposited beyond the shelf edge. Figure 5.5 shows a structure map of the top

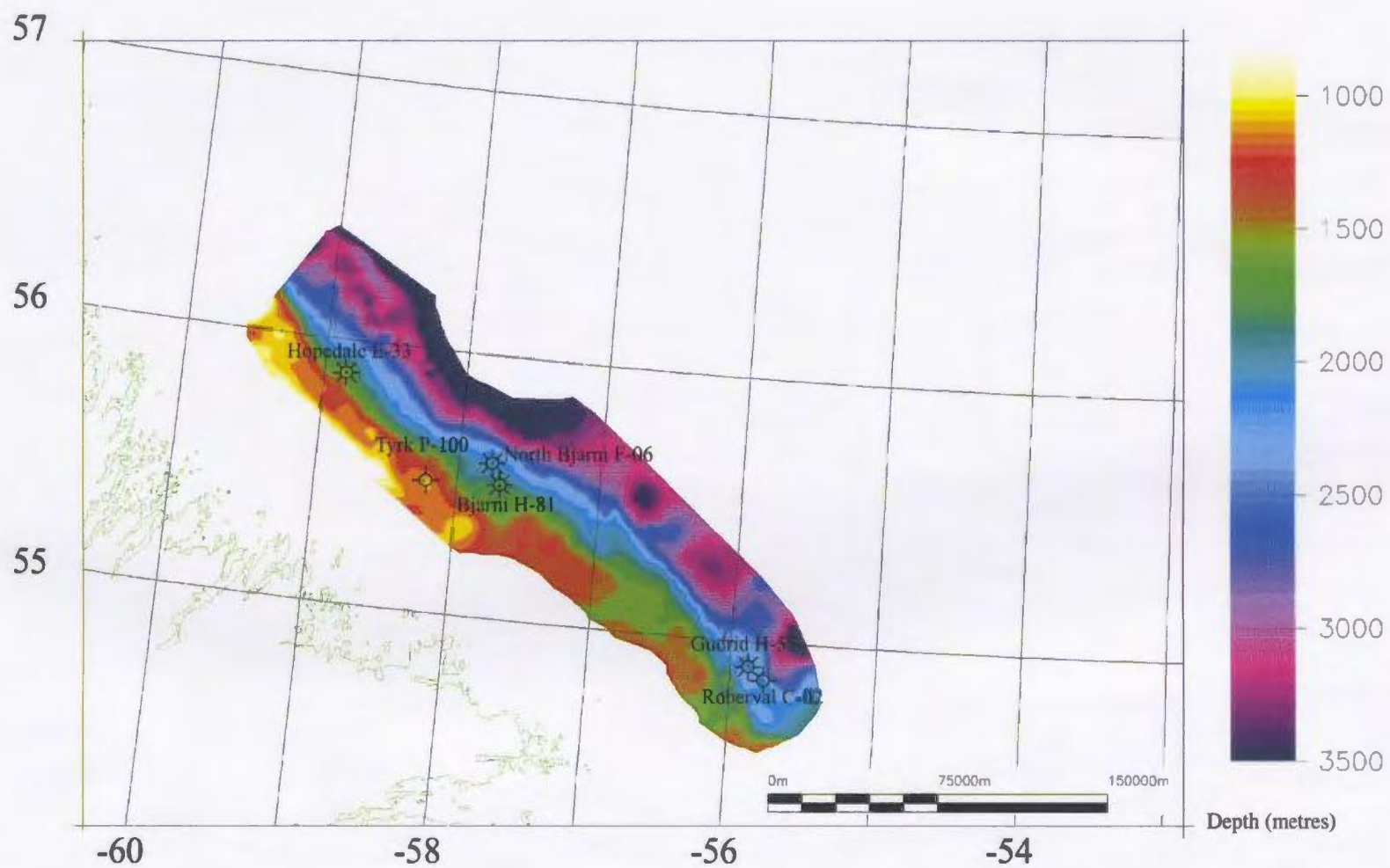


Figure 5.5 – Depth structure map of the top Cartwright Formation (horizon T2). The map was created in UTM Zone 21, NAD 83.

Cartwright Formation as determined through well ties. This map may also mark the top of the Gudrid Member in the area near shore. It is important to note that this horizon was tied to the Cartwright Formation through well ties so it can only be inferred to be representative of the Gudrid Member within the western side of the basin where sandstone was encountered in the wells. This sandstone does not extend past the shelf edge so all potential plays would be shallow water plays as already seen from the Snorri J-90 well which had gas shows from the Gudrid Member.

The porosity of the Gudrid Member within the Snorri J-90 well was determined to be 18% (C-NLOPB, 2003b). The Snorri J-90 well was the only well of the five significant discoveries to test gas from the Gudrid Member.

5.3.3 Leif Member

The Leif Member was not interpreted on these data due to the poor lateral extent of the sandstone, the difficulty correlating the marker, and the complexity of mapping the horizon using a large spacing between dip lines. The Leif Member of the Kenamu Formation is believed to be a potential reservoir and was penetrated by the following wells within the study area (C-NLOPB, 2003b): Gudrid H-55, Hopedale E-33 and Roberval C-02 but has only been tested in the Karlsefni A-13 well where it recovered water. In order to properly map the Leif Member, higher density seismic data is required.

5.3.4 Freydis Member

The Freydis Member of the Markland Formation is a difficult marker to identify on seismic lines. The Freydis Member has been encountered in limited wells: Freydis B-87, Gilbert F-53, Ogmund E-72 and Skolp E-07 - all of which are not in the study area. According to the C-NLOPB (2003a) the top of the Freydis Member was not interpreted within the wells in the study area. It is a shallow marine sandstone that was deposited along the shore line. Previously, it was noted that the depth required for maturation for both the Markland and Bjarni formations is further offshore therefore any hydrocarbons present within the Freydis Member would probably require lateral migration. In order to map this formation, Freydis Member well picks outside of the study area need to be projected into a denser seismic grid. More seismic data was recorded during 2006 and 2007 which will see more infill seismic in the area. While not mapped in this study, it is believed that the Freydis Member has reservoir potential along the Labrador shelf.

5.3.5 Carbonate Reservoirs

The carbonate reservoirs (limestones and dolomites) located within the seismic basement are difficult to interpret on 2D data. These carbonate reservoirs were only recognized in Gudrid H-55, Hopedale E-33, Roberval K-92, South Hopedale L-39, and Tyrk P-100 wells. It is worth noting that there were gas tests in the Gudrid H-55 and Hopedale E-33 wells from the carbonate interval therefore it must not be ignored when considering the hydrocarbon potential of the Hopedale Basin, and more broadly, the Labrador Shelf. It has been encountered in other wells within the Labrador basins and

has proven most widespread to the south of the study area. In order to map these carbonates with a relatively high degree of confidence, a 3D seismic grid would be required.

In the Gudrid H-55 well the Palaeozoic dolomite has porosity values of 10%. The Ordovician-aged limestone reservoir in the Hopedale E-33 well has porosity values of 8% (C-NLOPB, 2003b). Nonetheless, these carbonates yielded good tests with initial flow rates of 241 000 m³/day (Gudrid H-55) and 553373 m³/day (Hopedale E-33) to earn the areas surrounding these wells significant discovery designation.

Petrological studies of the Palaeozoic carbonates and the siliciclastics of the Bjarni Formation are currently ongoing at Memorial University. The results from these studies are contained within a Master of Science thesis by Schwartz (in progress) and may add additional insight into the petroleum prospectivity of the Labrador basins.

5.4 Regional Seals

Presence of regional seals pose few problems offshore Labrador. Thick sequences of shales are encountered at various stratigraphic levels. There are several regional shales which act as seals within the area. The Markland Formation restricts the vertical movement of potential hydrocarbons retained in the underlying Bjarni Formation (Figure 5.1). Similarly, the shales of the Kenamu Formation and the Mokami Formation act as seals for the underlying Gudrid Member and Leif Member sandstones respectively. Depth structure maps showing the lateral extent of the top Kenamu and top Mokami Formations can be seen in Figures 5.6 and 5.7.

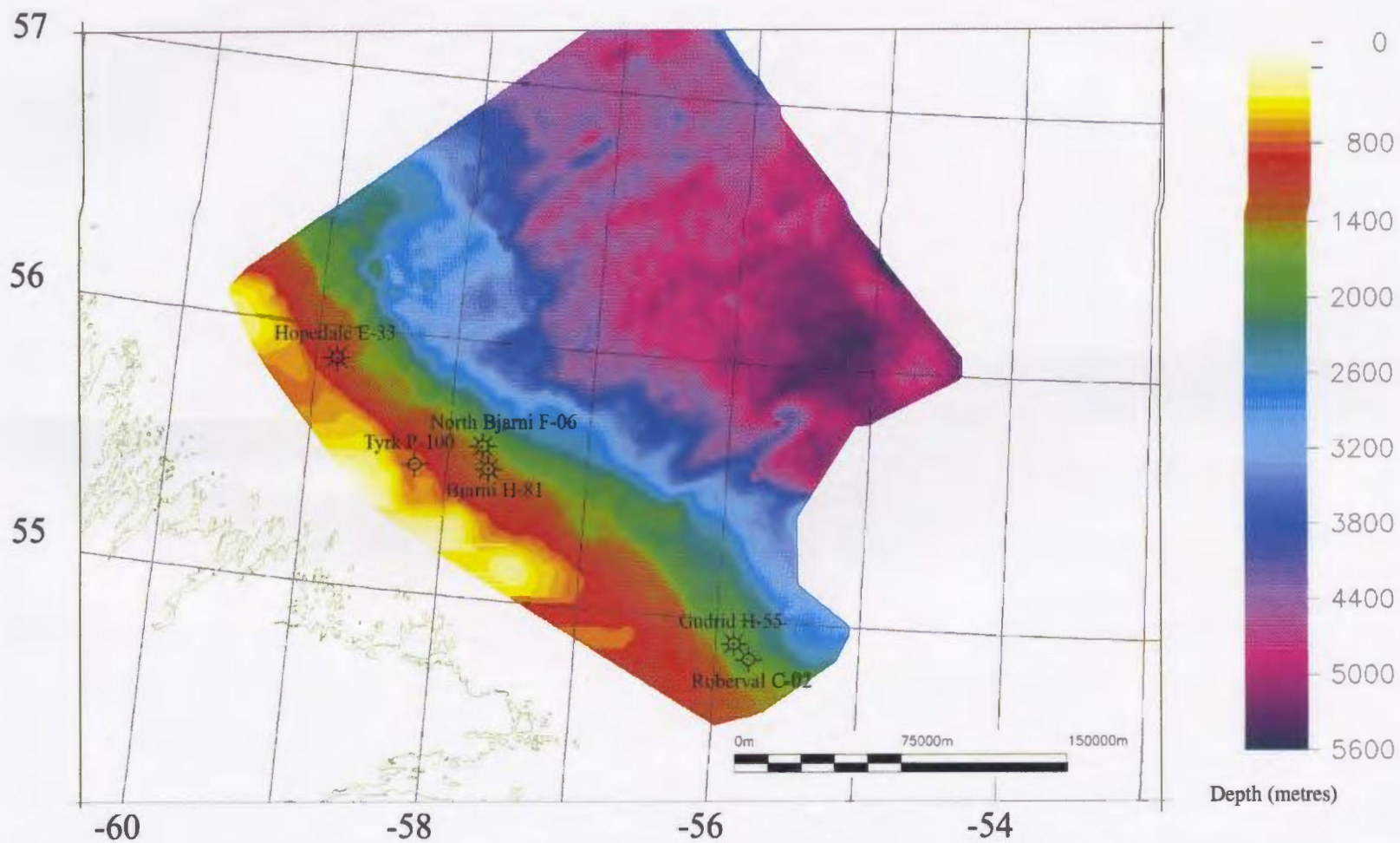


Figure 5.6— Depth structure map of the top Kenamu Formation (horizon T3). The map was created in UTM Zone 21, NAD 83.

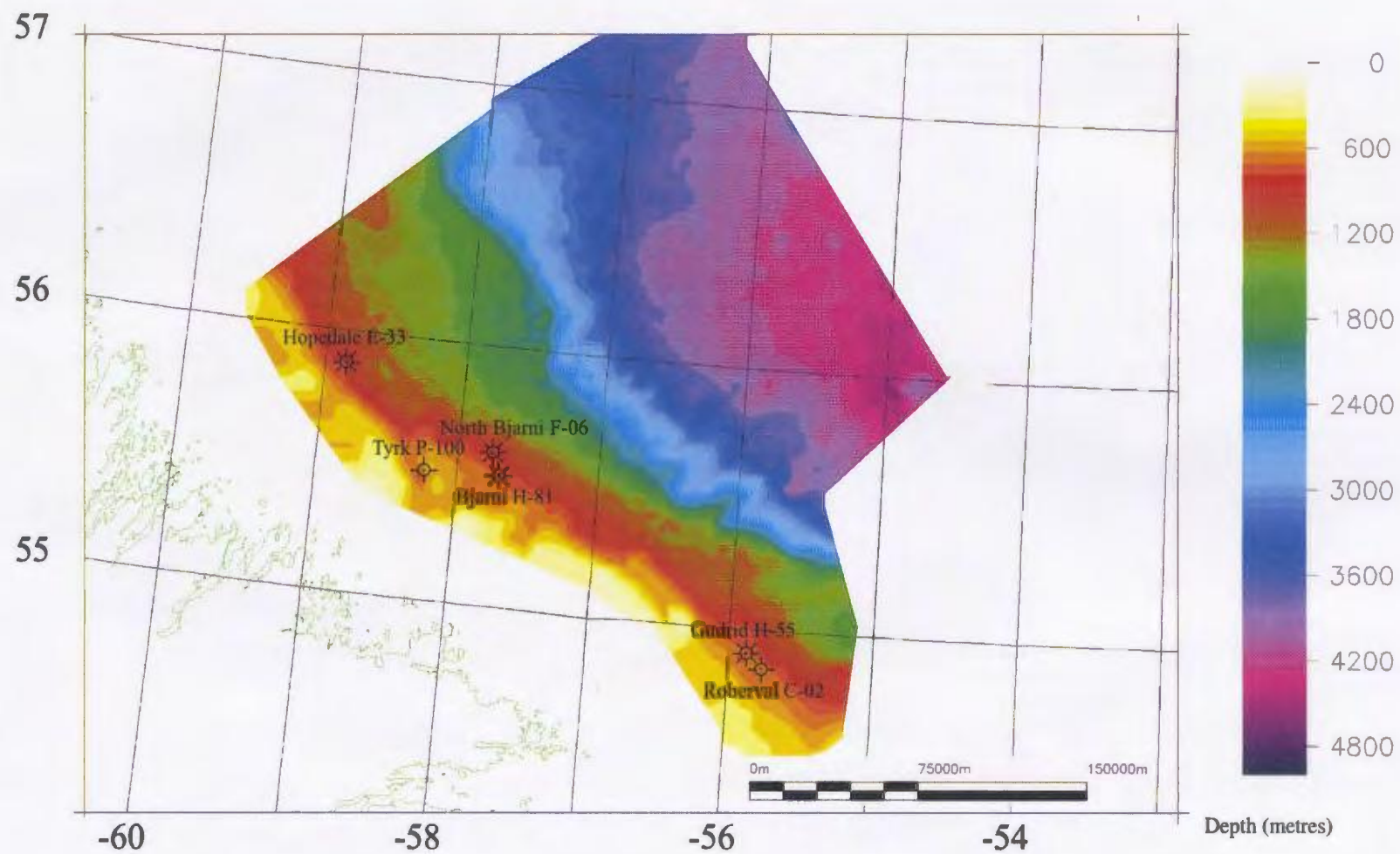


Figure 5.7 – Depth structure map of the top Mokami Formation (horizon T4). The map was created in UTM Zone 21, NAD 83.

The Kenamu Formation (Figure 5.6) is relatively thick, regionally deposited shale which lies stratigraphically higher than the Gudrid Member of the Cartwright Formation. Similarly, the Mokami Formation (Figure 5.7) is also regionally deposited therefore sealing any hydrocarbons that may be present within the Leif Member. There is very little faulting within these sequences thereby inhibiting any seeping of hydrocarbons from the underlying formation.

The mafic volcanics of the Alexis Formation and Markland shales would inhibit the vertical movement of the gas trapped in the underlying carbonate reservoirs. For further information regarding the carbonates present along the Labrador Shelf including petrological studies of these carbonates and other siliciclastic intervals within the Labrador Basins refer to Schwartz (M.Sc Thesis, in progress).

5.5 Structural and Stratigraphic Traps

There are numerous types of structural traps recognized within the Hopedale Basin. As seen in the large North Bjarni Field, basement highs can have preserved Lower Cretaceous Bjarni sandstones (Figure 5.8). This anticline is estimated to contain 2.2 Tcf of recoverable natural gas. Also, rotated basement blocks and horsts may preserve Palaeozoic carbonates especially in areas south of the Hopedale Basin. These basement highs have resulted in the Hopedale gas discovery (105 bcf recoverable) and the Gudrid gas discovery (924 bcf recoverable, Figure 5.9) which both tested 566336 m³/day from the Palaeozoic carbonates.

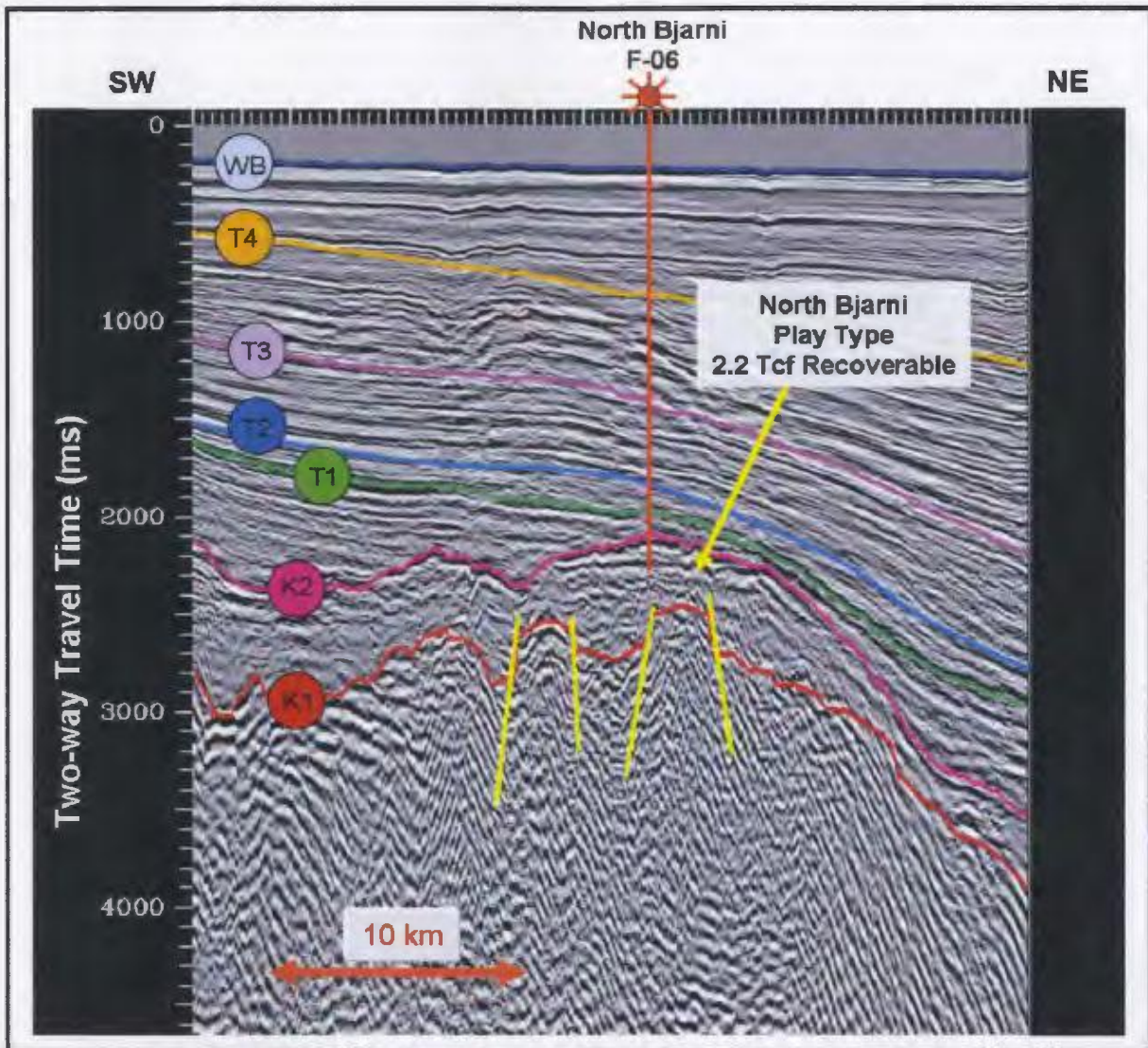


Figure 5.8 – Dip seismic section of the North Bjarni F-06 field illustrating the anticline containing the Bjarni Formation draped over a complex faulted basement high.

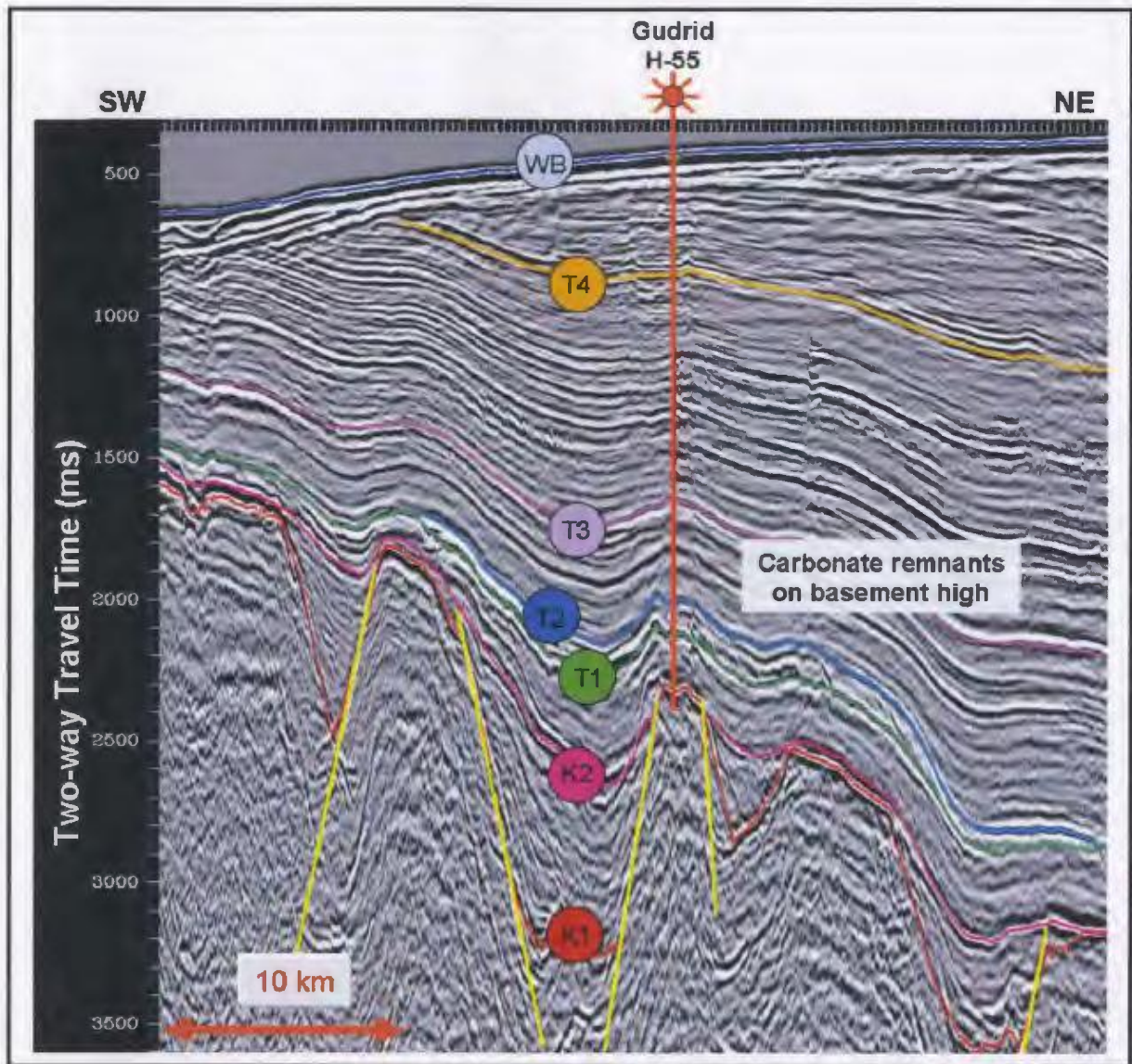


Figure 5.9 – Dip seismic section illustrating the Gudrid H-55 well location. Although difficult to image in seismic, there are remnants of Palaeozoic carbonates on top of a basement horst.

Another typical structural trapping mechanism along the Labrador Shelf is the draping of Bjarni sandstone over the tops of rotated basement blocks or horsts. Figure 5.10 illustrates two rotated basement blocks with Bjarni sandstones draping over them or possibly pinching out against the blocks. Traps created from the pinching out of Bjarni sandstone are considered stratigraphic traps or combination traps. This is the type of trap encountered at the North Leif I-05 location which is outside of the current study area. Wells drilled on top of the structure did not test hydrocarbons (Leif M-48) while the North Leif I-05 well, which was drilled on the east flank of this high, tested a small oil accumulation.

These are the typical structural and combination traps that have been identified along the Labrador Shelf. Enachescu (2006b) suggests that, although previously undrilled, there are probable stratigraphic turbidite traps along the slope and in deepwater. These traps will likely consist of lenses of sandstones (the Gudrid and Leif Member deep water equivalents) encased in thick shales. It is evident from the maturation data that younger sediments in the deep water may generate hydrocarbons due to an increase in geothermal gradient and therefore these stratigraphically shallower turbidite traps may likely be viable targets.

After creating time and depth structure maps of the Bjarni Formation it is evident that there are both large and small features with structural closure in the area. Figure 5.11 reproduces the Bjarni Formation structure map also shown in Figure 5.4. The map illustrates several areas of possible structural closure. Nevertheless, with the dip lines 5 km apart and the strike lines 20 km apart the definition of the structural closures may be

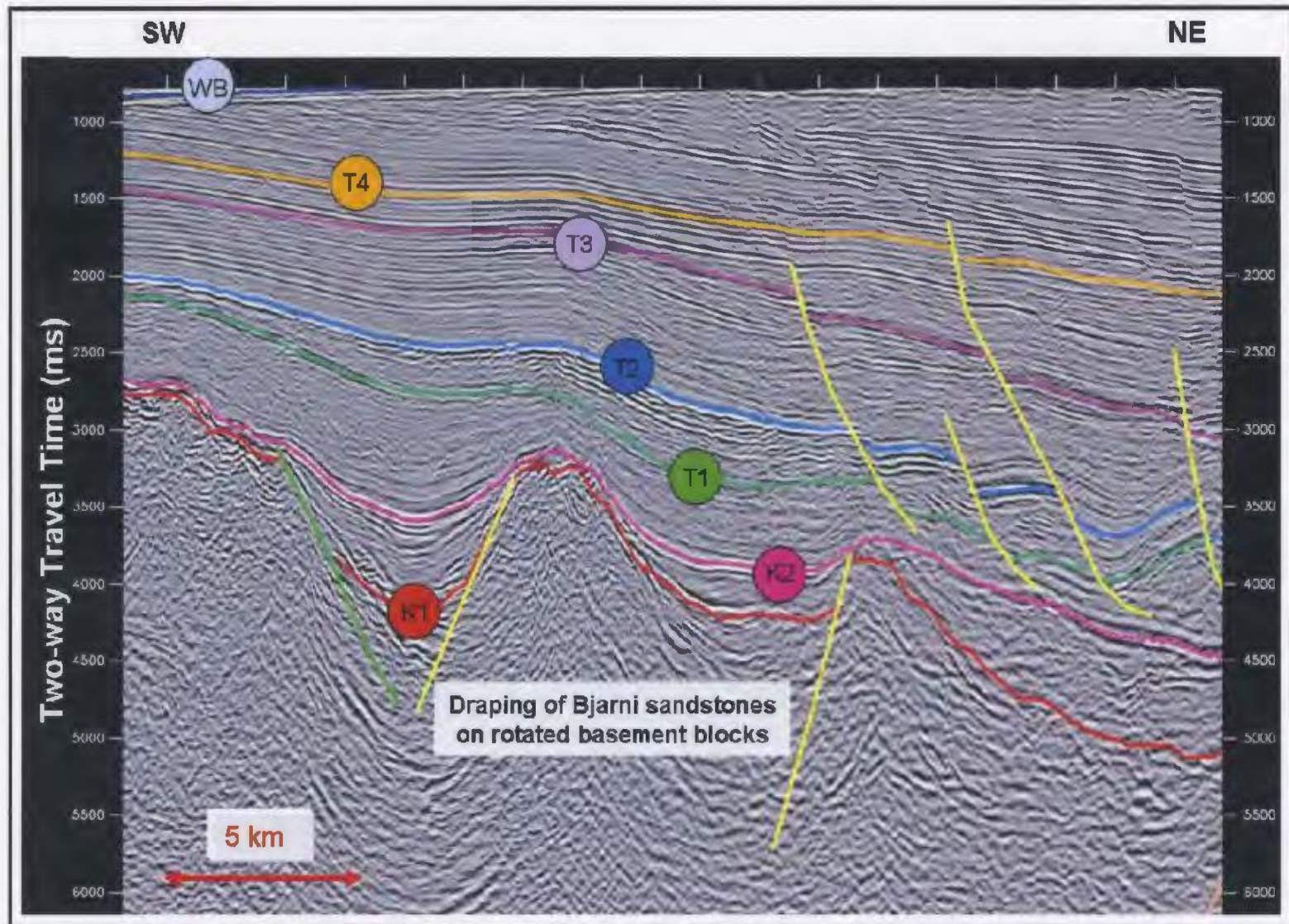


Figure 5.10 – Dip seismic section showing rotated basement blocks with Bjarni sandstones draped over rotated basement blocks and which are sometimes fault bounded.

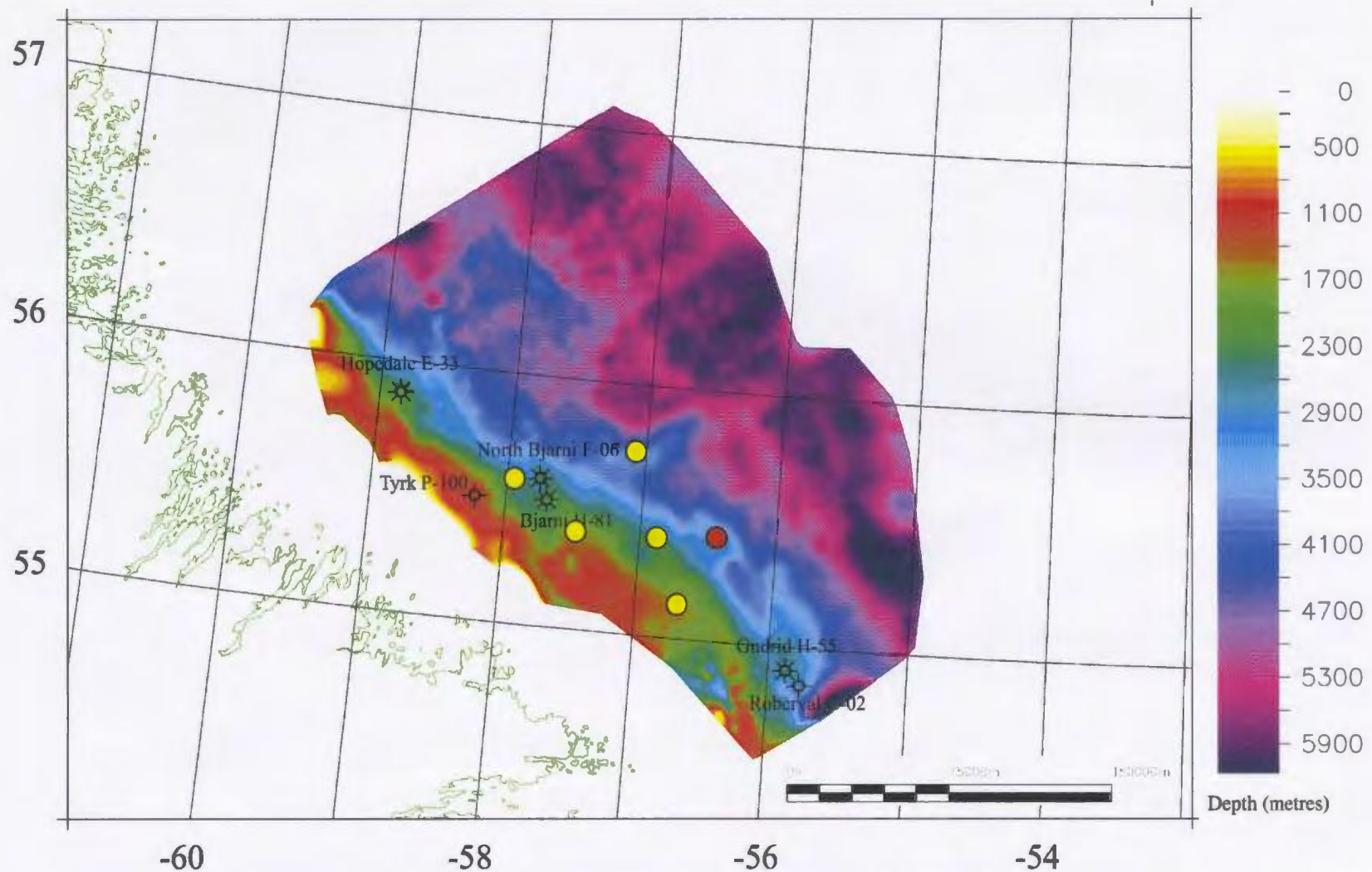


Figure 5.11 – Depth structure map of the top Bjarni Formation (K2 horizon). The map was created in UTM Zone 21, NAD 83. The location of the structure seen in Figures 5.12(A) and 5.12(B) is indicated by a red circle. Other possible structural traps with Bjarni sandstone reservoir potential are indicated by yellow circles.

uncertain. One of the closures which has not been drilled is denoted by a red circle (Figure 5.11). Figures 5.12(A) and 5.12(B) show approximate cross-sections through this structural high. Figure 5.12(A) shows a dip line trending SW-NE. This feature has Bjarni Formation draping over the top of the rotated basement block. Figure 5.12(B) is a strike line through the same feature trending NW-SE. This is just one example of an undrilled structural trap within the Hopedale Basin. Other trap types include possible anticlines which have been poorly imaged beneath the shelf breaks, rollover structures evident in the deep water as a result of gravity induced listric faulting as seen in Figure 4.2, and anticlinal structures created as a result of basement or serpentinite ridges situated within the deep water.

5.6 Discussion

The earlier drilling cycle in the Labrador Sea (1973-1983) has proven the existence of a working petroleum system. Several publications have documented these gas discoveries, described the stratigraphy, petroleum geology and the source geochemistry (McWhae and Michel, 1975; Gradstein and Williams, 1976; Barss, 1979; McWhae et al., 1980; Rashid et al., 1980; Issler and Beaumont, 1987; Bell et al., 1989; Balkwill and McMillan, 1990; Enachescu 2005; Enachescu and Hogg, 2005; Fowler et al., 2005; Enachescu 2006a; Enachescu 2006b; Martin et al., 2006 and others) while others have concentrated on the geodynamic evolution of the area (Grant, 1972, Grant, 1975; Gradstein and Srivastava, 1980; Grant, 1980; Keen, 1982; Balkwill, 1987; Enachescu, 1987; Chalmers, 1991; Chian and Loudon, 1994; Chalmers and Laursen,

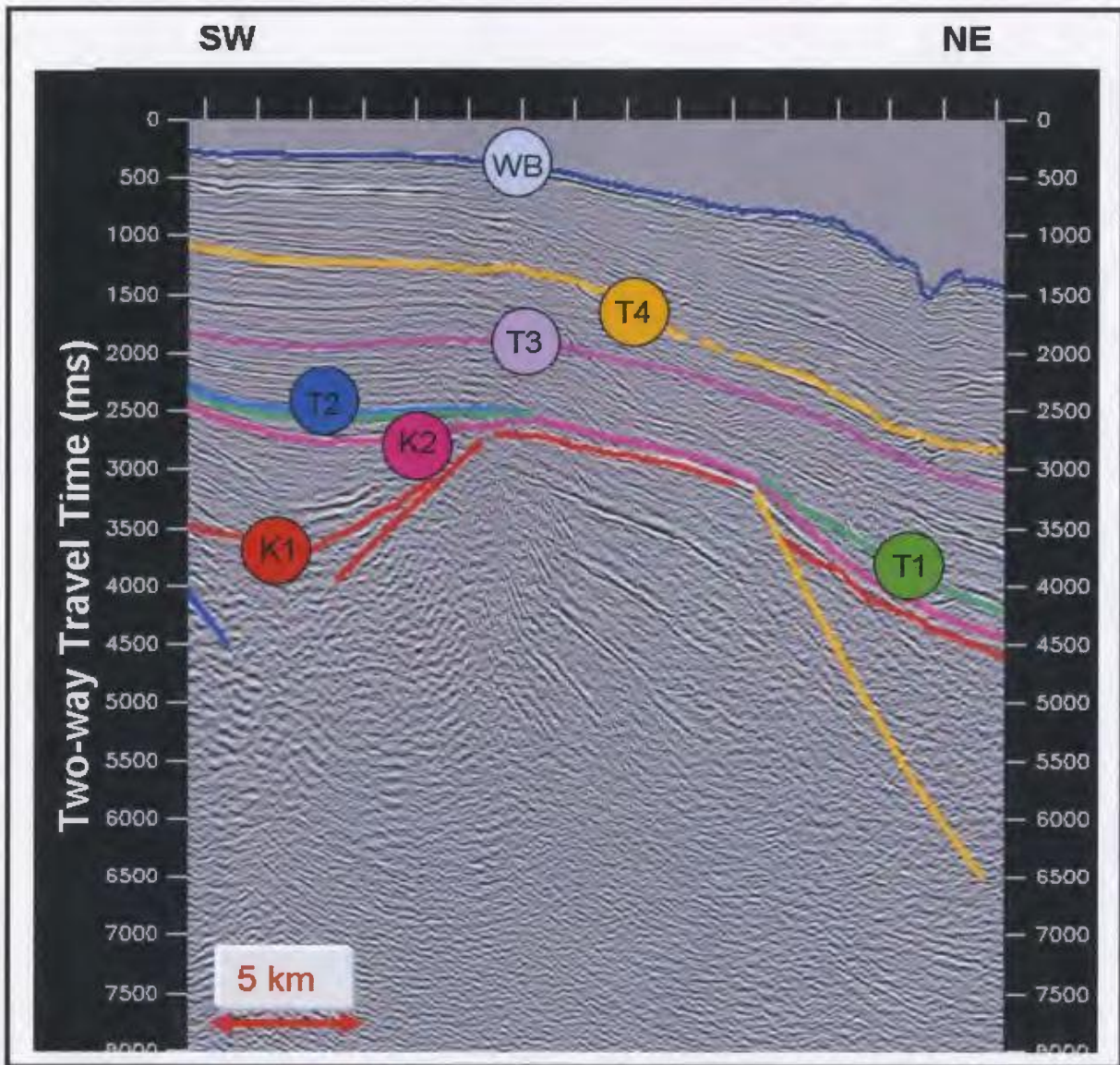


Figure 5.12(A) – Dip seismic section through a potential structural trap. Location of structure is shown in Figure 5.11.

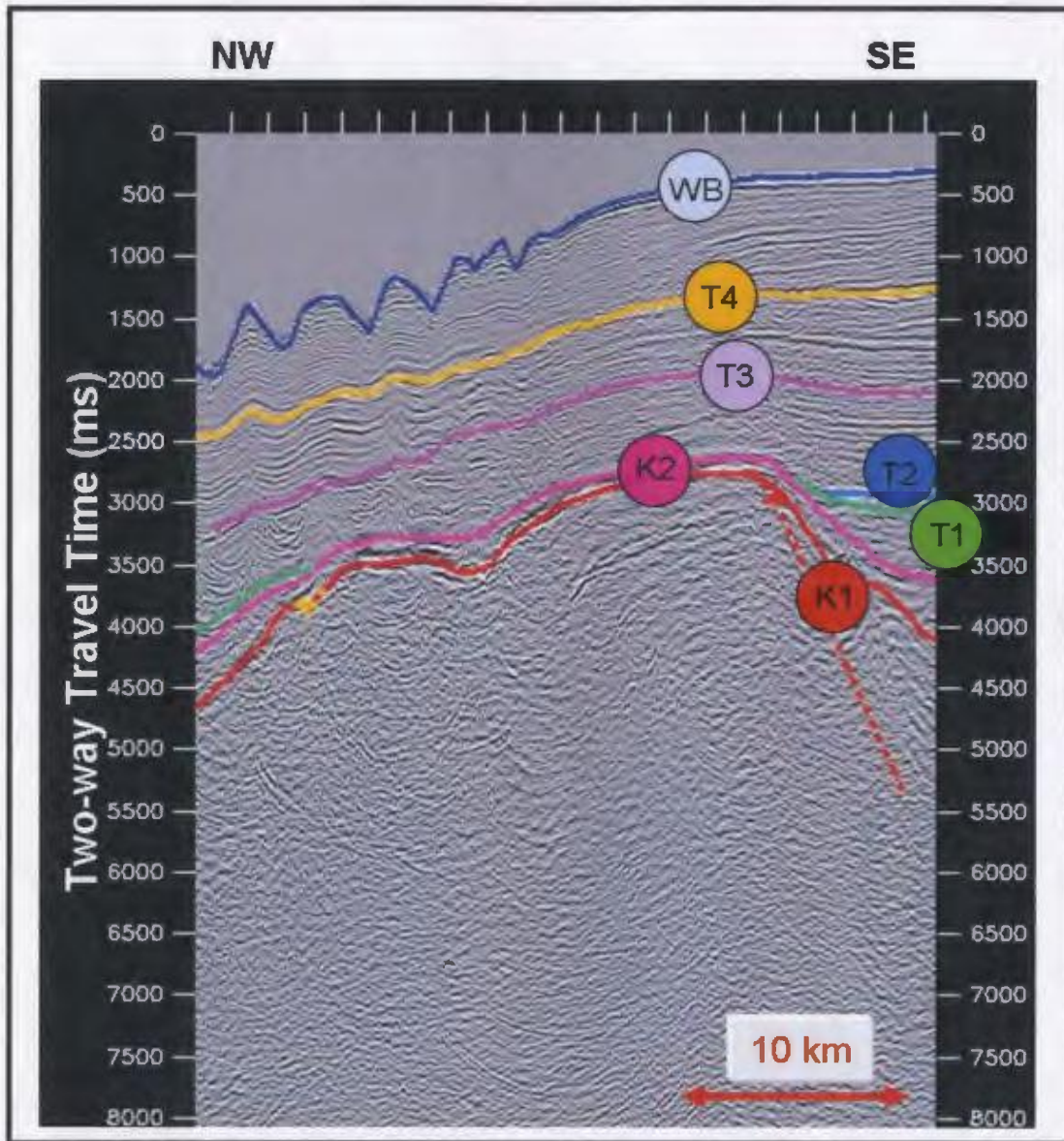


Figure 5.12(B) – Strike seismic section through a potential Bjarni structural trap. Location of structure is shown in Figure 5.11.

1995; Chian et al., 1995; Loudon et al., 1996; Chalmers and Pulvertaft, 2001; Loudon, 2002 and others). This thesis shows that there is a significant potential of finding hydrocarbons in the vicinity of the known Bjarni-North Bjarni field. It also points out that mature source rocks are widespread in the Hopedale Basin and that there are many undrilled structural and stratigraphic traps in the area. Several plays exist besides the proven Bjarni sandstone and Palaeozoic carbonates within rotated blocks and drape anticlines. One of the major concerns regarding drilling offshore Labrador is the risk of finding large enough closures to justify high-cost drilling. Aside from normal offshore exploration hazards such as shallow gas pockets, other obstacles exist which are unique to the Labrador Shelf and absent from other areas such as the Gulf of Mexico.

The first major obstacle is the short drilling season. Due to pack ice and persistently poor weather, safe drilling can only take place for approximately 3 months a year. Even then, poor weather conditions are still a problem therefore leaving little extra time to allow for the unexpected such as mechanical issues. The Orphan Basin already struggles with this issue and the drilling season for that region is significantly longer than Labrador. It would take some strategic planning and new innovations to overcome these issues (Enachescu, 2006a; 2006b).

Secondly, the quantity of icebergs which pass along the Labrador Shelf in shallow water is considerable. Trying to find ample protection against iceberg scour or towing the icebergs would be very challenging but definitely necessary. This would be a significant concern when considering production from fields located offshore Labrador

(Enachescu, 2006a; 2006b) although iceberg removal is already ongoing in the Grand Banks and appears to be effective as well as cost efficient.

Finally, the Labrador basins are far removed from major United States and Central Canadian markets or pipelines connections. Without finding economic and safe production solutions the hydrocarbons of the Hopedale Basin may remain stranded for more years to come (Enachescu, 2006a; 2006b). However gas price levels in North America will be the decisive factor for developing these reserves (Enachescu, 2006a; 2006b).

Obviously there are many things to consider when exploring offshore Labrador. If the demand for hydrocarbons continues to rise and conventional reserves become increasingly difficult to find, the Labrador basins will once again become the focus of exploration.

Chapter Six: Conclusions

6.1 Justification of Study

In recent years the need for new petroleum discoveries offshore Newfoundland has become increasingly important. Hibernia, Terra Nova and White Rose oil fields are approaching their maximum production plateau and other than recent land sales in the Orphan and Jeanne d'Arc basins there is little exploration carried out in the province's offshore region. During the time that the gas discoveries were made offshore Labrador, natural gas prices were low and there was no economic value in gas field development and production. Now, with the changes in natural gas prices and new drilling and development techniques it is time to take another look at what may potentially be another large resource for the province of Newfoundland and Labrador. The high exploration success rate recorded with the wells already drilled in this region is proof the richness of the Labrador Sea petroleum system and that large accumulations exist. Offshore Labrador cannot be ignored as a future gas production area.

The potential of the Labrador Sea has prompted Geophysical Services Incorporated (GSI) to collect more than thirty thousand kilometres of proprietary data in the Hopedale and Saglek basins. This data has been collected using better acquisition and processing techniques than the data collected in the 1970's and 1980's. The new lines extend further beyond the shelf and cover more than traditional structural traps of the past. With this dataset better regional interpretation can be carried out.

Numerous new concepts emerged in this thesis involving the seismic horizons, seismic sequences, geodynamic stages, transitional crust and potential hydrocarbon plays and are all valuable information. The work also confirms recent suggestions made by other researchers. Hopefully with the publication of this thesis and presentation of its main results, more information will be publicly available to raise new interest in the potential of the Hopedale Basin and ultimately, the Labrador Shelf.

6.2 Key Conclusions

This study includes a seismic sequence analysis, a kinematic model and petroleum system study. There are several key conclusions which can be drawn about the Bjarni area in the Hopedale Basin, Labrador Sea:

1. Seven key seismic markers can be defined and interpreted within the Hopedale Basin with varying degrees of confidence. These seven seismic horizons correspond with earlier identified major lithologic markers and regional unconformities and define six major seismic sequences.
2. Two other distinct seismic horizons were suggested which were correlated to the transitional crust zone. Large ridges of presumed serpentinized peridotites due to continental mantle exhumation and alteration appear at the eastern end of the 2003 and 2004 seismic lines. Also, characteristics of these areas are significantly bright seismic horizons which are believed to represent lava flows formed during and after mantle exhumation.

3. The geodynamic evolution of the Hopedale Basin, Labrador Sea can be divided into five stages of basin formation. These stages are: I) prerift, II) synrift, III) postrift (mantle exhumation), IV) syndrift (sea floor spreading) and V) postdrift (spreading cessation).

4. Most of the extension of the Labrador Sea took place in a continental setting during the Early Cretaceous creating numerous normal faults, rotated basement blocks, horsts and half grabens. Thermal subsidence occurred during the following postrift (Late Cretaceous - present) with the largest thermal subsidence occurring during the postdrift stage.

5. Early studies based on interpretation of 1970-1983 seismic cross-sections limited the distribution of the Bjarni Formation to the inner shelf region of the Hopedale Basin. New seismic data used in this thesis and derived time and depth structural maps illustrates that there is much wider distribution of the Bjarni Formation, with this predominantly sandstone formation extending on the outer shelf and deepwater regions.

6. Massive thermal subsidence took place in the Late Tertiary creating a thick succession of postdrift sediments on the shelf and in the deep water. This considerable subsidence along with margin tilting and some erosion and redeposition of Late Tertiary beds have created the present-day Labrador shelf.

7. Several intriguing structural features are present in the Hopedale Basin which includes compressional features due to transtensional movements and/or gravity sliding. Figure 6.1 illustrates these structural features as well as combines other important information presented in this thesis and described in numbers 1-6.

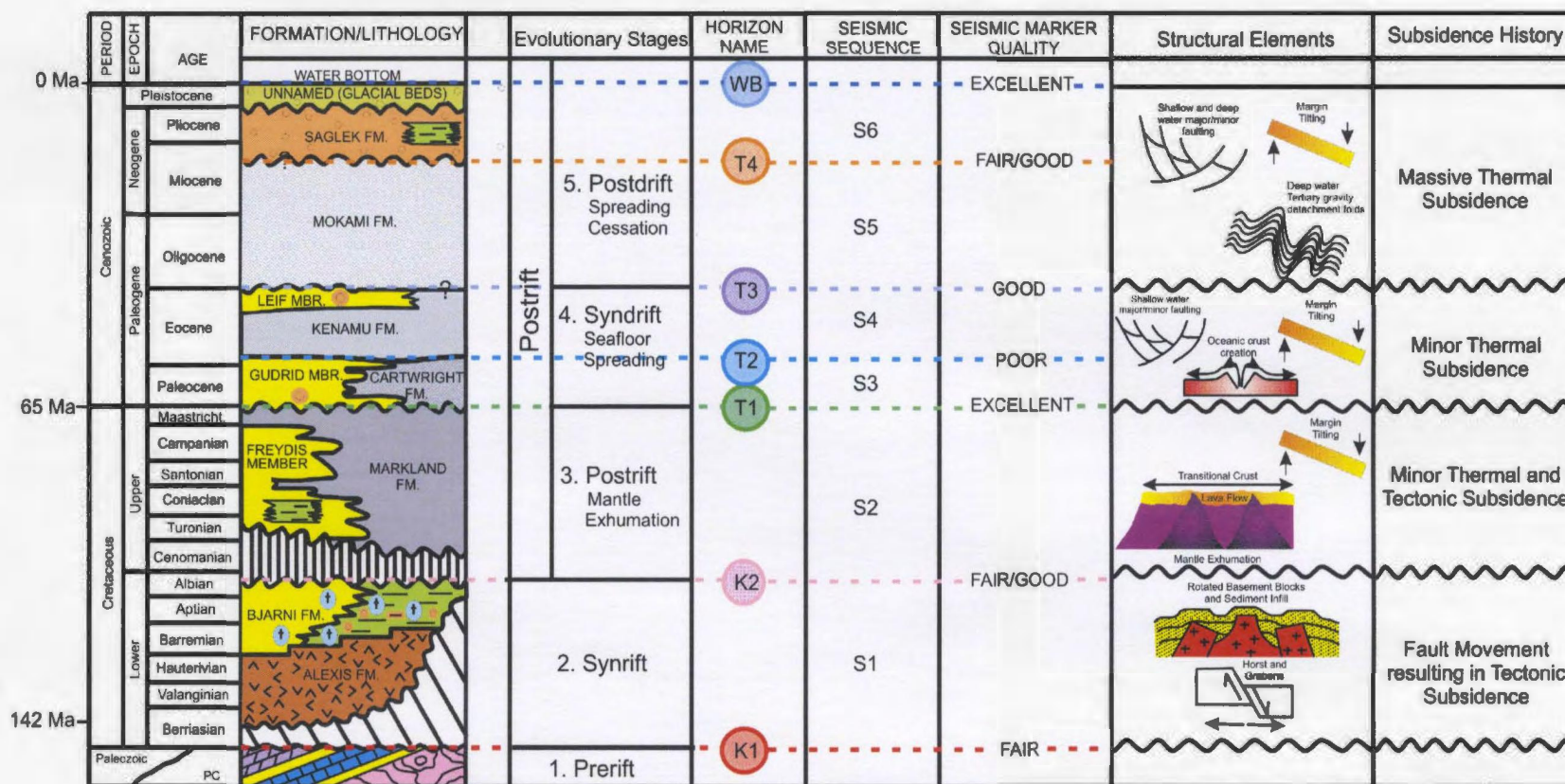


Figure 6.1 – Stratigraphic chart combining information determined and used in the previous sections of the study (modified after McWhae et al., 1980, GSC, 1987 and Enachescu, 2006).

8. Both the Markland Formation (identified earlier) and the Bjarni Formation (indicated only recently) were considered as potential source rocks for the hydrocarbons produced within the Hopedale Basin. It is evident that the structures which have been shown to have significant hydrocarbons reserves do not lie within the region that is predicted to have mature source rocks. This implies that there is lateral migration occurring from the down dip half-grabens. Also, the depth to maturation increases with distance from the shore. Therefore, in the deep water, younger formations may contain unidentified, yet mature, source rocks.

9. There is no shortage of potential reservoir rocks or seals along the Labrador Shelf. Widespread Bjarni Formation and local preservation of Palaeozoic carbonates are the most significant known reservoir rocks in the region. Other minor reservoirs include the Freydis Member of the Markland Formation, the Gudrid Member of the Cartwright Formation, and the Leif Member of the Kenamu Formation. Regionally deposited shales acting as seals include the Markland Formation, Kenamu Formation and Mokami Formation.

10. Known play mechanisms within the Hopedale Basin include preserved Bjarni Formation and Palaeozoic carbonates on top of basement highs. Bjarni sandstones draped over the top of rotated basement blocks or complex ridges forming large anticlines is the favorite exploration play. Another tested play that is widespread in the basin is represented by sand pinchouts and onlap of the Bjarni sandstones on Precambrian basement.

This study has confirmed information discussed by previous researchers in the area as well as introduced new observations and ideas adding to the knowledge of the geological evolution and petroleum geology of the basin.

6.3 Recommendations for Future Work

The regional seismic mapping done during this thesis is only a small portion of the work that could be completed using the entire Labrador GSI data set as well as other geophysical and geological data. Listed below are several recommendations for future work:

1. A complete integrated study using all of the available GSI data for offshore Labrador is essential for reconstructing the areas structural and tectonic evolution. This includes data to the north of the study area (Saglek Basin) as well as to the south.
2. Acquisition and use of stratigraphic and mechanical well logs in conjunction with the seismic data should be done in a future study. It would be beneficial to do an entire integrated study using seismic data, well core, well logs and potential field data such as magnetic and gravity data. This would include further geochemical and petrophysical research including reservoir provenance studies.
3. Unfortunately, the hydrocarbon-bearing Palaeozoic carbonates (as well as other potential reservoirs) were neglected during this thesis due to a low-degree of confidence when interpreting seismic markers beyond the well locations. Several wells in the Hopedale Basin and along the Labrador Shelf have proven that the carbonates are

good reservoirs and should not be forgotten when considering the hydrocarbon potential of the Labrador Shelf. After saying this, there is a need to further investigate the Palaeozoic carbonates in the area (dolomites and limestones) and study their petroleum potential.

4. Proper balanced geological reconstructions for the margin would also be beneficial especially when considering subsidence history and looking at hydrocarbon maturation within the Hopedale Basin. It would also be beneficial to do several of these balanced reconstructions, at different latitudes on other dip lines along the margin and use paleobathymetric information for a more reliable reconstruction. The model proposed in this study is a first approximation and will likely change with further data and more detailed modelling studies.

5. Comparison of the Labrador offshore geology with the geology of the conjugate Greenland margin should be done, using trans-Labrador Sea seismic lines or at least long lines from both margins.

References

Albertz, M., Beaumont, C., and Ings, S.J. 2006. Mobile shale basins - genesis, evolution and hydrocarbon systems. Presentation: AAPG/GSTT Hedberg Conference, Port of Spain, Trinidad and Tobago.

Balkwill, H.R. 1987. Labrador Basin; structural and stratigraphic style; sedimentary basins and basin-forming mechanisms, Atlantic Geoscience Society Special Publication, 5: 17-43, pp. 295-324.

Balkwill, H.R. and McMillan, N.J. 1990. Mesozoic-Cenozoic geology of the Labrador shelf; geology of the Labrador shelf, Baffin Bay, and Davis Strait. In Geology of the continental margin of Eastern Canada. Edited by M.J. Keen and G.L. Williams. Geological Society of America, United States (USA), United States (USA).

Bally, A.W., Watts, A.B., Grow, J.A., Manspeizer, W., Bernoulli, D., Schreiber, C., and Hunt, J.M. 1981. Atlantic-type margins; geology of passive continental margins; history, structure and sedimentologic record (with special emphasis on the Atlantic margin), AAPG Continuing Education Course Note Series, 19: 48.

Barss, M.S., Bujak, J.P., and Williams, G.L. 1979. Palynological zonation and correlation of sixty-seven wells, eastern Canada, Paper - Geological Survey of Canada. : 118.

Bell, J.S., Howie, R.D., McMillan, N.J., Hawkins, C.M., and Bates, J.L. 1989. Labrador Sea, East Coast Basin Atlas series. Geological Survey of Canada, Canada.

Blatt, H. and Tracy, R.J. 1996. Petrology: Igneous, sedimentary and metamorphic. W.H. Freeman and Company, USA.

Canada-Newfoundland and Labrador Offshore Petroleum Board. 2003. Schedule of wells [online]. Available from <http://www.cnlopb.nl.ca> [cited January - December 2006]

Canada-Newfoundland and Labrador Offshore Petroleum Board. 2003. Properties of gas bearing reservoirs [online]. Available from <http://cnlopb.nl.ca> [cited March 5 2007]

Chalmers, J.A. 1991. New evidence on the structure of Labrador Sea/Greenland continental margin, Journal of the Geological Society of London, 148: 899-908.

Chalmers, J.A. and Pulvertaft, T.C.R. 2001. Development of the continental margins of the Labrador Sea; a review; non-volcanic rifting of continental margins; a comparison of evidence from land and sea, Geological Society Special Publications, 187: 77-105.

Chalmers, J.A. and Laursen, K.H. 1995. Labrador Sea; the extent of continental and oceanic crust and the timing of the onset of seafloor spreading, Marine and Petroleum Geology, 12: 205-217.

Chian, D. and Loudon, K.E. 1994. The continent-ocean crustal transition across the southwest Greenland margin, Journal of Geophysical Research, 99: 9117-9135.

Chian, D., Loudon, K.E., and Reid, I. 1995. Crustal structure of the Labrador Sea conjugate margin and implications for the formation of nonvolcanic continental margins, *Journal of Geophysical Research*, 100: 24, pp. 239-253.

Coe, A. L. (ed.), 2003. *The Sedimentary Record of Sea-Level Change*, Cambridge, UK ; New York : Open University ; Cambridge University Press: 57-87.

Cutt, B.J. and Laving, J.G. 1977. Tectonic elements and geologic history of the south Labrador and Newfoundland continental shelf, eastern Canada, *Bulletin of Canadian Petroleum Geology*, 25: 1037-1058.

Dehler, S.A. and Keen, C.E. 1993. Effects of rifting and subsidence on thermal evolution of sediments in Canada's East Coast basins, *Canadian Journal of Earth Sciences*, 30: 1782-1798.

Enachescu, M.E. 2006a. Hopedale Basin; 1, favorable geology, advanced technology may unlock Labrador's substantial resource, *Oil and Gas Journal*, 104: 29-34.

Enachescu, M.E. 2006b. Hopedale Basin; 2, Atlantic off Labrador poised for modern exploration round, *Oil and Gas Journal*, 104: 36-42.

Enachescu, M.E. 2005. A story of stranded gas, Hopedale Basin, Labrador Sea: Its geologic evaluation and exploration potential, *Atlantic Business Magazine*, 16: 18-22.

Enachescu, M.E. 1987. Tectonic and structural framework of the northeast Newfoundland continental margin; sedimentary basins and basin-forming mechanisms, Atlantic Geoscience Society Special Publication, 5: 117-146.

Enachescu, M.E. and Fagan, A.J. 2005. Canada's offshore; 2, Newfoundland's Grand Banks presents untested oil and gas potential in eastern North America, Oil and Gas Journal, 103: 32-39.

Enachescu, M.E. and Hogg, J. 2005. Exploring for Atlantic Canada's next giant petroleum discovery, Canadian Society of Exploration Geophysicists RECORDER, 30: 19-30.

Enachescu, M.E., Fagan, A.J., and Smee, J. 2005a. Newfoundland Orphan Basin; 1, exploration opportunities abound in Orphan Basin off Newfoundland, Oil and Gas Journal, 103: 32-36.

Enachescu, M.E., Fagan, A.J., and Smee, J. 2005b. Newfoundland Orphan Basin; 2, Orphan Basin off Newfoundland set for multiyear exploration program, Oil and Gas Journal, 103: 32-34.

Enachescu, M.E., Kearsey, S., Hogg, J., Fagan, A.J., Einarsson, D., Atkinson, I., and Hardy, V. 2006. Hopedale Basin, offshore Labrador, Canada: Structural and tectonic framework and exploration potential. SEG 2006 Annual Meeting, New Orleans, LA.

Fowler, M.G., Stasiuk, L.D., and Avery, M. 2005. Potential petroleum systems in the Labrador and Baffin shelf areas, offshore eastern Canada. Abstract: GAC/MAC/CSPG/CSSS, Halifax, NS.

Geological Society of Canada. 2007. Atlantic Basin website [online]. Available from http://gsca.nrcan.gc.ca/BASIC/index_e.php.

Geophysical Services Incorporated. 2007. GSI website [online]. Available from <http://www.geophysicalservice.com>.

Gradstein, F.M. and Srivastava, S.P. 1980. Aspects of Cenozoic stratigraphy and paleoceanography of the Labrador Sea and Baffin Bay; Cenozoic history in and around the northern Atlantic and Arctic oceans. *Palaeogeography, Palaeoclimatology, Palaeoecology*, 30: 261-295.

Gradstein, F.M. and Williams, G.L. 1976. Biostratigraphy of the Labrador shelf; part 1. 349, Geological Survey of Canada, Calgary, AB, Canada (CAN), Canada (CAN), 39 pp.

Gradstein, F.M., Jansa, L.F., Srivastava, S.P., Williamson, M.A., Bonham-Carter, G., and Stam, B. 1990. Aspects of north Atlantic paleo-oceanography. In *Geology of the continental margin of Eastern Canada*. Edited by M.J. Keen and G.L. Williams. Geological Society of America, United States (USA), United States (USA).

Grant, A.C. 1980. Problems with plate tectonics; the Labrador Sea. *Bulletin of Canadian Petroleum Geology*, 28: 252-278.

Grant, A.C. 1975. Structural modes of the western margin of the Labrador Sea, Paper - Geological Survey of Canada, no.74-30, Offshore geology of eastern Canada; Vol.2, Regional geology: pp. 217-231.

Grant, A.C. 1972. The continental margin off Labrador and eastern Newfoundland; morphology and geology, Canadian Journal of Earth, 9: 1394-1430.

Hall, J., Loudon, K.E., Funck, T., and Deemer, S. 2002. Geophysical characteristics of the continental crust along the Lithoprobe Eastern Canadian Shield Onshore-Offshore Transect (ECSOOT); a review; Proterozoic evolution of the northeastern Canadian shield, Canadian Journal of Earth Sciences, 39: 569-587.

Issler, D.R. and Beaumont, C. 1987. Thermal and subsidence history of the Labrador and west Greenland continental margins; sedimentary basins and basin-forming mechanisms, Atlantic Geoscience Society Special Publication, 5: 45-69.

Keen, C.E. 1982. The continental margins of eastern Canada; a review; dynamics of passive margins, Geodynamics Series, 6: 45-58.

Keen, C.E. 1979. Thermal history and subsidence of rifted continental margins; evidence from wells on the Nova Scotian and Labrador shelves, Canadian Journal of Earth Science, 16: 505-522.

King, A.F. and McMillan, N.J. 1975. A mid-Mesozoic breccia from the coast of Labrador, Canadian Journal of Earth Science, 12: 44-51.

Laughton, A.S. 1971. South Labrador Sea and the evolution of the north Atlantic. *Nature* (London), 232: 612-616.

Louden, K.E. 2002. Tectonic evolution of the east coast of Canada. *Canadian Society of Exploration Geophysicists RECORDER*, 27: 37-49.

Louden, K.E., and Lau H. 2002. Insights from scientific drilling on rifted continental margins: *Geoscience Canada*, 28: 187-195.

Louden, K.E., Osler, J.C., Srivastava, S.P., and Keen, C.E. 1996. Formation of oceanic crust at slow spreading rates; new constraints from an extinct spreading center in the Labrador Sea, *Geology* (Boulder), 24: 771-774.

Majorowicz, J.A. and Osadetz, K.G. 2003. Natural gas hydrates stability in the east coast offshore, Canada. *Natural Resources Research* (International Association for Mathematical Geology), 12: 93-104.

Majorowicz, J.A. and Osadetz, K.G. 2001. Gas hydrate distribution and volume in Canada, *AAPG Bulletin*, 85: 1211-1230.

Martin, M.R., Enachescu, M.E., and Schwartz, S. 2006. New geoscience data and interpretation of Hopedale Basin reservoirs. Presentation: ILP Task Force on Sedimentary Basins, Quebec City, QC.

Mayhew, M.A., Drake, C.L., and Nafe, J.E. 1970. Marine geophysical measurements on the continental margins of the Labrador Sea, Canadian Journal of Earth Sciences = Journal Canadien des Sciences de la Terre, 7: 199-210.

McMillan, N.J., 1982. Canada's East Coast: the new super petroleum province; Journal of Canadian Petroleum Technology, 21/2: 1-15

McWhae, J.R.H. and Michel, W.F.E. 1975. Stratigraphy of Bjarni H-81 and Leif M-48, Labrador shelf, Bulletin of Canadian Petroleum Geology, 23: 361-382.

McWhae, J.R.H., Elie, R., Laughton, D.C., and Gunther, P.R. 1980. Stratigraphy and petroleum prospects of the Labrador shelf, Bulletin of Canadian Petroleum Geology, 28: 460-488.

Osler, J.C. and Loudon, K.E. 1995. Extinct spreading center in the Labrador Sea; crustal structure from a two-dimensional seismic refraction velocity model, Journal of Geophysical Research, 100: 2261-2278.

Osler, J.C. and Loudon, K.E. 1992. Crustal structure of an extinct rift axis in the Labrador Sea; preliminary results from a seismic refraction survey, Earth and Planetary Science Letters, 108: 243-258.

Pinheiro, L.M., Wilson, R.C.L., Pena dos Reis, R., Whitmarsh, R.B., and Ribeiro, A. 1996. The western Iberia margin: A geophysical and geological overview. In Proceedings of the Ocean Drilling Program, Scientific Results, Vol. 149 Edited by R.B. Whitmarsh,

D.S. Sawyer, A. Klaus and D.G. Masson. Ocean Drilling Program, College Station, TX, pp. 1-21.

Powell, T.G. 1979. Geochemistry of Snorri and Gudrid condensates, Labrador shelf; implications for future exploration; current research, part C, Paper - Geological Survey of Canada: 91-95.

Rashid, M.A., Purcell, L.P., and Hardy, I.A. 1980. Source rock potential for oil and gas of the east Newfoundland and Labrador shelf areas; facts and principles of world petroleum occurrence, Memoir - Canadian Society of Petroleum Geologists: 589-607.

Reston, T.J., Pennell, J., Stubenrauch, A., Walker, I., and Perez-Gussinye, M. 2001. Detachment faulting, mantle serpentinization, and serpentinite-mud volcanism beneath the Porcupine Basin, southwest of Ireland, *Geology (Boulder)*, 29: 587-590.

Roest, W.R. and Srivastava, S.P. 1989. Sea-floor spreading in the Labrador Sea; a new reconstruction, *Geology (Boulder)*, 17: 1000-1003.

Royden, L. and Keen, C.E. 1980. Rifting process and thermal evolution of the continental margin of eastern Canada determined from subsidence curves, *Earth and Planetary Science Letters*, 51: 343-361.

Schwartz, S. in progress. Diagenesis and porosity evolution of the lower Palaeozoic carbonate and Cretaceous-Tertiary siliciclastic reservoir intervals, Labrador shelf. MSc (Geology), Memorial University of Newfoundland, St. John's, NL.

Shillington, D.J., Holbrook, W.S., Tucholke, B.E., Hopper, J.R., Loudon, K.E., Larsen, H.C., Van Avendonk, H.J.A., Deemer, S., Hall, J., Tucholke, B.E., Sibuet, J., Klaus, A., Arnaboldi, M., Delius, H., Engstrom, A.V., Galbrun, B., Hiscott, R.N., Karner, G.D., Ladner, B.C., Leckie, R.M., Lee, C., Manatschal, G., Marsaglia, K.M., Pletsch, T.K., Pross, J., Robertson, A.H.F., Sawyer, D.S., Sawyer, D.E., Shillington, D.J., Shirai, M., Shryane, T., Stant, S.A., Takata, H., Urquhart, E., Wilson, C., Zhao, X., and Ocean Drilling Program, Leg 210, Shipboard Scientific Party, College Station, TX, United States (USA). 2004. Marine geophysical data on the Newfoundland nonvolcanic rifted margin around SCREECH transect 2; proceedings of the ocean drilling program; initial reports; drilling the Newfoundland half of the Newfoundland-Iberia transect; the first conjugate margin drilling in a nonvolcanic rift; covering leg 210 of the cruises of the drilling vessel JOIDES resolution; sites 1276 and 1277, 6 July - 6 September 2003, Proceedings of the Ocean Drilling Program, Part A: Initial Reports, 210: 36.

Sibuet, J., Srivastava, S.P., and Manatschal, G. *in press*. Exhumed mantle forming transitional crust in the Newfoundland-Iberia rift and associated magnetic anomalies.

Srivastava, S.P. 1978. Evolution of the Labrador Sea and its bearing on the early evolution of the north Atlantic, The Geophysical Journal of the Royal Astronomical Society, 52: 313-357.

Srivastava, S.P. and Roest, W.R. 1999. Extent of oceanic crust in the Labrador Sea, Marine and Petroleum Geology, 16: 65-84.

Srivastava, S.P., Falconer, R.K.H., and MacLean, B. 1981. Labrador Sea, Davis Strait, Baffin Bay; geology and geophysics; a review; geology of the north Atlantic borderlands, Memoir - Canadian Society of Petroleum Geologists, 7: 333-398.

Stead, J.E. in progress. Interpretation of seismic and wellbore data, Hawke basin (Labrador shelf). MSc (Geophysics), Memorial University of Newfoundland, St. John's, NL.

Tankard, A.J. and Welsink, H.J. 1989. Mesozoic extension and styles of basin formation in Atlantic Canada; extensional tectonics and stratigraphy of the north Atlantic margins, AAPG Memoir, 46: 175-195.

Taylor, A., Weitmiller, R., and Judge, A. 1979. Two risks to drilling and production off the east coast of Canada-earthquakes and gas hydrates. In Proc. Vol. Symp. Research on the Labrador Coastal and Offshore Region Edited by W. Denver. Memorial University of Newfoundland, St. John's, NL, pp. 91-105.

Taylor, F.C. 1981. Precambrian geology of the Canadian north Atlantic borderlands; geology of the north Atlantic borderlands, Memoir - Canadian Society of Petroleum Geologists, 7: 11-30.

Taylor, F.C. 1979. Reconnaissance geology of a part of the Precambrian shield, northeastern Quebec, northern Labrador and Northwest Territories. Geological Survey of Canada, Ottawa, ON, Canada (CAN), Canada (CAN), no. 393, 99 pp.

Tucholke, B.E., Sibuet, J., Klaus, A., Arnaboldi, M., Delius, H., Engstrom, A.V., Galbrun, B., Gardin, S., Hiscott, R.N., Karner, G.D., Ladner, B.C., Leckie, R.M., Lee, C., Manatschal, G., Marsaglia, K.M., Pletsch, T.K., Pross, J., Robertson, A.H.F., Sawyer, D.S., Sawyer, D.E., Shillington, D.J., Shirai, M., Shryane, T., Stant, S.A., Takata, H., Urquhart, E., Wilson, C., Zhao, X., Ocean Drilling Program, Leg 210, Shipboard Scientific Party, College Station, TX, United States (USA), Tucholke, B.E., Sibuet, J., Klaus, A., Arnaboldi, M., Delius, H., Engstrom, A.V., Galbrun, B., Hiscott, R.N., Karner, G.D., Ladner, B.C., Leckie, R.M., Lee, C., Manatschal, G., Marsaglia, K.M., Pletsch, T.K., Pross, J., Robertson, A.H.F., Sawyer, D.S., Sawyer, D.E., Shillington, D.J., Shirai, M., Shryane, T., Stant, S.A., Takata, H., Urquhart, E., Wilson, C., Zhao, X., and Ocean Drilling Program, Leg 210, Shipboard Scientific Party, College Station, TX, United States (USA). 2004. Leg 210 summary; proceedings of the ocean drilling program; initial reports; drilling the Newfoundland half of the Newfoundland-Iberia transect; the first conjugate margin drilling in a nonvolcanic rift; covering leg 210 of the cruises of the drilling vessel JOIDES resolution; sites 1276 and 1277, 6 July - 6 September 2003, Proceedings of the Ocean Drilling Program, Part A: Initial Reports, 210: 78.

Umpleby, D.C. 1979. Geology of the Labrador shelf, Paper - Geological Survey of Canada: 34.

Vail, P.R. 1977. Seismic recognition of depositional facies on slopes and rises, AAPG Bulletin, 61: 5, 837 pp.

Vogt, P.R. and Avery, O.E. 1974. Detailed magnetic surveys in the northeast Atlantic and Labrador Sea, *Journal of Geophysical Research*, 79: 363-389.

Wanless, R.K., Stevens, R.D., Lachance, G.R., and Delabio, R.N.D. 1974. Age determinations and geological studies; K-Ar isotopic ages, report 12, Paper - Geological Survey of Canada, : 72.

Whitmarsh, R.B., Wallace, P.J., Abe, N., Basile, C., Beard, J.S., Froitzheim, N., Gardien, V., Hebert, R., Hopkinson, L.J., Kudless, K.E., Louvel, V., Manatschal, G., Newton, A.C., Rubenach, M.J., Skelton, A.D.L., Smith, S.E., Takayama, H., Tompkins, M.J., Turrin, B.D., Urquhart, E., Wallrabe-Adams, H., Wilkens, R.H., Wilson, R.C.L., Wise, S.W., Jr, Zhao, X., and Ocean Drilling Program, Leg 173, Shipboard Scientific Party, College Station, TX, United States (USA). 2001. The rift-to-drift development of the west Iberia nonvolcanic continental margin; a summary and review of the contribution of ocean drilling program leg 173; proceedings of the ocean drilling program; scientific results, return to Iberia; covering leg 173 of the cruises of the drilling vessel JOIDES resolution; Lisbon, Portugal, to Halifax, Nova Scotia; sites 1065-1070, 15 April-15 June 1997, *Proceedings of the Ocean Drilling Program, Scientific Results*, 173: 36.

Young, J. 2005. The stratigraphy and structural history of the Mesozoic and Cenozoic of the central Nova Scotian slope, eastern Canada. MSc (Geology), Memorial University of Newfoundland, St. John's, NL.

APPENDIX A:
Time-depth data for
the wells within the study area
collected from the C-NLOPB

Well Name: Bjarni H-81

MD (m)	TVD (m)	Two Way Time (ms)
13.00	0.00	0.00
152.66	139.66	183.20
243.86	230.86	259.60
396.26	383.26	396.80
670.58	657.58	636.00
944.90	931.90	886.20
1219.22	1206.22	1124.60
1432.58	1419.58	1308.60
1828.82	1815.82	1635.80
2026.94	2013.94	1789.80
2159.52	2146.52	1887.40

Well Name: Bjarni O-82

MD (m)	TVD (m)	Two Way Time (ms)
12.30	0.00	0.00
182.30	170.00	223.00
372.00	359.70	391.40
495.00	482.70	495.60
565.00	552.70	553.60
755.00	742.70	713.80
918.00	905.70	859.80
1080.00	1067.70	1009.80
1170.00	1157.70	1083.80
1357.00	1344.70	1237.80
1445.00	1432.70	1307.80
1582.00	1569.70	1413.80
1727.00	1714.70	1531.80
1861.00	1848.70	1645.80
1960.00	1947.70	1723.80
2058.00	2045.70	1798.00
2160.00	2147.70	1874.00
2283.00	2270.70	1974.00
2402.00	2389.70	2042.00
2500.00	2487.70	2084.00
2648.00	2635.70	2154.00

Well Name: Corte Real P-85 (UNRELIABLE)

MD (m)	TVD (m)	Two Way Time (ms)
13.40	0.00	0.00
463.40	450.00	20.69
899.98	886.58	1017.80
1718.26	1704.86	1748.00
1785.15	1771.75	1812.00
1856.03	1842.63	1876.00
1933.03	1919.62	1940.00
2022.72	2009.32	2004.00
2121.11	2107.71	2068.00
2221.40	2208.00	2132.00
2322.80	2309.40	2200.00
2443.99	2430.59	2284.00
2564.28	2550.88	2368.00
2700.97	2687.57	2476.00
2852.16	2838.76	2592.00
2976.84	2963.44	2678.00
3081.63	3068.23	2754.00
3191.12	3177.72	2836.00
3302.41	3289.01	2916.00
3400.39	3386.99	2988.00
3509.37	3495.97	3060.00
3637.15	3623.75	3140.00
3763.04	3749.64	3220.00
3885.54	3872.14	3300.00
4003.41	3990.01	3380.00
4111.56	4098.16	3460.00
4225.84	4212.44	3540.00
4324.40	4311.00	3609.00

Well Name: Gudrid H-55

MD (m)	TVD (m)	Two Way Time (ms)
12.30	0.00	0.00
311.60	299.30	393.00
518.30	506.00	604.60
731.63	719.33	840.40
1005.95	993.65	1069.80
1127.87	1115.57	1173.20
1585.07	1572.77	1532.80
1828.91	1816.61	1715.00
2133.71	2121.41	1943.80
2359.26	2346.96	2074.40

Well Name: Herjolf M-92

MD (m)	TVD (m)	Two Way Time (ms)
26.80	0.00	0.00
192.61	165.81	217.60
496.80	470.00	506.20
659.87	633.07	649.20
1127.74	1100.94	1031.00
1371.58	1344.78	1230.80
1429.49	1402.69	1275.40
1630.66	1603.86	1434.20
1767.82	1741.02	1537.20
2005.56	1978.76	1737.00
2133.58	2106.78	1833.60
2156.44	2129.64	1850.60
2255.50	2228.70	1917.20
2474.95	2448.15	2090.20
2569.44	2542.64	2156.20
2636.50	2609.70	2192.60
2746.23	2719.43	2246.40
2791.95	2765.15	2263.80
3148.56	3121.76	2433.40
3240.00	3213.20	2482.20
3425.93	3399.13	2566.40
3547.85	3521.05	2624.40
3617.95	3591.15	2658.40
3785.59	3758.79	2733.40

Well Name: Hopedale E-33

MD (m)	TVD (m)	Two Way Time (ms)
12.80	0.00	0.00
562.60	549.80	758.34
1638.80	1626.00	1912.80
1645.80	1633.00	1922.00
1653.80	1641.00	1932.00
1673.80	1661.00	1952.00
1683.80	1671.00	1962.00
1696.80	1684.00	1972.00
1707.80	1695.00	1982.00
1719.80	1707.00	1992.00
1731.80	1719.00	2002.00
1743.80	1731.00	2012.00
1767.80	1755.00	2032.00
1790.80	1778.00	2052.00
1802.80	1790.00	2062.00
1813.80	1801.00	2072.00
1825.80	1813.00	2082.00
1837.80	1825.00	2092.00
1848.80	1836.00	2102.00
1860.80	1848.00	2112.00
1872.80	1860.00	2122.00
1884.80	1872.00	2132.00
1895.80	1883.00	2142.00
1905.80	1893.00	2152.00
1915.80	1903.00	2162.00
1926.80	1914.00	2172.00
1938.80	1926.00	2182.00
1951.80	1939.00	2192.00
1965.80	1953.00	2202.00
1980.80	1968.00	2212.00
2000.80	1988.00	2222.00
2022.80	2010.00	2232.00
2045.80	2033.00	2242.00
2069.80	2057.00	2250.60

Well Name: North Bjarni F-06

MD (m)	TVD (m)	Two Way Time (ms)
12.00	0.00	0.00
162.00	150.00	193.50
650.00	638.00	655.40
856.00	844.00	838.60
1050.00	1038.00	1005.80
1265.00	1253.00	1193.80
1481.00	1469.00	1374.00
1600.00	1588.00	1460.00
1713.00	1701.00	1545.80
1850.00	1838.00	1654.00
2014.00	2002.00	1789.00
2150.00	2138.00	1892.00
2290.00	2278.00	1990.00
2430.00	2418.00	2093.00
2519.00	2507.00	2139.00
2592.00	2580.00	2179.00
2630.00	2618.00	2199.00
2703.00	2691.00	2236.00
2815.00	2803.00	2292.00

Well Name: Roberval C-02

MD (m)	TVD (m)	Two Way Time (ms)
13.70	0.00	0.00
313.70	300.00	400.00
603.70	590.00	680.00
863.70	850.00	980.00
1098.70	1085.00	1160.00
1303.70	1290.00	1320.00
1498.70	1485.00	1480.00
1688.70	1675.00	1630.00
1893.70	1880.00	1760.00
2003.70	1990.00	1850.00
2193.70	2180.00	1994.00
2273.70	2260.00	2050.00
2393.70	2380.00	2120.00
2478.70	2465.00	2150.00
2603.70	2590.00	2240.00
2743.70	2730.00	2340.00

Well Name: Roberval K-92

MD (m)	TVD (m)	Two Way Time (ms)
13.00	0.00	0.00
281.50	268.50	364.00
633.00	620.00	710.00
968.00	955.00	1020.00
1243.00	1230.00	1250.00
1353.00	1340.00	1340.00
1523.00	1510.00	1460.00
1578.00	1565.00	1510.00
1813.00	1800.00	1700.00
1893.00	1880.00	1750.00
2008.00	1995.00	1830.00
2128.00	2115.00	1910.00
2208.00	2195.00	1960.00
2353.00	2340.00	2080.00
2563.00	2550.00	2190.00
2683.00	2670.00	2260.00
2893.00	2880.00	2420.00
3053.00	3040.00	2520.00
3083.00	3070.00	2540.00
3138.00	3125.00	2560.00
3208.00	3195.00	2600.00
3333.00	3320.00	2650.00
3513.00	3500.00	2720.00

Well Name: South Hopedale L-39

MD (m)	TVD (m)	Two Way Time (ms)
11.60	0.00	0.00
591.60	580.00	761.00
1806.60	1795.00	1927.00
1906.00	1894.40	2007.80
2011.60	2000.00	2091.20
2061.60	2050.00	2117.40
2111.60	2100.00	2139.80
2161.60	2150.00	2157.20
2231.60	2220.00	2183.80
2377.00	2365.40	2240.00

Well Name: Tyrk P-100

MD (m)	TVD (m)	Two Way Time (ms)
11.80	0.00	0.00
129.80	118.00	154.80
384.80	373.00	391.20
489.80	478.00	493.60
649.80	638.00	655.80
764.80	753.00	769.80
796.80	785.00	803.80
874.80	863.00	870.00
949.80	938.00	944.00
1032.80	1021.00	1026.00
1082.80	1071.00	1074.00
1132.80	1121.00	1110.00
1177.80	1166.00	1142.00
1242.80	1231.00	1202.00
1292.80	1281.00	1240.20
1342.80	1331.00	1276.20
1392.80	1381.00	1314.20
1442.80	1431.00	1354.20
1492.80	1481.00	1388.20
1515.80	1504.00	1402.20
1588.80	1577.00	1446.20
1638.80	1627.00	1476.20
1697.80	1686.00	1506.20
1734.80	1723.00	1524.20

5263

